UNIVERSITY OF CALIFORNIA, SAN DIEGO

Mammary Gland Development and Function Depend upon the Structure of Heparan Sulfate

A Dissertation submitted in partial satisfaction of the requirements

for the degree Doctor of Philosophy

in

Biomedical Sciences

by

Omai Brant Garner

Committee in charge:

Professor Jeffrey D. Esko, Chair
Professor Sanjay Nigam
Professor Ajit Varki
Professor Anthony Wynshaw-Boris
Professor Benjamin Yu

2007

The Dissertation of Omai Brant Garner is approved, and it is acceptable in quality and form for publication on microfilm:

_____

_____

_____

_____

_____
Chair

University of California, San Diego

2007

Dedication

I would like to dedicate this thesis to my mother and father. John and Olivia Garner always instilled in me a sense of love, self worth and the confidence to do anything.

Table of Contents

List of Figures and Tables

Acknowledgements

Many people contributed to the success of this thesis project. First and foremost, I would like to thank Jeff Esko. I could not have asked for a better mentor for my graduate career. Through his efforts, I'm not only a better scientist, but I also have the problem solving skills to approach any situation my career presents, scientific or otherwise. I want to thank Brett Crawford, for starting us down the road of heparan sulfate and mammary glands. I especially want to thank Rusty Bishop. Having a friend and mentor to look up to on a daily basis is an invaluable gift. I also want to thank my future wife and best friend, Simone Moore. I'm a better man, because of her. Finally I'd like to thank everyone who was in the Esko lab during my tenure. You all made work an absolute joy.

Chapter 2 is a reprint of material intended to be submitted for publication by Garner, B. Omai; Crawford E. Brett; and Esko D. Jeffrey. The dissertation author was the primary researcher and author of this paper.

Chapter 3 is a reprint of material intended to be submitted for publication by Garner, B. Omai; and Esko D. Jeffrey. The dissertation author was the primary researcher and author of this paper.

Chapter 4 is a reprint of material intended to be submitted for publication by Crawford, E. Brett; Garner, B. Omai; Bishop, R. Joseph; Zhang, Y. David; Castagnola, Jan; and Esko, D. Jeffery. The dissertation author was the co-primary researcher and author of this paper.

Appendix 1 is a reprint of material intended to be submitted for publication by Garner, B. Omai; Esko, D. Jeffery; Videm, V. Vibeke. The dissertation author was the primary researcher and author of this paper.

Appendix 2 is a reprint of material as it is published in the Journal of Biological Chemistry, Elson-Schwab, Lev; Garner, B. Omai; Schuksz, Manuela; Crawford, E. Brett; Esko, D. Jeffery; Tor, Yitzhak. The dissertation author was a secondary researcher and author of this paper.

Vita

Education/Training

2000 Bachelor of Science, Genetics/Bacteriology, University of Wisconsin, Madison, (Madison, WI)

2007 Doctor of Philosophy, Biomedical Sciences, University of California, San Diego, (La Jolla, CA)

Honors and Awards

Chancellor Scholar – University of Wisconsin, Madison – 1996-2001

McNair Scholar – University of Wisconsin, Madison – 1998-2001

Individual NRSA – NIH/University of California, San Diego – 2002-2007

Carl Storm Fellowship – Gordon Research Conference for Mammary Gland Biology – 2005

Best Poster Award – Gordon Research Conference for Proteoglycan Biology – 2006

Publications

"Guanidinoglycosides deliver large bioactive cargo into cells through a heparan sulfate dependent pathway" Lev Elson-Schwab, **Omai B. Garner**, Manuela Schuksz, Brett Crawford, Jeffrey D. Esko, and Yitzhak Tor. Journal of Biological Chemistry. Vol. 282, No.18, pp. 13585-13591

"Lymphocyte specific inactivation of heparan sulfate biosynthetic enzymes leads to subtle changes in lymphocyte development and function". **Omai B. Garner**, Vibeke Videm, and Jeffrey D. Esko (In preparation)

"Defective lobuloalveolar development in mice containing a mammary epithelial cell-specific inactivation of a heparan sulfate sulfotransferase" Brett E. Crawford*, **Omai B. Garner***, Joseph R. Bishop, David Y. Zhang, Jan Castagnola, and Jeffrey D. Esko (In preparation), * these authors contributed equally

"A cell autonomous requirement for heparan sulfate during mammary gland branching morphogenesis". **Omai B. Garner**, Brett E Crawford, and Jeffrey D. Esko (In preparation)

"The HGF tyrosine kinase receptor C-met is not required for branching morphogenesis in the mammary gland". **Omai B. Garner**, Jeffrey D. Esko (In preparation)

ABSTRACT OF THE DISSERTATION

Mammary Gland Development and Function Depend upon the Structure of Heparan Sulfate

by

Omai Brant Garner

Doctor of Philosophy in Biomedical Sciences

University of California, San Diego, 2007

Professor Jeffery D. Esko, Chair

To understand the function of heparan sulfate in branching morphogenesis in the mammary gland, we have generated mice containing conditional mutations of heparan sulfate biosynthetic enzymes in mammary epithelial cells. Tissue specific alteration of heparan sulfate was accomplished by crossbreeding mice bearing loxP flanked alleles with transgenic mice that express the Cre recombinase specifically in mammary epithelia before ductal branching (MMTV Cre).In chapter 2 we show that altering the polymerization or overall sulfation of the chain inhibits mammary epithelial proliferation leading to failure of ductal branching. Inhibition of 2-O-

sulfation of the chain did not inhibit proliferation but blocked dichotomous and side branching. In contrast, diminution of overall sulfation of the chain had no effect on branching, but blocked lobuloalveolar formation (chapter 4). In vitro studies show that the activity of multiple heparin binding growth factors was affected. Prior studies suggested an crucial role for hepatocyte growth factor (HGF) in mammary ductal development, but deletion of the Met receptor (through which HGF signals) did not effect mammary development (chapter 3). These studies demonstrate that heparan sulfate is a key regulator in mammary development and function. This thesis provides a springboard for examining individual growth factors in branching morphogenesis.

Chapter 1: Heparan Sulfate in Branching Morphogenesis

1.1 Structure of Heparan Sulfate

Heparan sulfate is a type of glycosaminoglycan (GAG) characterized by alternating uronic acid (iduronic (IdoA) or glucuronic (GlcA) acid) and D-glucosamine units (GlcNAc). The chains are covalently linked to specific core proteins, and the composite structures are called proteoglycans. Mammals express at least 17 different proteoglycan core proteins. These are divided into three different subfamilies. The membrane spanning proteoglycans include four syndecans, betaglycan and CD44v3, and six glycophosphatidylinositol (GPI) linked membrane proteoglycans called glypicans. There is also a group of secreted or extracellular matrix (ECM) proteoglycans that include agrin, collagen XVIII, perlecan, and serglycin. In addition, several minor species are expressed in a tissue specific manner (Esko and Lindahl, 2001). Extreme heterogeneity of heparan sulfate arises by modification of the sugar backbone, including substoichiometric epimerization of D-GlcA to L-IdoA, N-deacetylation and N-sulfation of GlcNAc units, and O-sulfation of both glucosamine residues and uronic acids (Esko and Lindahl, 2001). Consequently, the composition of heparan sulfate can vary widely among different tissues giving rise to unique binding sites for various ligands such as growth factors, morphogens, and matrix proteins (Rapraeger et al., 1991).

The structure of heparan sulfate depends on the action of multiple glycosyltransferases and sulfotransferases. Synthesis begins in the Golgi apparatus

with the assembly of a linkage tetrasaccharide on serine residues on the proteoglycan core protein. The initiating reaction is the addition of xylose by one of two xylosyltransferases (XYLT) to specific sites found on the core protein defined by Ser-Gly residues flanked by one or more acidic amino acids (Zhang et al., 1995). Two galactose residues are subsequently added by galactosyltransferases, and this linkage region is variably sulfated. Then one or more GlcNAc transferases (GLCAT) add a single α1,4-linked GlcNAc unit to the chain, committing it toward the assembly of heparan sulfate. Polymerization occurs by alternating addition of GlcAβ1,4 and GlcNAcα1,4 residues under control of the EXT1/EXT2 co-polymerase. As the chain grows, it undergoes a series of modifications that include GlcNAc N-deacetylation and N-sulfation, uronic acid epimerization of glucuronic acid to iduronic acid, and variable O-sulfation (Esko and Lindahl, 2001). Four N-deacetylase/N-sulfotransferase isozymes (NDST 1-4) exist that vary in their relative ratios of N-deacetylase and N-sulfotransferase activity as well as in their expression in different tissues. NDST enzyme action is necessary for any further enzyme modification (epimerization or O-sulfation) to the heparan sulfate chain. The C5 epimerase (HSGLCE) has one family member that catalyzes the stereoisomeric transition form glucuronic acid to iduronic acid. The glucosaminyl 6-O-sulfotransferase (HS6ST) catalyzes the addition of a sulfate to the C6 position of GlcNAc. There are three known HS6STs that are expressed in a tissue specific manner. The glucosaminyl 3-O-sulfotransferase (HS3ST) catalyzes the addition of a sulfate to the C3 position of GlcNAc. There are seven HS3ST enzymes that catalyze a similar reaction with different substrates.

Lastly, the 2-O-sulfotransferase (HS2ST) enzyme has only one family member that catalyzes the addition of a sulfate to the C2 position of iduronic acid. This enzyme can also add sulfate to the C2 position of glucuronic acid. These are the enzymes active in heparan sulfate formation in vertebrate cells (Figure 1-1). Lower organisms such as *Drosophila melanogaster* and *Caenorhabditis elegans* also express heparan sulfate proteoglycans but have fewer total proteoglycans and less isozymes for modification of the heparan sulfate chain (Selleck, 2001).

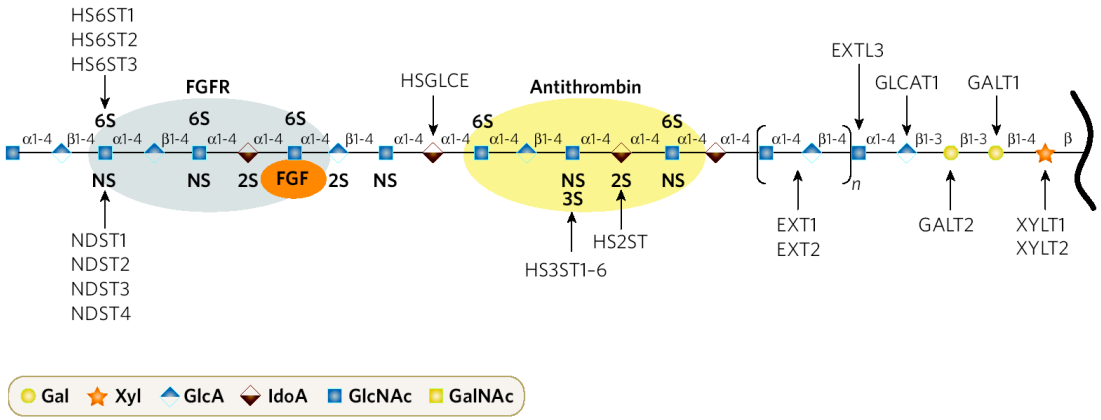

Figure 1-1: Assembly of heparan sulfate and formation of binding sites for ligands. At least 26 enzymes participate in the formation of a fully modified heparan sulfate chain. The modifications include the addition of a sulfate group to different dissacharides that impart a negative charge to the chain. The pattern of negatively charged sulfates and uronic acids creates binding sites for various protein ligands. Figure reprinted from (Bishop, 2007).

1.2 Many Growth Factors Bind to Heparan Sulfate

Cell surface heparan sulfate proteoglycans bind growth factors and extracellular matrix (ECM) proteins (Bernfield et al., 1999). Cellular events associated with heparan sulfate include cell-cell adhesion, cell-extracellular matrix adhesion, growth factor, cytokine, and chemokine action, lipoprotein internalization and clearance. Many growth factors including fibroblast growth factor (FGFs) (Rapraeger et al., 1991), (Yayon et al., 1991), hepatocyte growth factor (HGF) (Zioncheck et al., 1995), heparin binding epidermal growth factor (HB-EGF) (Aviezer and Yayon, 1994), Wnts (Lin and Perrimon, 1999; Reichsman et al., 1996; Tsuda et al., 1999), bone morphogenetic proteins (BMPs) (Jackson et al., 1997b; Ruppert et al., 1996), and a number of interleukins have been found to bind to heparin (Taipale and Keski-Oja, 1997) and/or interact directly with heparan sulfate proteoglycans. Binding could have many functions including; localization of a growth factor to the cell surface, sequestration of a growth factor in the ECM, or increasing the affinity of the ligand for its receptor, as has been shown for HGF and its receptor, Met, and FGFs (Sakata et al., 1997) (Najjam et al., 1998). Interaction with heparan sulfate may shield the growth factor from proteolytic degradation, which could result in a considerably longer half-life.

Although much is known about binding and receptor activation from *in vitro* studies, the role of heparan sulfate *in vivo* is very poorly understood. Recent advances in gene knockout technology have helped to shed some light on the role of heparan sulfate in development. Mice deficient in heparan sulfate tend to exhibit an early

embryonic lethality. For example, systemic deletion of *Ext1* or *Ext2* (heparan sulfate co-polymerase) results in early embryonic death (E6-7) due to failure to form mesoderm during gastrulation. These embryos show reduced Indian hedgehog signaling (Lin et al., 2000), (Stickens et al., 2005). Heterozygotes in either gene exhibit ectopic bone growth (exostoses), coupled with cartilage abnormalities. Deletion of the gene encoding heparan sulfate GlcNAc N-deacetylase/N-sulfotransferase-1 (*Ndst1*), one of a family of four enzymes involved in the initial sulfation of the heparan sulfate chains, leads to perinatal lethality with lung, brain and skeletal defects (Fan et al., 2000; Grobe et al., 2005; Ringvall et al., 2000). The lungs exhibit atelectasis, a collapsing of the lung due to an increased glycogen content in type II pneumocytes and a reduced number of microvilli. The forebrain defects include cerebral hypoplasia, lack of olfactory bulbs, eye defects and axon guidance errors. These phenotypes correlate well with mutant animals with impaired Sonic hedge hog and FGF signaling. Deletion of two other modifying enzymes, uronyl 2-O-sulfotransferase (*Hs2st*) and the glucuronyl C5 epimerase (*Hsglce*), causes perinatal death due to kidney agenesis. The relevant growth factor in this system may be GDNF (Bullock et al., 1998; Li et al., 2003; Merry et al., 2001).

Some systemic genetic modifications to the heparan sulfate chain are tolerated. The systemic deletion of *Ndst2* (Forsberg et al., 1999; Humphries et al., 1999) in mice manifests as a deficiency in connective-tissue-type mast cells. These cells typically make heparin (a highly sulfated form of heparan sulfate) and loss of *Ndst2* results in undersulfated chains. Most mammalian cells express both *Ndst1* and *2*, and the loss of

Ndst2 is compensated by *Ndst1* as no change in the heparan sulfate composition occurs in most tissues. The systemic deletion of xylosyltransferase-2 (one of a family of two enzymes that catalyzes the addition of xylose to the core protein) also has a mild developmental phenotype. These animals mature normally, but then develop polycystic kidney and liver disease which includes renal tubule dilation and biliary epithelial cysts (Condac et al., 2007). This is probably another example of compensation as one would predict a complete loss of xylosyltransferase activity would lead to the absence of both heparan and chondroitin sulfate, and early arrest of embryonic development. These knockout animals show that sulfated GAGs are essential for embryonic development and physiology.

Conditional knockouts of heparan sulfate biosynthetic genes have revealed specific roles for heparan sulfate in mammalian physiology. Mice lacking *Ndst1* specifically in endothelial cells and leukocytes develop normally, but show impaired neutrophil infiltration during inflammation due to altered rolling velocity correlated with weaker binding of L-selectin. Chemokine trancytosis and presentation on the endothelial cell surface is also reduced (Wang et al., 2005). Mice deficient in *Ndst1* specifically in hepatocytes are viable and healthy, but accumulate triglyceride rich lipoprotein particles, indicating that heparan sulfate plays a crucial role in clearance of hepatic lipoprotein particles (MacArthur et al., 2007). These experiments show that heparan sulfate plays specific roles in organ function as well as development.

1.3 Branching Morphogenesis

Various organs rely on ductal branching, including the lung, kidney, pancreas, salivary gland, lacrimal gland, and mammary gland (Figure 1-2). These branches are a system of highly organized epithelial tubular networks that transport gases or fluids and serve to increase the utilized surface area within an organ (Affolter et al., 2003). The development of a branched epithelial organ begins with the formation of an epithelial anlage, or bud, from an epithelial sheet. Invagination and budding are followed by branch initiation and outgrowth. This process is repeated until the organ is spatially organized with arborized tubules. The amount and complexity of branching depends on the organ. Finally, differentiation of organ specific structures and functions occurs, that are as varied as oxygen transfer in the lungs and milk production and delivery in the mammary gland (Affolter et al., 2003). That these processes depend on heparan sulfate is not surprising since heparan sulfate is a major component of basement membranes, which coordinates the interactions between stroma and epithelia and signaling events between numerous growth factors and their receptors.

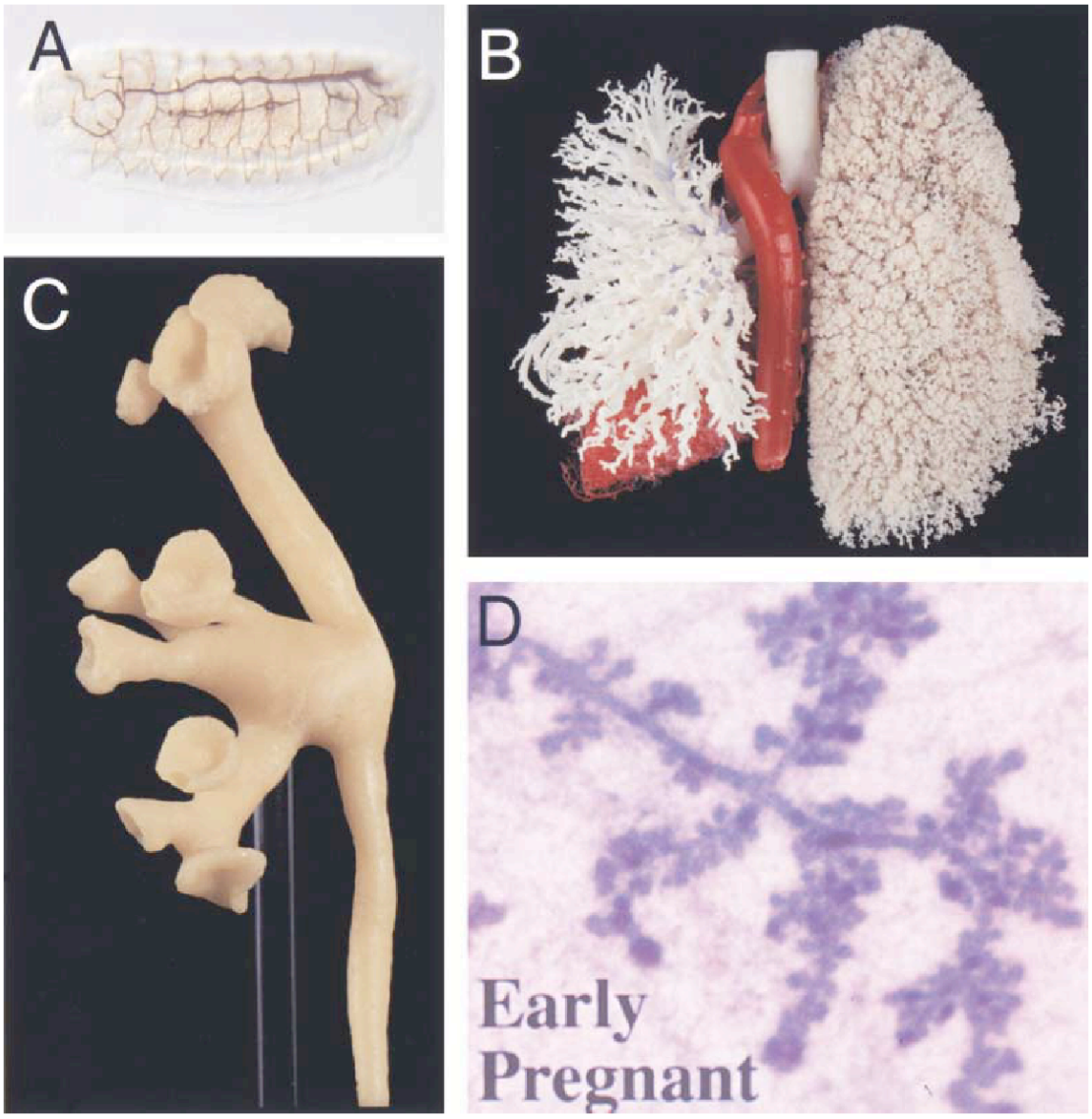

Figure 1-2: Multiple organs rely on branching morphogenesis. (**A**) The Drosophila trachea at a stage 15 embryo. (**B**) Preparation of a human lung with acryl polyester. (**C**) The branched collecting duct of the adult kidney. (**D**) Mammary gland branching at early pregnancy. Figure reprinted from (Affolter et al., 2003).

1.4 Heparan Sulfate, Tracheal Branching, and Lung Development

Embryonic and larval tracheal branching in *Drosophila melanogaster* serves as a simple model of branching morphogenesis and give insight into mammalian epithelial tubulogenesis as occurs in the lung and mammary gland. Both tracheal branching and mammalian branching morphogenesis develop epithelia lined tubules with a luminal spaces designed for the movement of air or biological fluids.

Drosophila tracheal branching begins from a single, 80 cell, epithelial sac. Six primary branches migrate from each sac, followed by secondary and tertiary branching (Ghabrial et al., 2003). The branches consist of an epithelial monolayer surrounding a central lumen. This process is in part controlled by the expression of two genes, *breathless* (btl)/FGFR and *branchless* (bnl)/FGF. Btl/FGFR is expressed on the epithelial cells while bnl/FGF is expressed in cells surrounding the tracheal placode. Mutant flies in either of these genes show a complete failure in tracheal branching (Klambt et al., 1992; Reichman-Fried et al., 1994).

Heparan sulfate facilitates signaling between FGF and the FGF receptor. Drosophila deficient in two genes critical to heparan sulfate formation, *sugarless* (UDP-D-glucose dehydrogenase) and *sulfateless* (N-deacetylase/N-sulfotransferase (Ndst)), show a similar, though less severe phenotype, in that tracheal branch formation is incomplete (Lin et al., 1999). These mutants show a deficiency in btl/FGF dependent downstream mitogen-activated protein kinase (MAPK) activation as well. Overexpression of *branchless* was able to partially rescue tracheal cell branching in both s*ulfateless* and *sugarless*. This is common to heparan sulfate/FGF interactions

that an increase in ligand overcomes the requirement for the low affinity co-receptor (heparan sulfate).

Drosophila deficient in heparan sulfate 6-O-sulfotransferase (*dHs6st*) gene, also have tracheal branching defects. RNAi interference of dHS6ST causes reduced enzyme activity and leads to stalled tracheal branches and migration defects (Kamimura et al., 2001). Mimicking both sugarless and sulfateless, the *dHs6st* deficient fly shows a reduction in FGF-dependent mitogen activated protein kinase activation. Thus, one of the necessary signaling components in the FGF/heparan sulfate complex is the addition of a 6-o-sulfate modification to the heparan sulfate chain. Other studies show that the binding of FGF to heparan sulfate does not depend on 6-O-sulfate groups, but binding of the receptor does. Recent work on both the Hs6st and the Hs2st Drosophila mutants show a compensatory increase of sulfation at other positions in response to the mutations, which maintains the overall level of heparan sulfate charge. These findings suggest that in Drosophila, the overall sulfation level is more important than defined heparan sulfate modifications (Kamimura et al., 2006), and it is clear that heparan sulfate is critical to tracheal branching.

Branching morphogenesis in the mammalian lung shares many similarities with tracheal branching in Drosophila. Lung morphogenesis includes dichotomous branching from the tips of large ducts and is dependent on cell proliferation and migration (Chuang and McMahon, 2003). Lung development begins with the formation of two respiratory progenitors (lung and trachea) from the ventral foregut endoderm at E9. Two endodermal lung buds invade the adjacent mesoderm and form

primary buds. Secondary buds arise as outgrowth from the primary buds. Between E10.5 and E17 the epithelium undergoes ductal branching, including bud outgrowth and dichotomous subdivisions at the branch points(Cardoso and Lu, 2006).

Several growth factors are known to be involved in branching morphogenesis of the lung, including Hedgehog, FGFs, and Wnt. In the FGF family, there are four ligands expressed in the lung; FGF 1, 7, 9 and 10. (Chuang and McMahon, 2003). Knockout models have shown that FGF10 and its receptor FGFR2b are critical to branching morphogenesis in the lung. Genetic inactivation of either of these genes inhibits main stem bronchial development and pulmonary branching morphogenesis (Min et al., 1998), (Ohuchi et al., 2000).

3G10, an antibody to the heparan sulfate stub on a proteoglycan remains after heparinases treatment, strongly labeled airway basement membranes and the surrounding mesenchyme. EW4G27, a different antibody that recognizes a specific structural epitope on heparan sulfate chains, only stained airway basement membranes (Thompson et al., 2007). These findings suggest that the fine structure of heparan sulfate is altered in a cell type specific manner to coordinate growth factor action in the mammalian lung.

In order to explore the necessity for heparan sulfate in lung branching, *in vitro* models of branching morphogenesis have been examined. Branching morphogenesis of the lung can be partially modeled by culturing E11.5 lung explants for 72 hours with FGF-10. Culturing lung explants in FGF-10 containing medium plus sodium chlorate (25mM) (a heparan sulfate inhibitor) results in death within 24 hours. This is

similar to the effect of culture without FGF-10 (Izvolsky et al., 2003). In heparinase-III (an enzyme that cleaves heparan sulfate) treated lungs, branching morphogenesis is disrupted as well. Excess FGF-10 provided by an implanted bead can locally overcome the HS deficiency brought on by heparinase treatment.

Finally, the *Ndst1*-deficient mice show lung abnormalities. The *Hsglce*-deficient mutant also displays poorly inflated lungs, but detailed studies of the cells and relevant growth factors have not been done. By analogy to *Drosophila* tracheal development, lung epithelial branching morphogenesis and function presumably requires heparan sulfate to facilitate growth factor signaling and regulation.

1.5 Heparan Sulfate and Kidney Development/Function

Kidney branching morphogenesis is reminiscent of the other branching systems. Multiple growth factors interact with an epithelial layer to produce a tubular network through proliferation, remodeling, and branching. Kidney development begins with an epithelial tube called the Wolffian duct. An epithelial outgrowth forms from this duct called the ureteric bud (UB) that grows into the surrounding mesenchyme and produces the collecting duct system of the kidney through ductal branching. During each successive round of dichotomous branching, the number of ureteric bud tips doubles. The direction of this branching process is thought to be dictated by morphogenetic gradients of soluble factors (Pohl et al., 2000). The epithelium can be stimulated to branch by growth factors produced from the mesenchyme acting on the epithelium (paracrine) or from the epithelium producing its

own autocrine factors. A wide variety of growth factors implicated in kidney ductal branching including FGFs, transforming growth factor β (TGFβ) superfamily, glial cell derived neurotrophic factor (GDNF), pleiotrophin, BMPs, Wnt, and hedgehog, interact with heparan sulfate and can require this interaction for downstream signaling (Steer et al., 2004). The extracellular matrix and basement membrane between the cell layers may facilitate the molecular communication that regulates kidney ductal branching.

Sulfated GAGs are present in the glomerular basement membrane (GBM) (Kanwar and Farquhar, 1979). The GBM is the basal lamina that sits between the epithelial podocytes and the endothelia and is the actual site of filtration between the two cell layers. The sulfated GAGs were identified as heparan sulfate (Kanwar and Farquhar, 1979). The heparan sulfate proteoglycans were originally thought to impart an electric charge to the glomerular capillaries to restrict the passage of macromolecules.

Heparan sulfate proteoglycans have also been found in the kidney (Kanwar et al., 1984). Secreted ECM proteoglycans perlecan, agrin, and collagenXVIII are spatially and temporally regulated in the kidney. Agrin mRNA is prominent in the adult kidney, and seen at low levels in the fetal kidney (Groffen et al., 1998). Agrin accumulation is most prominent in the GBM but the Bowman's capsule, tubule and vascular basement membranes also stain positive. The presence of collagen XVIII has been confirmed by both Northern blot and immunohistochemical localization (Muragaki et al., 1995). Both syndecans and the glypicans are found in the

mesenchyme and embryonic epithelium (Kanwar et al., 2004). Array analysis confirms the presence of high expression of syndecan-1, and, glypican-1, 2 and 3 during early rat kidney development. The highest levels of expression are at E13-15, when initial ureteric bud branching takes place. Syndecan-2 and syndecan-4 are found to be highly expressed during late embryonic kidney development (Steer et al., 2004).

The function of heparan sulfate proteoglycans in renal development and function were initially studied using chemical inhibitors of sulfation. Embryonic kidneys dissected at E13 of embryonic development and placed in organ culture media, will go through a few rounds of ductal branching and some differentiation after seven days. These cultures contain both epithelia and mesenchyme. Organ explants treated with xylosides, an inhibitor of GAG attachment to the proteoglycan core protein, have a dramatic effect on explant development. Treated explants show loose interstitial matrix and a decrease in developing nephron elements with a poorly developed ureteric bud and only a few remnants of branches (Lelongt et al., 1988). Embryonic kidneys isolated from E11 and placed in an organ culture system display ureteric bud growth and successive branching that induces the formation of nephrons. Treatment with sodium chlorate, a PAPS (sulfate donor) inhibitor that reduces GAG chain sulfation, inhibits branching and growth but does not inhibit nephron formation (Davies et al., 1995). Treatment of E11 organ explants with heparitinase (an enzyme that cleaves heparan sulfate) exhibited a partial inhibition of ureteric bud branching.

Subsequently, a new model of ureteric bud branching has further helped to define the role of heparan sulfate in kidney branching. The UB can be isolated and

cultured in Matrigel/collagen extracellular matrix. This system only contains epithelia. When exposed to conditioned media, the isolated UB goes through extensive ductal branching (Steer et al., 2004). The three chemical inhibitors (chlorate, heparitinase, and xylosides) show severe effects on both the overall size and extent of UB branching (Steer et al., 2004). Further analysis shows that chlorate treatment diminished FGF-2 binding. Treated ureteric buds also show a diminished rate of proliferation (Steer et al., 2004).

Systemic genetic knock outs in heparan sulfate proteoglycans and biosynthetic enzymes have confirmed the role of heparan sulfate in kidney development. Glypican-3 (*Gpc3*) deficient animals show kidney abnormalities. Induction of ureteric bud branching is normal, however overgrowth of ureteric ductal branching is seen. This overgrowth is accompanied by an increase in ureteric bud cell and collecting duct cell proliferation (Cano-Gauci et al., 1999). Further analysis showed that medullary cell proliferation was decreased, coupled with an increase in apoptosis, and BMP and FGF7 signaling is modulated in an *in vitro* model. Thus the removal of one proteoglycan in both the epithelia and stroma caused hyperbranching. In contrast to these results, inactivation of both the *Hs2st* and *Hsglce* led to the complete loss of kidney ductal branching. However, in both glypican-3 and the biosynthetic mutants, it is not known whether this is due to stromal or epithelial effects. These examples show that determining the biological role of heparan sulfate in branching morphogenesis has to consider the contribution of the stromal and epithelial heparan sulfate, the

proteoglycans that are present, their spatial and temporal characteristics, and the specific sulfation pattern on the HS chains.

1.6 Heparan Sulfate and Mammary Gland Development/Function

Unlike the lung and kidney, most of mammary gland development occurs postnatally. At birth, the mammary fat pad (stroma consisting of adipocytes, fibroblasts and immune cells) holds a rudimentary ductal structure of approximately 10 branches connected to an exterior nipple. This gland remains quiescent until the beginning of the mouse estrous cycle at about 4 weeks in age. Ovarian hormones induce rapid branching that fills the entire fat pad with arborized ductal epithelia by 10 to 12 weeks of age. At this time, the gland is capable of differentiating into a milk producing structure with the onset of pregnancy (Figure 1-3).

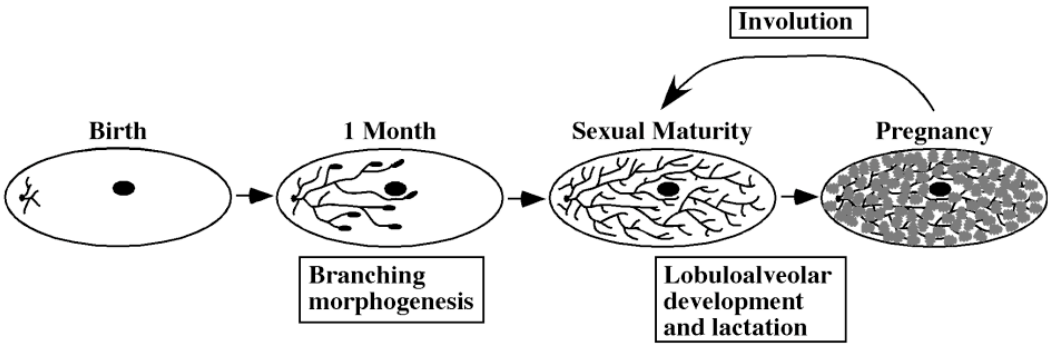

Figure 1-3: Picture representation of mammary epithelial branching. Pubertal ductal branching begins with a small ductal tree. At the start of the estrous cycle (4 weeks), epithelial ductal branching fills the mammary fat pad. The gland sits quiescent at sexual maturity until pregnancy, where new sets of hormones induce lobuloalveolar development and lactation. Upon weening, the gland involutes back to a state of sexual maturity. Figure adapted from thesis by Dr. Brett Crawford.

Epithelial ductal branching in the mouse mammary gland is facilitated by a bulbous cellular structure known as the terminal end bud (TEB). These form at the ends of growing epithelial branches. TEBs consist of an outer layer of bipotent stem cells that proliferate into the mammary fat pad creating a layer of myoepithelia, which constitutes the outer layer of the ducts. The inner layer of the TEB consists of body cells that apoptose to form the lumen inside the duct (Figure 1-4). The myoepithelia lay down a thick basement membrane that surrounds the branched ductal structures. A thick layer of stroma sits along the neck of the light bulb-shaped terminal end bud, and may play a role in stability and direction of growth. Secondary branching can occur along previously formed ductal branches. This coordinated process of ductal bifurcation and branching fills the gland with a spatially regulated ductal structure. The arborized branches are far enough apart to allow for the additional branching and lobuloalveolar formation that happens during pregnancy.

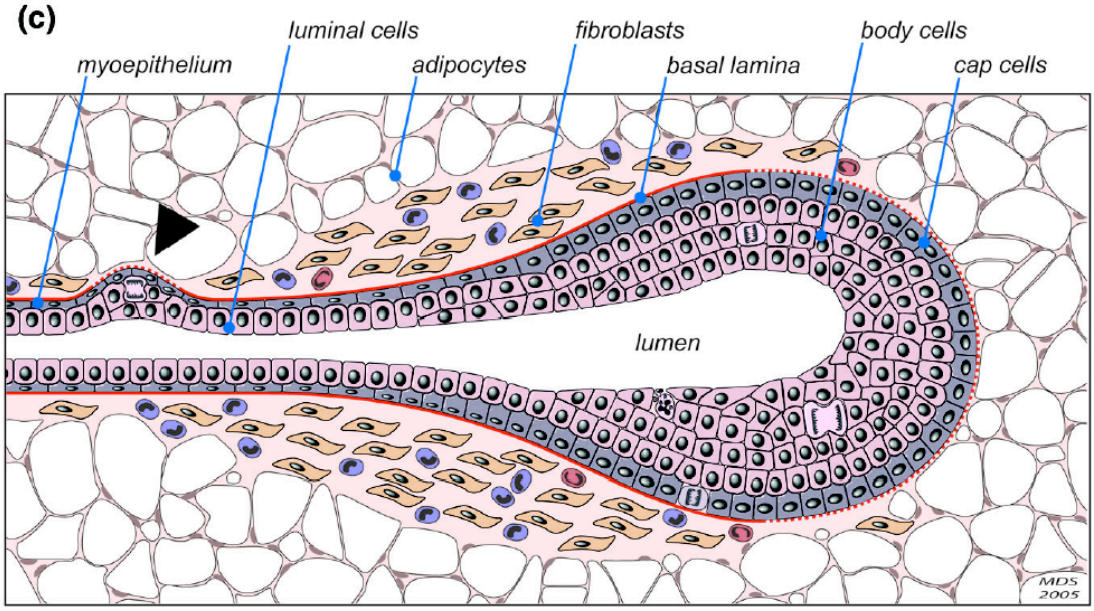

Figure 1-4: Schematic diagram of a mammary epithelial terminal end bud. This picture depicts a bilayered duct with a central lumen connected to a terminal end bud composed of cap cells and body cells. A thick stroma surrounding the neck region of the terminal end bud consists of fibroblasts and immune cells. Adipocytes shown in white compose the rest of the stroma. The large black arrow head points to the beginning of a side branch. Figure reprinted from (Sternlicht, 2006).

Sulfated GAGs are found associated with the basement membrane of epithelial tubes. The posterior regions of TEBs are sites of intense sulfated GAG synthesis. GAGs are also found in the stroma between ducts (Gordon and Bernfield, 1980; Silberstein and Daniel, 1982).

Pubertal growth of the mammary epithelial ductal tree is regulated by endocrine hormones. Estrogen is the primary hormone that promotes ductal epithelial branching, but genetic studies have shown that glucocorticoid and growth hormone are involved in primary branching, while progesterone is involved in side branching (Howlin et al., 2006). The steroid-receptor expressing cells in the mammary gland are found in the stroma adjacent to the epithelia. This means that endocrine hormones act via a release of local growth factors by the stroma that act in a paracrine nature on the epithelia. These growth factors include insulin like growth factor (IGF), FGFs, epidermal growth factor (EGFs), TGFβ, HGF, and others. This relay system has been eloquently shown by looking at the knockout phenotypes of growth hormone and its direct local growth factor, IGF. The addition of IGF to the growth hormone knockout in the mammary gland reestablished ductal branching (Ruan and Kleinberg, 1999).

1.7 Heparan Sulfate/FGF and Mammary Gland Development/Function

The FGF family of growth factors are spatially and temporally regulated during branching morphogenesis. FGF-1, FGF-2 and FGF-7 are highly expressed during branching and produced by the stroma (Coleman-Krnacik and Rosen, 1994). FGF-10 is expressed during mammary placode formation (Mailleux et al., 2002).

FGFs signal through tyrosine kinase receptors known as FGFRs and a single FGF can bind to multiple FGFR family members. There are four different receptor genes, FGFR1-4 that encode multiple isoforms. Members of the FGFR family are localized to the epithelia of the mammary gland (Plath et al., 1998).

Estrogen treatment of pubertal animals have shown an increase in FGF-7 mRNA levels (Pedchenko and Imagawa, 2000). This experiment suggests that FGFs could serve as a messenger between hormones and epithelia. Genetic manipulation of FGF family members and receptors has served to help explain their role in mammary gland biology. Single family member knock outs of FGF-2 or FGF-7 have no aberrant mammary phenotype, which could be due to signaling compensation by other FGF family members (Dono et al., 1998; Guo et al., 1996). FGF-10 and FGFR2b have been shown to be required for early mammary gland biology, but their role in pubertal branching is unknown (Mailleux et al., 2002). Dominant negative expression of FGFR2(IIIb) (a receptor for a number of FGF family members) causes an inhibition of lobuloalveolar development during pregnancy that manifests as an underdeveloped ductal tree with fewer alveoli (Jackson et al., 1997a). These experiments show that FGFs play a role in mammary gland development, but single growth factor knockouts may not be an effective strategy in determining the exact role of FGFs in mammary gland development.

The interaction of FGFs with FGFRs has been shown to involve heparan sulfate. FGF-2 is localized to the heparan sulfate in basement membranes (Rudland et al., 1993). Interactions with heparan sulfate is thought to increase the affinity between

growth factor and receptor, protect growth factors from degradation, regulate diffusion through tissue and possibly create a storage depot for later release (Bernfield et al., 1999; Delehedde et al., 2001; Lander et al., 2002). These interactions have been well characterized in multiple systems. In mammary gland biology, the interaction between FGF, FGFR, and heparan sulfate may be crucial for mammary epithelial development.

1.8 Heparan Sulfate/EGF and Mammary Gland Development/Function

The EGF family of growth factors including EGF, TGFα, and amphiregulin (AR) are all expressed during ductal branching (Snedeker et al., 1991), (Kenney et al., 1995). HB-EGF (another EGF family member) is known to bind to EGF receptors implicated in mammary gland development (Stern, 2003). EGF family members signal through the ErbB family of receptor tyrosine kinases. The four ErbB receptors display a dynamic expression and phosphorylation pattern depending on the stage of mammary gland development (Schroeder and Lee, 1998).

Multiple *in vitro* and *in vivo* experiments suggest that EGF family members and receptors are critical to mammary gland development. Retrovirally transduced mammary transplants that overexpress AR develop overgrown tertiary ducts and increased lateral branching (Kenney et al., 1996) suggesting that EGF family members are involved in ductal branching. Mice lacking AR exhibit severely stunted ductal growth but still maintain the capacity for lobuloalveolar development. Single knockouts of the other EGF ligand family members do not produce mammary phenotypes. Mice lacking EGF or TGFα also do not show no mammary phenotype.

Systemic knockout of HB-EGF were uninformative, because the mice die shortly after birth (Jackson et al., 2003). A triple null animal for EGF, AR, TGFα exhibit a more severe defect showing irregular alveolar morphology with undifferentiated epithelia (Luetteke et al., 1999). This experiment suggests that branching depends on multiple growth factor action.

Another method of analyzing the role of EGF growth factors in mammary development is to target the receptors that often interact with more than one ligand. Mammary targeted expression of a dominant negative EGFR causes a reduction in ductal branching and a smaller mammary fat pad (Xie et al., 1997). Analysis of the null EGFR animal was uninformative because the animals die perinatally. To avoid this problem transplantation methods were employed to show that EGFR is essential in the stroma to support mammary epithelial ductal branching, but is dispensable on the surface of the epithelium. Wildtype epithelia can not grow in a fat pad devoid of EGFR (Wiesen et al., 1999). ErbB2 (another EGF receptor) deficient epithelia exhibit a penetration defect in which the epithelial tree advances slowly through the mammary fat pad (Jackson-Fisher et al., 2004). These experiments provide genetic proof that the interactions between EGF family members and receptors play an important role in mammary gland development.

Some of the interactions between EGF ligands and receptors are regulated by heparan sulfate. While EGF signals without the assistance of heparan sulfate, both amphiregulin and HB-EGF are known to interact with heparan sulfate proteoglycans. Amphiregulin can induce growth in lung epithelia, and this interaction is disrupted by

treatment with a heparan sulfate degrading enzyme (Schuger et al., 1996). HB-EGF, unlike EGF or TGFα, binds strongly to heparin (Raab and Klagsbrun, 1997) and HB-EGF stimulation of smooth muscle cell migration is dependent on heparan sulfate (Higashiyama et al., 1993). These experiments suggest that the interaction between EGF family members and heparan sulfate may be critical for mammary development.

1.9 Heparan Sulfate/TGF-β and Mammary Gland Development/Function

Another growth factor that is spatially and temporally regulated throughout mammary gland development is TGF-β. Early studies revealed overlapping expression patterns of TGF-β1, 2, and 3 during pubertal ductal branching. Localization studies confirm the presence of mature TGF-β1 along the mammary epithelium. In order to determine the role of TGF-β in ductal branching, slow release pellets containing either of the three TGF-β isoforms were implanted into a mammary fat pad. TGF-β release inhibited mammary ductal elongation (Robinson et al., 1991). Upon closer examination, it was found that ductal structures, in which budding is inhibited, show mature TGFβ in the basement membrane. In all areas of ductal growth including terminal end buds and lateral branches, there is an inhibition of TGF-β1localization (Silberstein et al., 1992). These studies confirm that TGF-β1 acts as an inhibitor of growth.

Evidence confirming the inhibitory role of TGF-β has been obtained in vivo by examining mutant and transgenic mice. Mice overexpressing TGF-β1 show a

reduction in total ductal tree volume, but lactation is unaffected (Pierce et al., 1993). Transgenic mice that overexpress a dominant negative form of the TGF-β type II receptor show a loss of responsiveness to TGF-β1 with an increase in lateral branching (Joseph et al., 1999). Conditional knock outs of the type II TGF-β receptor gene in mammary epithelia exhibit lobuloalveolar hyperplasia, but this phenotype regresses after 20 weeks (Forrester et al., 2005). These experiments suggest that TGF-β is an important inhibitor of ductal growth, but may not be the only inhibitor expressed in ductal branching.

TGF-β1 signaling and interactions with the ECM could be mediated by heparan sulfate proteoglycans. TGF-β family members bind to both heparin and highly modified heparan sulfate (Lyon et al., 1997). Betaglycan, a membrane bound proteoglycan, is referred to as the type III TGF-β receptor (Massague and Chen, 2000). Syndecan-2 has been found to regulate the TGF-β dependent increase of matrix deposition in vitro. These findings suggest that heparan sulfate proteoglycans could play a role in TGF-β action, and that interaction may be important for mammary development.

1.10 Heparan Sulfate/HGF and Mammary Gland Development/Function

HGF (hepatocyte growth factor) is a growth factor that signals through the Met tyrosine kinase receptor. The HGF-Met interaction has been implicated to play an important role in mammary epithelial morphogenesis. In early embryonic studies, HGF is found expressed by mesenchymal cells, and Met is found in the proximal

epithelia (Sonnenberg et al., 1993). HGF and Met are also found to be expressed in mouse mammary tissue. Their expression is temporally regulated; the genes are expressed during virgin branching morphogenesis (6 weeks) and during the process of ductal hyperbranching found in the early stages of pregnancy (Niranjan et al., 1995). Mouse mammary fibroblasts produce HGF, while c-met is expressed on both luminal and myoepithelia.

In vitro branching models have shown that HGF-Met may be able to facilitate ductal branching. HGF is able to induce tubular branching morphogenesis in TAC-2 clonal human mammary epithelia cells plated in a collagen matrix (Soriano et al., 1998) and EpH4 clonal mouse mammary epithelial cells plated in Matrigel (Niemann et al., 1998), (Berdichevsky et al., 1994). HGF treatment of primary mouse mammary epithelia induces tube formation in collagen gels (Kamalati et al., 1999). Finally, organ culture reveals that HGF treatment is able to induce intensified growth resulting in numerous main ducts. Expression of antisense oligonucleotides to HGF blocks ductal branching of the glands (Yang et al., 1995). *In vivo* overexpression studies of HGF induces a range of alterations in the virgin mammary gland. Transgenic overexpression of HGF in the whole animal induces a broad range of epithelial tumors including mammary tumors (Takayama et al., 1997). Transplanted epithelia, virally overexpressing HGF, affects the structure and multiplicity of terminal end buds, resulting in a more highly branched gland (Yant et al., 1998). These results suggest that HGF plays a role in ductal branching *in vivo*. Whole animal knockout models

have not been informative since systemic HGF and Met knockout animals exhibit incomplete development and die *in utero* (Bladt et al., 1995; Schmidt et al., 1995).

The interaction of HGF and Met may be facilitated by heparan sulfate proteoglycans. *In vitro*, heparin increases the mitogenic action of HGF and causes the oligermization of HGF (Zioncheck et al., 1995), which may facilitate interaction with Met. Basic clusters found in HGF facilitate the interaction between HGF and heparin (Mizuno et al., 1994). HGF also interacts with heparan sulfate, and the interaction requires a sequence containing iduronic acid and 6-O-sulfate modifications, differentiating it from the FGF-heparan sulfate interaction (Lyon et al., 1994). Addition of heparin to heparan sulfate-deficient CHO cells restored HGF signaling through Met tyrosine phosphorylation (Sakata et al., 1997). Met has also been found to interact with heparan sulfate (Rubin et al., 2001). Chlorate (sulfation inhibitor) treatment of renal epithelia inhibits HGF binding to the cell surface and diminishes HGF dependent downstream signaling (Deakin and Lyon, 1999). Taken cumulatively, this data suggests heparan sulfate facilitates the interaction between HGF and Met and this may be crucial to mammary gland development

1.11 Heparan Sulfate/ECM and Mammary Gland Development/Function

What precedes is a list of growth factors relevant to mammary gland function that have known heparan sulfate interactions, but this is not an exhaustive list. Other growth factors in mammary gland biology include Wnts, which also bind to heparan sulfate. Recent studies demonstrate that altering 6-O-sulfation of heparan sulfate has a

positive influence on Wnt signaling (Ai et al., 2003). The interaction of stromally produced growth factors with the epithelial surface is regulated by the extracellular matrix contained in the basement membrane. This basement membrane contains proteoglycans, collagens, laminin, integrins and ECM degrading proteinases including matrix metalloproteinases (MMPs). Both integrins and MMPs can interact with heparan sulfate and play important roles in mammary gland biology.

ECM remodeling of the basement membrane has been suggested to be important in ductal branching. An advancing epithelial duct would need to be able to alter its immediate environment to facilitate movement. One key family of players in this process are basement membrane degrading matrix metalloproteinases (MMPs). These enzymes, including stromelysin-1, 3, and gelatinase A, are expressed during ductal branching (Witty et al., 1995). MMP-2 is concentrated in the stroma with a reduction in expression around growing branch points. MMP-3 is also found in the stroma but shows no difference around sites of branch initiation (Wiseman et al., 2003). These experiments suggest that MMP expression is dynamically regulated during ductal branching. Mammary glands treated with a broad chemical inhibitor of MMP activity show a reduction in terminal end bud number and a lack of fat pad invasion. Targeted expression of stromelysin-1 (MMP) in rat mammary glands leads to hyperbranching and precocious alveolar development during pubertal branching (Sympson et al., 1994). MMP2 mutant animals exhibit retarded invasion of mammary ducts showing twice as much apoptosis in terminal end buds as the wildtype counterparts. These mutant animals also show an increase in lateral buds. MMP3

deficient animals show a reduction in the frequency of branching and total number of branch points (Wiseman et al., 2003). Presumably, MMPs act by helping to reshape the ECM in front of an advancing TEB, and make progression through the gland easier.

MMP-2, -7, -9 and –13 all bind to heparin (Yu and Woessner, 2000). Heparan sulfate proteoglycans can act as extracellular docking molecules for MMPs. Matrilysin (MMP7) co-localizes with heparan sulfate in uterine glandular epithelial cells. Finally, CD44 heparan sulfate proteoglycan recruits MMP-7 and HB-EGF to the lactating mammary epithelium and this process is disrupted in a CD44 deficient animal having a dramatic effect on lactation (Yu et al., 2002). Thus one way heparan sulfate regulates mammary gland biology is through interaction with MMPs.

Integrins are heterodimers composed of an α and a β subunit that interact with growth factor receptors. These proteins are transmembrane adhesive receptors that transmit signals from the ECM to the cell to coordinates cytoskeletal rearrangement and cell movement. Previous experiments suggest that integrins are involved in mammary gland development. Implanted pellets containing function blocking antibodies to β1 integrin reduce the number of end buds per gland and the extent of ductal branching (Klinowska et al., 1999). Mice expressing a dominant negative form of β1 integrin show reduced mammary epithelial cell proliferation and increased apoptosis during lactation (Faraldo et al., 2001). Mice deficient in α2β1 integrins show a reduction in branching complexity during pubertal branching (Chen et al., 2002). While the phenotypes in these animals are not overly dramatic, they show that

integrins play a role in mammary development, but there may be compensation based on the large numbers of different integrins. Integrins cooperate with heparan sulfate proteoglycans to facilitate adhesion (Coombe et al., 1994), (Diamond et al., 1995).

1.12 Genetic Manipulation of Heparan Sulfate Proteoglycans and Mammary Gland Development/Function

Previous genetic evidence in the mammary field supports a role for heparan sulfate in mammary gland development. Mammary glands of transgenic mice overexpressing a human heparinases (degrades heparan sulfate) show hyperbranching and precocious alveolar development (Zcharia et al., 2001) suggesting that cell surface heparan sulfate chains help to regulate the space found between ductal branches. Mutants lacking syndecan-1, a cell surface proteoglycan found on mammary epithelial cells, show reduced mammary gland branching and have a 50% reduction in terminal end buds during pubertal branching suggesting that this proteoglycan is partially involved in terminal end bud formation (Liu et al., 2004). Both of these mutants are systemic, affecting both the stroma and the epithelia in the mammary gland. The question still remains whether epithelial heparan sulfate is critical for mammary ductal branching. Mutants lacking other proteoglycans either die embryonically, or do not display severe mammary phenotypes. Multiple proteoglycans are expressed in mammary epithelia. Thus, it is possible that dramatic effects on mammary gland branching are not exhibited in single proteoglycan knock out animals due to compensation by other proteoglycans. This thesis clearly defines the importance of

heparan sulfate in mammary gland ductal branching and demonstrates selective changes in development dependent on structural attributes of the chains.

1.13 Conclusions

The mammary gland represents a unique system for the study of epithelial ductal branching. Since the majority of mammary development occurs postnatally, the system imparts some advantages including work on adult animals and transplantation. Mammary gland development has been well characterized using a large number of knockout animals, and important roles for many growth factors and extracellular matrix components have been proven. Many, if not all, of these factors bind to heparan sulfate proteoglycans or heparin. Therefore, it is likely that endogenous heparan sulfate plays a critical regulatory role in mammary epithelial branching and development. This hypothesis is consistent with previous data from other branching systems, including the *Drosophila* trachea, and mammalian lung and kidney.

Earlier work in mammary gland biology has confirmed the presence of sulfated GAGs in mammary development. Surviving mice deficient in single proteoglycans did not show overt mammary phenotypes, probably due to the fact that multiple families of proteoglycans exist in the mammary gland. A better strategy to study heparan sulfate *in vivo*, would be to target the biosynthetic machinery responsible for glycan addition and sulfation.

Mice systemically deficient in heparan sulfate biosynthetic enzymes and core proteins reveal the requirements of specific mutations in embryonic and organ

development. However, many of these mutant animals display phenotypes that precede mammary gland development, and therefore they are uninformative. In this thesis, conditional knockouts of biosynthetic enzymes have been prepared. Mammary epithelial specific alterations of any gene was accomplished through tissue specific deletion of genes using Cre-loxP system (Wagner et al., 1997)(Wagner et al., 2001). Transgenic mice that express the Cre recombinase specifically in mammary epithelia before ductal branching (MMTV Cre) were used. This system allows for a structure/function analysis of heparan sulfate in the mammary gland. It also permits one to distinguish between epithelial cell versus stromal effects.

In chapter 2 we show that epithelial heparan sulfate is critical to mammary ductal branching by altering the polymerization or overall sulfation of the chain. Furthermore, small changes in chain sulfation lead to different ductal phenotypes. In chapter 4, we show that lobuloalveolar formation and milk production rely on Ndst1 expression. We believe an inefficient signaling, mediated by multiple growth factors, causes these phenotypes.

1.14 References

Affolter, M., Bellusci, S., Itoh, N., Shilo, B., Thiery, J. P., and Werb, Z. (2003). Tube or not tube: remodeling epithelial tissues by branching morphogenesis. Dev Cell *4*, 11-18.

Ai, X., Do, A. T., Lozynska, O., Kusche-Gullberg, M., Lindahl, U., and Emerson, C. P., Jr. (2003). QSulf1 remodels the 6-O sulfation states of cell surface heparan sulfate proteoglycans to promote Wnt signaling. J Cell Biol *162*, 341-351.

Aviezer, D., and Yayon, A. (1994). Heparin-dependent binding and autophosphorylation of epidermal growth factor (EGF) receptor by heparin-binding EGF-like growth factor but not by EGF. ProcNatlAcadSciUSA *91*, 12173-12177.

Berdichevsky, F., Alford, D., D'Souza, B., and Taylor-Papadimitriou, J. (1994). Branching morphogenesis of human mammary epithelial cells in collagen gels. J Cell Sci *107 (Pt 12)*, 3557-3568.

Bernfield, M., Gotte, M., Park, P. W., Reizes, O., Fitzgerald, M. L., Lincecum, J., and Zako, M. (1999). Functions of cell surface heparan sulfate proteoglycans. Annu Rev Biochem *68*, 729-777.

Bladt, F., Riethmacher, D., Isenmann, S., Aguzzi, A., and Birchmeier, C. (1995). Essential role for the c-met receptor in the migration of myogenic precursor cells into the limb bud. Nature *376*, 768-771.

Bullock, S. L., Fletcher, J. M., Beddington, R. S., and Wilson, V. A. (1998). Renal agenesis in mice homozygous for a gene trap mutation in the gene encoding heparan sulfate 2-sulfotransferase. Genes Dev *12*, 1894-1906.

Cano-Gauci, D. F., Song, H. H., Yang, H., McKerlie, C., Choo, B., Shi, W., Pullano, R., Piscione, T. D., Grisaru, S., Soon, S., *et al.* (1999). Glypican-3-deficient mice exhibit developmental overgrowth and some of the abnormalities typical of Simpson-Golabi-Behmel syndrome. JCell Biol *146*, 255-264.

Cardoso, W. V., and Lu, J. (2006). Regulation of early lung morphogenesis: questions, facts and controversies. Development *133*, 1611-1624.

Chen, J., Diacovo, T. G., Grenache, D. G., Santoro, S. A., and Zutter, M. M. (2002). The alpha(2) integrin subunit-deficient mouse: a multifaceted phenotype including defects of branching morphogenesis and hemostasis. Am J Pathol *161*, 337-344.

Chuang, P. T., and McMahon, A. P. (2003). Branching morphogenesis of the lung: new molecular insights into an old problem. Trends Cell Biol *13*, 86-91.

Coleman-Krnacik, S., and Rosen, J. M. (1994). Differential temporal and spatial gene expression of fibroblast growth factor family members during mouse mammary gland development. Mol Endocrinol *8*, 218-229.

Condac, E., Silasi-Mansat, R., Kosanke, S., Schoeb, T., Towner, R., Lupu, F., Cummings, R. D., and Hinsdale, M. E. (2007). Polycystic disease caused by deficiency in xylosyltransferase 2, an initiating enzyme of glycosaminoglycan biosynthesis. Proc Natl Acad Sci U S A *104*, 9416-9421.

Coombe, D. R., Watt, S. M., and Parish, C. R. (1994). Mac-1 (CD11b/CD18) and CD45 mediate the adhesion of hematopoietic progenitor cells to stromal cell elements via recognition of stromal heparan sulfate. Blood *84*, 739-752.

Davies, J., Lyon, M., Gallagher, J., and Garrod, D. (1995). Sulphated proteoglycan is required for collecting duct growth and branching but not nephron formation during kidney development. Development *121*, 1507-1517.

Deakin, J. A., and Lyon, M. (1999). Differential regulation of hepatocyte growth factor scatter factor by cell surface proteoglycans and free glycosaminoglycan chains. JCell Sci *112*, 1999-2009.

Delehedde, M., Lyon, M., Sergeant, N., Rahmoune, H., and Fernig, D. G. (2001). Proteoglycans: pericellular and cell surface multireceptors external stimuli in the mammary gland. J Mammary Gland Biol Neoplasia *6*, 253-273.

Diamond, M. S., Alon, R., Parkos, C. A., Quinn, M. T., and Springer, T. A. (1995). Heparin is an adhesive ligand for the leukocyte integrin Mac-1 (CD11b/CD18). JCell Biol *130*, 1473-1482.

Dono, R., Texido, G., Dussel, R., Ehmke, H., and Zeller, R. (1998). Impaired cerebral cortex development and blood pressure regulation in FGF-2-deficient mice. Embo J *17*, 4213-4225.

Esko, J. D., and Lindahl, U. (2001). Molecular diversity of heparan sulfate. JClinInvest *108*, 169-173.

Fan, G., Xiao, L., Cheng, L., Wang, X., Sun, B., and Hu, G. (2000). Targeted disruption of NDST-1 gene leads to pulmonary hypoplasia and neonatal respiratory distress in mice. FEBS Lett *467*, 7-11.

Faraldo, M. M., Deugnier, M. A., Thiery, J. P., and Glukhova, M. A. (2001). Growth defects induced by perturbation of beta1-integrin function in the mammary gland

epithelium result from a lack of MAPK activation via the Shc and Akt pathways. EMBO Rep *2*, 431-437.

Forrester, E., Chytil, A., Bierie, B., Aakre, M., Gorska, A. E., Sharif-Afshar, A. R., Muller, W. J., and Moses, H. L. (2005). Effect of conditional knockout of the type II TGF-beta receptor gene in mammary epithelia on mammary gland development and polyomavirus middle T antigen induced tumor formation and metastasis. Cancer Res *65*, 2296-2302.

Forsberg, E., Pejler, G., Ringvall, M., Lunderius, C., Tomasini-Johansson, B., Kusche-Gullberg, M., Eriksson, I., Ledin, J., Hellman, L., and Kjellén, L. (1999). Abnormal mast cells in mice deficient in a heparin-synthesizing enzyme. Nature *400*, 773-776.

Ghabrial, A., Luschnig, S., Metzstein, M. M., and Krasnow, M. A. (2003). Branching morphogenesis of the Drosophila tracheal system. Annu Rev Cell Dev Biol *19*, 623-647.

Gordon, J. R., and Bernfield, M. R. (1980). The basal lamina of the postnatal mammary epithelium contains glycosaminoglycans in a precise ultrastructural organization. Dev Biol *74*, 118-135.

Grobe, K., Inatani, M., Pallerla, S. R., Castagnola, J., Yamaguchi, Y., and Esko, J. D. (2005). Cerebral hypoplasia and craniofacial defects in mice lacking heparan sulfate Ndst1 gene function. Development *132*, 3777-3786.

Groffen, A. J., Ruegg, M. A., Dijkman, H., van de Velden, T. J., Buskens, C. A., van den Born, J., Assmann, K. J., Monnens, L. A., Veerkamp, J. H., and van den Heuvel, L. P. (1998). Agrin is a major heparan sulfate proteoglycan in the human glomerular basement membrane. J Histochem Cytochem *46*, 19-27.

Guo, L., Degenstein, L., and Fuchs, E. (1996). Keratinocyte growth factor is required for hair development but not for wound healing. Genes Dev *10*, 165-175.

Higashiyama, S., Abraham, J. A., and Klagsbrun, M. (1993). Heparin-binding EGF-like growth factor stimulation of smooth muscle cell migration: Dependence on interactions with cell surface heparan sulfate. JCell Biol *122*, 933-940.

Howlin, J., McBryan, J., and Martin, F. (2006). Pubertal mammary gland development: insights from mouse models. J Mammary Gland Biol Neoplasia *11*, 283-297.

Humphries, D. E., Wong, G. W., Friend, D. S., Gurish, M. F., Qiu, W. T., Huang, C. F., Sharpe, A. H., and Stevens, R. L. (1999). Heparin is essential for the storage of specific granule proteases in mast cells. Nature *400*, 769-772.

Izvolsky, K. I., Shoykhet, D., Yang, Y., Yu, Q., Nugent, M. A., and Cardoso, W. V. (2003). Heparan sulfate-FGF10 interactions during lung morphogenesis. Dev Biol *258*, 185-200.

Jackson, D., Bresnick, J., Rosewell, I., Crafton, T., Poulsom, R., Stamp, G., and Dickson, C. (1997a). Fibroblast growth factor receptor signalling has a role in lobuloalveolar development of the mammary gland. J Cell Sci *110 (Pt 11)*, 1261-1268.

Jackson, L. F., Qiu, T. H., Sunnarborg, S. W., Chang, A., Zhang, C., Patterson, C., and Lee, D. C. (2003). Defective valvulogenesis in HB-EGF and TACE-null mice is associated with aberrant BMP signaling. Embo J *22*, 2704-2716.

Jackson, S. M., Nakato, H., Sugiura, M., Jannuzi, A., Oakes, R., Kaluza, V., Golden, C., and Selleck, S. B. (1997b). dally, a Drosophila glypican, controls cellular responses to the TGF-β-related morphogen, Dpp. Development *124*, 4113-4120.

Jackson-Fisher, A. J., Bellinger, G., Ramabhadran, R., Morris, J. K., Lee, K. F., and Stern, D. F. (2004). ErbB2 is required for ductal morphogenesis of the mammary gland. Proc Natl Acad Sci U S A *101*, 17138-17143.

Joseph, H., Gorska, A. E., Sohn, P., Moses, H. L., and Serra, R. (1999). Overexpression of a kinase-deficient transforming growth factor-beta type II receptor in mouse mammary stroma results in increased epithelial branching. Mol Biol Cell *10*, 1221-1234.

Kamalati, T., Niranjan, B., Yant, J., and Buluwela, L. (1999). HGF/SF in mammary epithelial growth and morphogenesis: in vitro and in vivo models. J Mammary Gland Biol Neoplasia *4*, 69-77.

Kamimura, K., Fujise, M., Villa, F., Izumi, S., Habuchi, H., Kimata, K., and Nakato, H. (2001). *Drosophila* heparan sulfate 6-*O*-sulfotransferase (*dHS6ST*) gene - Structure, expression, and function in the formation of the tracheal system. JBiolChem *276*, 17014-17021.

Kamimura, K., Koyama, T., Habuchi, H., Ueda, R., Masu, M., Kimata, K., and Nakato, H. (2006). Specific and flexible roles of heparan sulfate modifications in Drosophila FGF signaling. J Cell Biol *174*, 773-778.

Kanwar, Y. S., and Farquhar, M. G. (1979). Anionic sites in the glomerular basement membrane. In vivo and in vitro localization to the laminae rarae by cationic probes. JCell Biol *81*, 137-153.

Kanwar, Y. S., Jakubowski, M. L., Rosenzweig, L. J., and Gibbons, J. T. (1984). De novo cellular synthesis of sulfated proteoglycans of the developing renal glomerulus in vivo. ProcNatlAcadSciUS A *81*, 7108-7111.

Kanwar, Y. S., Wada, J., Lin, S., Danesh, F. R., Chugh, S. S., Yang, Q., Banerjee, T., and Lomasney, J. W. (2004). Update of extracellular matrix, its receptors, and cell adhesion molecules in mammalian nephrogenesis. Am J Physiol Renal Physiol *286*, F202-215.

Kenney, N. J., Huang, R. P., Johnson, G. R., Wu, J. X., Okamura, D., Matheny, W., Kordon, E., Gullick, W. J., Plowman, G., Smith, G. H., and et al. (1995). Detection and location of amphiregulin and Cripto-1 expression in the developing postnatal mouse mammary gland. Mol Reprod Dev *41*, 277-286.

Kenney, N. J., Smith, G. H., Rosenberg, K., Cutler, M. L., and Dickson, R. B. (1996). Induction of ductal morphogenesis and lobular hyperplasia by amphiregulin in the mouse mammary gland. Cell Growth Differ *7*, 1769-1781.

Klambt, C., Glazer, L., and Shilo, B. Z. (1992). breathless, a Drosophila FGF receptor homolog, is essential for migration of tracheal and specific midline glial cells. Genes Dev *6*, 1668-1678.

Klinowska, T. C., Soriano, J. V., Edwards, G. M., Oliver, J. M., Valentijn, A. J., Montesano, R., and Streuli, C. H. (1999). Laminin and beta1 integrins are crucial for normal mammary gland development in the mouse. Dev Biol *215*, 13-32.

Lander, A. D., Nie, Q., and Wan, F. Y. (2002). Do morphogen gradients arise by diffusion? Dev Cell *2*, 785-796.

Lelongt, B., Makino, H., Dalecki, T. M., and Kanwar, Y. S. (1988). Role of proteoglycans in renal development. DevBiol *128*, 256-276.

Li, J. P., Gong, F., Hagner-McWhirter, A., Forsberg, E., Abrink, M., Kisilevsky, R., Zhang, X., and Lindahl, U. (2003). Targeted disruption of a murine glucuronyl C5-epimerase gene results in heparan sulfate lacking L-iduronic acid and in neonatal lethality. J Biol Chem *278*, 28363-28366.

Lin, X., Wei, G., Shi, Z. Z., Dryer, L., Esko, J. D., Wells, D. E., and Matzuk, M. M. (2000). Disruption of gastrulation and heparan sulfate biosynthesis in EXT1-deficient mice. Dev Biol *224*, 299-311.

Lin, X. H., Buff, E. M., Perrimon, N., and Michelson, A. M. (1999). Heparan sulfate proteoglycans are essential for FGF receptor signaling during *Drosophila* embryonic development. Development *126*, 3715-3723.

Lin, X. H., and Perrimon, N. (1999). Daily cooperates with *Drosophila* Frizzled 2 to transduce Wingless signalling. Nature *400*, 281-284.

Liu, B. Y., McDermott, S. P., Khwaja, S. S., and Alexander, C. M. (2004). The transforming activity of Wnt effectors correlates with their ability to induce the accumulation of mammary progenitor cells. Proc Natl Acad Sci U S A *101*, 4158-4163.

Luetteke, N. C., Qiu, T. H., Fenton, S. E., Troyer, K. L., Riedel, R. F., Chang, A., and Lee, D. C. (1999). Targeted inactivation of the EGF and amphiregulin genes reveals distinct roles for EGF receptor ligands in mouse mammary gland development. Development *126*, 2739-2750.

Lyon, M., Deakin, J. A., and Gallagher, J. T. (1994). Liver heparan sulfate structure. A novel molecular design. J Biol Chem *269*, 11208-11215.

Lyon, M., Rushton, G., and Gallagher, J. T. (1997). The interaction of the transforming growth factor-βs with heparin heparan sulfate is isoform-specific. JBiolChem *272*, 18000-18006.

MacArthur, J. M., Bishop, J. R., Wang, L., Stanford, K. I., Bensadoun, A., Witztum, J. L., and Esko, J. D. (2007). Liver heparan sulfate proteoglycans mediate clearance of triglyceride-rich lipoproteins independently of LDL receptor family members. J Clin Invest *117*, 153-164.

Mailleux, A. A., Spencer-Dene, B., Dillon, C., Ndiaye, D., Savona-Baron, C., Itoh, N., Kato, S., Dickson, C., Thiery, J. P., and Bellusci, S. (2002). Role of FGF10/FGFR2b signaling during mammary gland development in the mouse embryo. Development *129*, 53-60.

Massague, J., and Chen, Y. G. (2000). Controlling TGF-beta signaling. Genes Dev *14*, 627-644.

Merry, C. L. R., Bullock, S. L., Swan, D. C., Backen, A. C., Lyon, M., Beddington, R. S. P., Wilson, V. A., and Gallagher, J. T. (2001). The molecular phenotype of heparan sulfate in the *Hs2st*$^{-/-}$ mutant mouse. J Biol Chem *276*, 35429-35434.

Min, H., Danilenko, D. M., Scully, S. A., Bolon, B., Ring, B. D., Tarpley, J. E., DeRose, M., and Simonet, W. S. (1998). Fgf-10 is required for both limb and lung development and exhibits striking functional similarity to Drosophila branchless. Genes Dev *12*, 3156-3161.

Mizuno, K., Inoue, H., Hagiya, M., Shimizu, S., Nose, T., Shimohigashi, Y., and Nakamura, T. (1994). Hairpin loop and second kringle domain are essential sites for

heparin binding and biological activity of hepatocyte growth factor. J Biol Chem *269*, 1131-1136.

Muragaki, Y., Timmons, S., Griffith, C. M., Oh, S. P., Fadel, B., Quertermous, T., and Olsen, B. R. (1995). Mouse Col18a1 is expressed in a tissue-specific manner as three alternative variants and is localized in basement membrane zones. Proc Natl Acad Sci U S A *92*, 8763-8767.

Najjam, S., Mulloy, B., Theze, J., Gordon, M., Gibbs, R., and Rider, C. C. (1998). Further characterization of the binding of human recombinant interleukin 2 to heparin and identification of putative binding sites. Glycobiology *8*, 509-516.

Niemann, C., Brinkmann, V., Spitzer, E., Hartmann, G., Sachs, M., Naundorf, H., and Birchmeier, W. (1998). Reconstitution of mammary gland development in vitro: requirement of c-met and c-erbB2 signaling for branching and alveolar morphogenesis. J Cell Biol *143*, 533-545.

Niranjan, B., Buluwela, L., Yant, J., Perusinghe, N., Atherton, A., Phippard, D., Dale, T., Gusterson, B., and Kamalati, T. (1995). HGF/SF: a potent cytokine for mammary growth, morphogenesis and development. Development *121*, 2897-2908.

Ohuchi, H., Hori, Y., Yamasaki, M., Harada, H., Sekine, K., Kato, S., and Itoh, N. (2000). FGF10 acts as a major ligand for FGF receptor 2 IIIb in mouse multi-organ development. Biochem Biophys Res Commun *277*, 643-649.

Pedchenko, V. K., and Imagawa, W. (2000). Estrogen treatment in vivo increases keratinocyte growth factor in the mammary gland. J Endocrinol *165*, 39-49.

Pierce, D. F., Jr., Johnson, M. D., Matsui, Y., Robinson, S. D., Gold, L. I., Purchio, A. F., Daniel, C. W., Hogan, B. L., and Moses, H. L. (1993). Inhibition of mammary duct development but not alveolar outgrowth during pregnancy in transgenic mice expressing active TGF-beta 1. Genes Dev *7*, 2308-2317.

Plath, A., Einspanier, R., Gabler, C., Peters, F., Sinowatz, F., Gospodarowicz, D., and Schams, D. (1998). Expression and localization of members of the fibroblast growth factor family in the bovine mammary gland. J Dairy Sci *81*, 2604-2613.

Pohl, M., Sakurai, H., Stuart, R. O., and Nigam, S. K. (2000). Role of hyaluronan and CD44 in *in vitro* branching morphogenesis of ureteric bud cells. DevBiol *224*, 312-325.

Raab, G., and Klagsbrun, M. (1997). Heparin-binding EGF-like growth factor. Biochim Biophys Acta *1333*, F179-199.

Rapraeger, A. C., Krufka, A., and Olwin, B. B. (1991). Requirement of heparan sulfate for bFGF-mediated fibroblast growth and myoblast differentiation. Science *252*, 1705-1708.

Reichman-Fried, M., Dickson, B., Hafen, E., and Shilo, B. Z. (1994). Elucidation of the role of breathless, a Drosophila FGF receptor homolog, in tracheal cell migration. Genes Dev *8*, 428-439.

Reichsman, F., Smith, L., and Cumberledge, S. (1996). Glycosaminoglycans can modulate extracellular localization of the *wingless* protein and promote signal transduction. JCell Biol *135*, 819-827.

Ringvall, M., Ledin, J., Holmborn, K., Van Kuppevelt, T., Ellin, F., Eriksson, I., Olofsson, A. M., Kjellén, L., and Forsberg, E. (2000). Defective heparan sulfate biosynthesis and neonatal lethality in mice lacking N-deacetylase/N-sulfotransferase-1. J Biol Chem *275*, 25926-25930.

Robinson, S. D., Silberstein, G. B., Roberts, A. B., Flanders, K. C., and Daniel, C. W. (1991). Regulated expression and growth inhibitory effects of transforming growth factor-beta isoforms in mouse mammary gland development. Development *113*, 867-878.

Ruan, W., and Kleinberg, D. L. (1999). Insulin-like growth factor I is essential for terminal end bud formation and ductal morphogenesis during mammary development. Endocrinology *140*, 5075-5081.

Rubin, J. S., Day, R. M., Breckenridge, D., Atabey, N., Taylor, W. G., Stahl, S. J., Wingfield, P. T., Kaufman, J. D., Schwall, R., and Bottaro, D. P. (2001). Dissociation of heparan sulfate and receptor binding domains of hepatocyte growth factor reveals that heparan sulfate-c-met interaction facilitates signaling. J Biol Chem *276*, 32977-32983.

Rudland, P. S., Platt-Higgins, A. M., Wilkinson, M. C., and Fernig, D. G. (1993). Immunocytochemical identification of basic fibroblast growth factor in the developing rat mammary gland: variations in location are dependent on glandular structure and differentiation. J Histochem Cytochem *41*, 887-898.

Ruppert, R., Hoffmann, E., and Sebald, W. (1996). Human bone morphogenetic protein 2 contains a heparin-binding site which modifies its biological activity. EurJBiochem *237*, 295-302.

Sakata, H., Stahl, S. J., Taylor, W. G., Rosenberg, J. M., Sakaguchi, R., Wingfield, P. T., and Rubin, J. S. (1997). Heparin binding and oligomerization of hepatocyte growth factor scatter factor isoforms - Heparan sulfate glycosaminoglycan requirement for Met binding and signalling. JBiolChem *272*, 9457-9463.

Schmidt, C., Bladt, F., Goedecke, S., Brinkmann, V., Zschiesche, W., Sharpe, M., Gherardi, E., and Birchmeier, C. (1995). Scatter factor/hepatocyte growth factor is essential for liver development. Nature *373*, 699-702.

Schroeder, J. A., and Lee, D. C. (1998). Dynamic expression and activation of ERBB receptors in the developing mouse mammary gland. Cell Growth Differ *9*, 451-464.

Schuger, L., Skubitz, A. P. N., Gilbride, K., Mandel, R., and He, L. (1996). Laminin and heparan sulfate proteoglycan mediate epithelial cell polarization in organotypic cultures of embryonic lung cells: Evidence implicating involvement of the inner globular region of laminin β 1 chain and the heparan sulfate groups of heparan sulfate proteoglycan. DevBiol *179*, 264-273.

Selleck, S. B. (2001). Genetic dissection of proteoglycan function in Drosophila and C. elegans. Semin Cell Dev Biol *12*, 127-134.

Silberstein, G. B., and Daniel, C. W. (1982). Glycosaminoglycans in the basal lamina and extracellular matrix of the developing mouse mammary duct. Dev Biol *90*, 215-222.

Silberstein, G. B., Flanders, K. C., Roberts, A. B., and Daniel, C. W. (1992). Regulation of mammary morphogenesis: evidence for extracellular matrix-mediated inhibition of ductal budding by transforming growth factor-beta 1. Dev Biol *152*, 354-362.

Snedeker, S. M., Brown, C. F., and DiAugustine, R. P. (1991). Expression and functional properties of transforming growth factor alpha and epidermal growth factor during mouse mammary gland ductal morphogenesis. Proc Natl Acad Sci U S A *88*, 276-280.

Sonnenberg, E., Meyer, D., Weidner, K. M., and Birchmeier, C. (1993). Scatter factor/hepatocyte growth factor and its receptor, the c-met tyrosine kinase, can mediate a signal exchange between mesenchyme and epithelia during mouse development. J Cell Biol *123*, 223-235.

Soriano, J. V., Pepper, M. S., Orci, L., and Montesano, R. (1998). Roles of hepatocyte growth factor/scatter factor and transforming growth factor-beta1 in mammary gland ductal morphogenesis. J Mammary Gland Biol Neoplasia *3*, 133-150.

Steer, D. L., Shah, M. M., Bush, K. T., Stuart, R. O., Sampogna, R. V., Meyer, T. N., Schwesinger, C., Bai, X., Esko, J. D., and Nigam, S. K. (2004). Regulation of ureteric bud branching morphogenesis by sulfated proteoglycans in the developing kidney. Dev Biol *272*, 310-327.

Stern, D. F. (2003). ErbBs in mammary development. Exp Cell Res *284*, 89-98.

Sternlicht, M. D. (2006). Key stages in mammary gland development: the cues that regulate ductal branching morphogenesis. Breast Cancer Res *8*, 201.

Stickens, D., Zak, B. M., Rougier, N., Esko, J. D., and Werb, Z. (2005). Mice deficient in Ext2 lack heparan sulfate and develop exostoses. Development *132*, 5055-5068.

Sympson, C. J., Talhouk, R. S., Alexander, C. M., Chin, J. R., Clift, S. M., Bissell, M. J., and Werb, Z. (1994). Targeted expression of stromelysin-1 in mammary gland provides evidence for a role of proteinases in branching morphogenesis and the requirement for an intact basement membrane for tissue-specific gene expression. J Cell Biol *125*, 681-693.

Taipale, J., and Keski-Oja, J. (1997). Growth factors in the extracellular matrix. FASEB J *11*, 51-59.

Takayama, H., LaRochelle, W. J., Sharp, R., Otsuka, T., Kriebel, P., Anver, M., Aaronson, S. A., and Merlino, G. (1997). Diverse tumorigenesis associated with aberrant development in mice overexpressing hepatocyte growth factor/scatter factor. Proc Natl Acad Sci U S A *94*, 701-706.

Thompson, S. M., Connell, M. G., Fernig, D. G., Ten Dam, G. B., van Kuppevelt, T. H., Turnbull, J. E., Jesudason, E. C., and Losty, P. D. (2007). Novel 'phage display antibodies identify distinct heparan sulfate domains in developing mammalian lung. Pediatr Surg Int *23*, 411-417.

Tsuda, M., Kamimura, K., Nakato, H., Archer, M., Staatz, W., Fox, B., Humphrey, M., Olson, S., Futch, T., Kaluza, V., *et al*. (1999). The cell-surface proteoglycan Dally regulates Wingless signalling in *Drosophila*. Nature *400*, 276-280.

Wagner, K. U., McAllister, K., Ward, T., Davis, B., Wiseman, R., and Hennighausen, L. (2001). Spatial and temporal expression of the Cre gene under the control of the MMTV-LTR in different lines of transgenic mice. Transgenic Res *10*, 545-553.

Wagner, K. U., Wall, R. J., St-Onge, L., Gruss, P., Wynshaw-Boris, A., Garrett, L., Li, M., Furth, P. A., and Hennighausen, L. (1997). Cre-mediated gene deletion in the mammary gland. Nucleic Acids Res *25. 25*, 4323-4330.

Wang, L., Fuster, M., Sriramarao, P., and Esko, J. D. (2005). Endothelial heparan sulfate deficiency impairs L-selectin- and chemokine-mediated neutrophil trafficking during inflammatory responses. Nat Immunol *6*, 902-910.

Wiesen, J. F., Young, P., Werb, Z., and Cunha, G. R. (1999). Signaling through the stromal epidermal growth factor receptor is necessary for mammary ductal development. Development *126*, 335-344.

Wiseman, B. S., Sternlicht, M. D., Lund, L. R., Alexander, C. M., Mott, J., Bissell, M. J., Soloway, P., Itohara, S., and Werb, Z. (2003). Site-specific inductive and inhibitory activities of MMP-2 and MMP-3 orchestrate mammary gland branching morphogenesis. J Cell Biol *162*, 1123-1133.

Witty, J. P., Wright, J. H., and Matrisian, L. M. (1995). Matrix metalloproteinases are expressed during ductal and alveolar mammary morphogenesis, and misregulation of stromelysin-1 in transgenic mice induces unscheduled alveolar development. Mol Biol Cell *6*, 1287-1303.

Xie, W., Paterson, A. J., Chin, E., Nabell, L. M., and Kudlow, J. E. (1997). Targeted expression of a dominant negative epidermal growth factor receptor in the mammary gland of transgenic mice inhibits pubertal mammary duct development. Mol Endocrinol *11*, 1766-1781.

Yang, Y., Spitzer, E., Meyer, D., Sachs, M., Niemann, C., Hartmann, G., Weidner, K. M., Birchmeier, C., and Birchmeier, W. (1995). Sequential requirement of hepatocyte growth factor and neuregulin in the morphogenesis and differentiation of the mammary gland. J Cell Biol *131*, 215-226.

Yant, J., Buluwela, L., Niranjan, B., Gusterson, B., and Kamalati, T. (1998). In vivo effects of hepatocyte growth factor/scatter factor on mouse mammary gland development. Exp Cell Res *241*, 476-481.

Yayon, A., Klagsbrun, M., Esko, J. D., Leder, P., and Ornitz, D. M. (1991). Cell surface, heparin-like molecules are required for binding of basic fibroblast growth factor to its high affinity receptor. Cell *64*, 841-848.

Yu, W. H., and Woessner, J. F., Jr. (2000). Heparan sulfate proteoglycans as extracellular docking molecules for matrilysin (matrix metalloproteinase 7). J Biol Chem *275*, 4183-4191.

Yu, W. H., Woessner, J. F., Jr., McNeish, J. D., and Stamenkovic, I. (2002). CD44 anchors the assembly of matrilysin/MMP-7 with heparin-binding epidermal growth factor precursor and ErbB4 and regulates female reproductive organ remodeling. Genes Dev *16*, 307-323.

Zcharia, E., Metzger, S., Chajek-Shaul, T., Friedmann, Y., Pappo, O., Aviv, A., Elkin, M., Pecker, I., Peretz, T., and Vlodavsky, I. (2001). Molecular properties and involvement of heparanase in cancer progression and mammary gland morphogenesis. J Mammary Gland Biol Neoplasia *6*, 311-322.

Zhang, L., David, G., and Esko, J. D. (1995). Repetitive Ser-Gly sequences enhance heparan sulfate assembly in proteoglycans. JBiolChem *270*, 27127-27135.

Zioncheck, T. F., Richardson, L., Liu, J., Chang, L., King, K. L., Bennett, G. L., Fügedi, P., Chamow, S. M., Schwall, R. H., and Stack, R. J. (1995). Sulfated oligosaccharides promote hepatocyte growth factor association and govern its mitogenic activity. JBiolChem *270*, 16871-16878.

Chapter 2: Mammary Ductal Branching Depends on Heparan Sulfate Fine Structure

2.1 Summary

We have examined the role of epithelial heparan sulfate in mammary gland branching by specifically targeting the biosynthetic machinery responsible for heparan sulfate polymerization and modification *in vivo*. Mammary epithelia lacking EXT1 (heparan sulfate co-polymerase) fail to undergo ductal branching in response to pubertal hormones released at the onset of the estrous cycle. This phenotype is dramatic and highly penetrant. Some variability in the penetrance was observed due to inefficient Cre recombinase activity. Mammary epithelia lack *Ndst1* and *Ndst2* (heparan sulfate sulfotranseferases necessary for all chain modification) exhibit a similar phenotype. Inhibition of chain polymerization and overall sulfation block epithelial proliferation leading to a loss of all tubular structures. In contrast, mammary epithelia deficient in *Hs2st* (an enzyme that adds 2-O-sulfate groups to uronic acids in heparan sulfate) show defects in the number and complexity of branched epithelia. Mutant glands had decreased secondary branches and fewer bifurcated terminal end buds. These studies show that (i) MEC heparan sulfate exhibits a cell autonomous effect on development and (ii) the pattern of sulfation of the chain determines the extent of dichotomous branching and side branching. These findings suggest that a

specific set of growth factors or extracellular matrix components interact with the heparan sulfate side chains of epithelial proteoglycans.

2.2 Introduction

Various organs undergo branching morphogensis, including the lung, kidney, pancreas, salivary gland, lacrimal gland, and mammary gland. Ductal branches formed in this way constitute a system of highly organized tubular networks lined with epithelia that transport gases or fluids. Branching serves to increase the utilized surface area within an organ (Affolter et al., 2003). The molecular mechanisms responsible for proliferation and arborization of the epithelial tree have not been fully characterized. Extracellular matrix molecules, such as proteoglycans, are produced by epithelial cells and deposited in basement membranes surrounding the ducts. Their role in branching morphogenesis has not been studied genetically.

The mammary gland provides an excellent system for studying the role of proteoglycans in branching morphogenesis. At birth, the mammary fat pad stroma consisting of adipocytes, fibroblasts and immune cells holds a rudimentary ductal structure of approximately 10 branches connected to an exterior nipple. The gland remains quiescent until the beginning of the mouse estrous cycle at about 4 weeks postpartum. Ovarian hormones induce rapid branching morphogenesis, which results in arborized ductal epithelia filling the entire fat pad by 10 to 12 weeks of age. At this time, the gland is capable of differentiating into a milk producing structure consisting of lobuloalveoli with the onset of pregnancy.

Epithelial ductal branching in the mouse mammary gland occurs via a bulbous cellular structure known as the terminal end bud (TEB). TEBs consist of an outer layer of bipotent stem cells that proliferate into the mammary fat pad creating a layer of myoepithelia, which constitutes the outer layer of the ducts. The inner layer of the TEB consists of body cells that apoptose to form the lumen inside the duct. The myoepithelia lay down a thick basement membrane that surrounds the branched ductal structures. Secondary branching can also occur along previously formed ductal branches. Coordination of TEB growth and secondary branching fills the gland during puberty.

Pubertal growth of the mammary epithelial ductal tree is regulated by endocrine hormones. Estrogen, glucocorticoids and growth hormone are involved in primary branching, while progesterone is involved in side branching (Howlin et al., 2006). Mammary epithelial cells do not express steroid-receptors, but the surrounding stroma responds to steroid hormones by releasing growth factors that act in a paracrine fashion on the epithelia. These growth factors include insulin like growth factor (IGF), fibroblast growth factors (FGF), epidermal growth factor (EGF), transforming growth factor β (TGFβ), hepatocyte growth factor (HGF), and others. All of these factors interact with heparin or heparan sulfate, which is found associated with the basement membrane of epithelial tubes and on the surface of epithelial cells (Gordon and Bernfield, 1980; Silberstein and Daniel, 1982).

Previous genetic evidence supports a role for heparan sulfate in mammary gland development. Mammary glands of transgenic mice overexpressing a human

heparanase, an enzyme that degrades heparan sulfate, show hyperbranching and precocious alveolar development (Zcharia et al., 2001). Mutants lacking syndecan-1, a cell surface proteoglycan found on mammary epithelial cells, show reduced mammary gland branching and have a 50% reduction in terminal end buds during pubertal branching (Liu et al., 2004). However, because these mutations are systemic, they do not provide insight into the relative contribution of heparan sulfate from the epithelial cells versus the stroma. Furthermore, the results may have underestimated the importance of heparan sulfate since the mutations did not completely inhibit heparan sulfate production.

To study further the role of epithelial heparan sulfate in mammary gland branching, we have inactivated genes responsible for heparan sulfate polymerization and modification specifically in mammary epithelial cells using the Cre-loxP system. Mammary epithelia lacking EXT1, the heparan sulfate co-polymerase, fail to undergo ductal branching. Mammary epithelia lacking *Ndst1* and *Ndst2* (heparan sulfate sulfotransferases necessary for all subsequent chain modifications) exhibit a similar phenotype. In contrast, mammary epithelia deficient in *Hs2st* (an enzyme that adds 2-O-sulfate groups to heparan sulfate) show defects in the number and complexity of branched epithelia.

2.3 Results

Ductal branching depends on sulfation. To study the role of heparan sulfate in ductal branching, we analyzed the affect of chlorate, an inhibitor of sulfation, on a model of ductal branching. Primary mammary epithelia plated into growth factor reduced Matrigel form a spheroid within 24 hours (Fig 2-1A, black arrow). Treatment with FGF-2 for 7 days induces ductal branching (Fig 2-1B, black arrow). Heparan sulfate interacts with growth factors through variable sulfation tracks found along the carbohydrate chain. Treatment with chlorate inhibits PAPS, the sulfate donor, and can reduce the amount of functional heparan sulfate on the surface of the cell. FGF-2 binds specifically to heparan sulfate on the cell surface, so FGF-2 binding can be used as an heparan sulfate specific marker. Primary mammary epithelial cells grown in tissue culture dishes showed a significant reduction in cell surface heparan sulfate upon treatment with chlorate (Fig 2-1C, grey line wild type, black line chlorate treated.) To test the role of heparan sulfate in this model of branching, we treated primary mammary epithelia in Matrigel with FGF-2, in the presence of increasing amounts of chlorate. Treatment with 45mM chlorate reduced the percent of branched spheroids (spheroids that grow from a sphere to a ductal structure) from 90% to 15% (Fig 2-1D). This inhibition increased from 45mM chlorate to 90mM chlorate but was concurrent with an overall loss of spheroids to due cell death. There was no reduction in overall spheroid number after 7 days of treatment with 45mM chlorate versus untreated epithelia (Fig 2-1E). These data indicate that FGF-2 mediated ductal branching is dependent on sulfation.

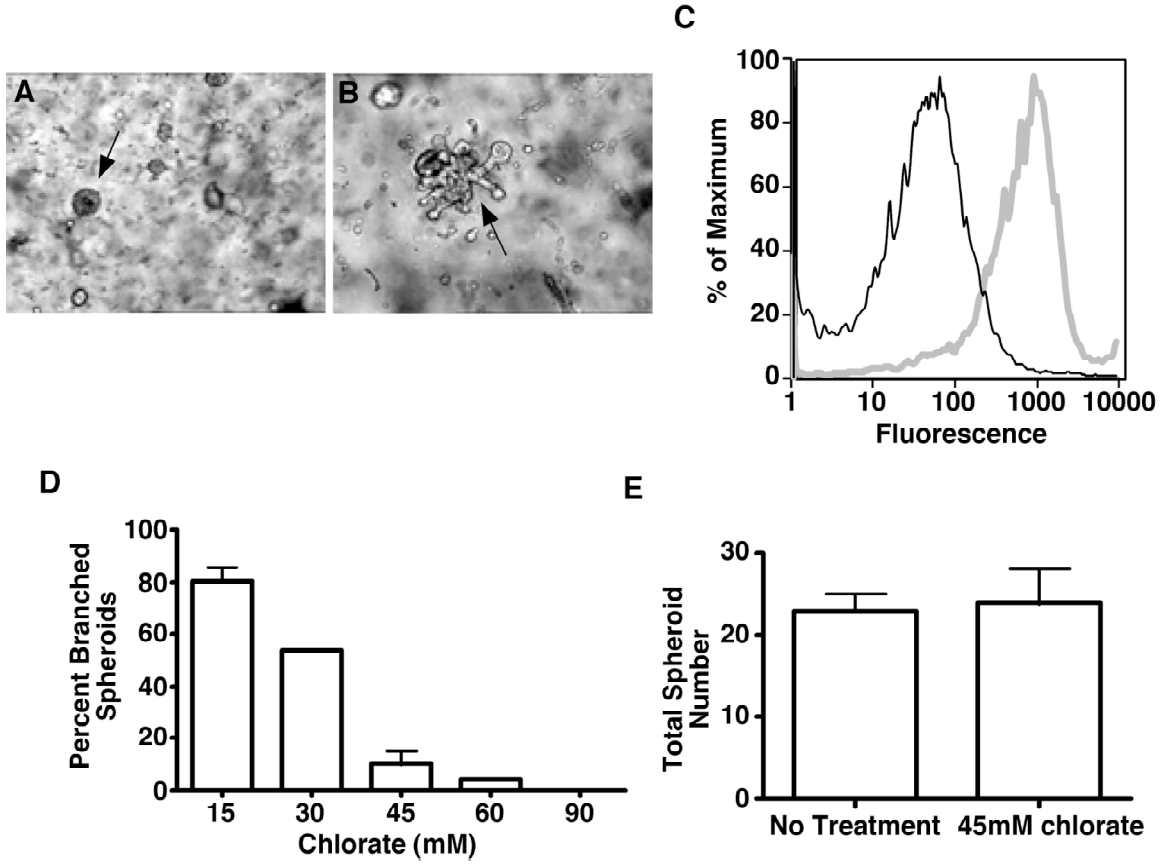

Figure 2-1: FGF-2 mediated *in vitro* mammary epithelial ductal branching is sulfate dependent. Isolated primary mammary epithelial cells were plated into growth factor reduced Matrigel in Hams F12, ITS buffer, and penicillin. **(A, black arrow)** Spheroids formed within 24 hours. **(B, black arrow)** Upon treatment with FGF-2 (300ng/ml) for 7 days, spheroids formed branched organoids structures. **(C)** Mammary epithelial cells were reacted with biotinylated FGF-2, stained with PE-Cy5-streptavidin and analyzed by flow cytometry. Black line curve, Wild type mammary epithelial cells with biotinylated FGF-2 grown in the presence of 45mM sodium chlorate for three days; grey line curve, Wildtype mammary epithelial cells with biotinylated FGF-2. **(D)** Increasing concentrations of sodium chloride had an inhibitory affect on spheroid branching. **(E)** At 45mM sodium chlorate, there is no adverse affect on spheroid formation.

Multiple growth factors in mammary gland development depend on sulfation. The mammary gland uses a variety of local growth factors to translate hormonal signals from outside the gland, through the stroma, and to the growing epithelia. This list of growth factors includes members of the FGF family and members of the EGF family. To test whether these growth factors rely on heparan sulfate to facilitate signaling, growth, and ductal branching, we used chlorate to inhibit sulfation in the model of ductal branching shown in Figure 2-1. Singular treatment with a variety of growth factors is able to produce ductal structures from spheroids. We tested FGF-2, -7, -10, and HB-EGF with 45mM chlorate (Fig. 2-2). Spheroids branched at a rate of 80% with treatment of FGF-2 for 7 days (Fig. 2-2A). 45mM chlorate treatment was able to inhibit branching by 70% (Fig. 2-2A). Treatment with 45mM sodium chloride had minimal affect on ductal branching, showing that the inhibitory response was not an osmotic effect (Fig. 2-2A). The inhibitory response to 45mM chlorate could be overcome by adding 5mM sulfate back to the media (Fig. 2-2A). All of the other growth factors tested behaved in a similar manner as FGF-2, suggesting that multiple growth factors involved in mammary epithelial ductal branching rely on sulfation to mediate branching.

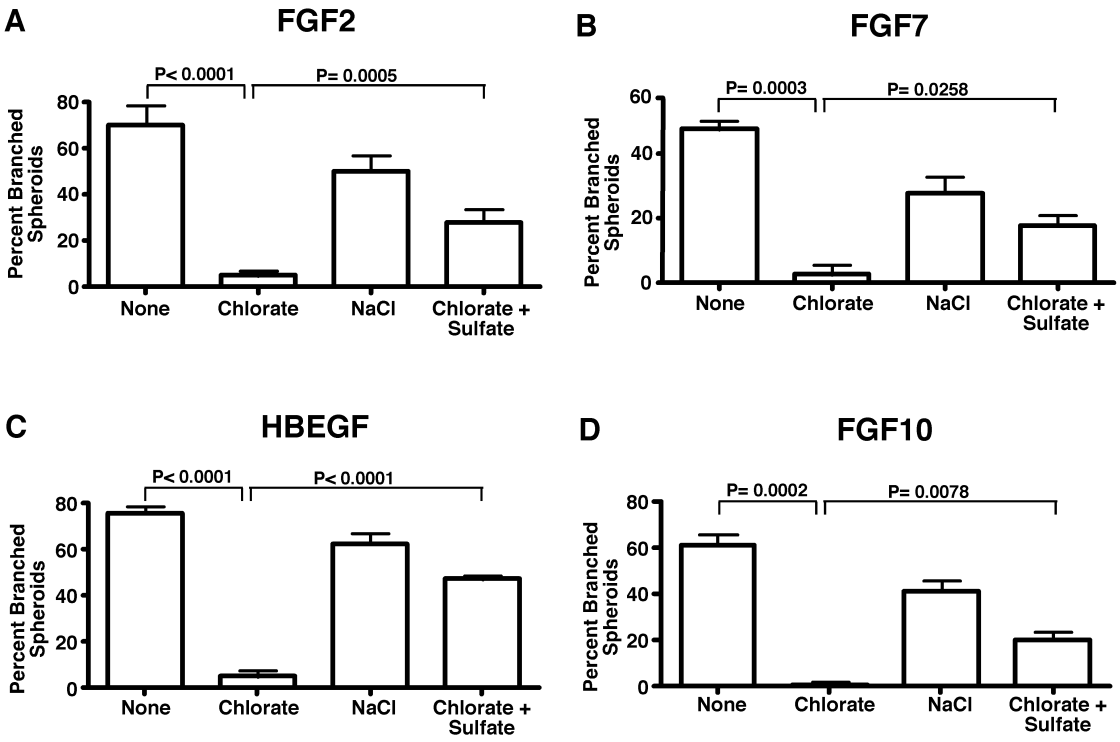

Figure 2-2: Multiple growth factors are sensitive to chlorate treatment. **(A)** FGF-2 treated spheroids branched at 80%. 45mM sodium chlorate treatment inhibited branching to 10%. 45mM sodium chloride treatment showed minimal effect. Treatment of spheroids with 45mM sodium chlorate and 5 mM sodium sulfate rescued branching to 30%. Other growth factors **(B)** FGF-7, **(C)** HB-EGF, **(D)** FGF-10 showed a similar sensitivity.

Mammary ductal branching depends on heparan sulfate. To study the role of heparan sulfate in mammary gland branching morphogenesis, we inactivated *Ext1*, the copolymerase, selectively in mammary epithelial cells. *MMTV Cre* mice express the Cre recombinase in mammary epithelia at day 6 postpartum (Wagner et al., 2001). Cross breeding mice with a conditional allele of *Ext1* (*Ext1*$^{f/f}$) resulted in littermate pairs of *Ext1*$^{f/f}$ *MMTV Cre*$^{+}$ (mutant) mice and *Ext1*$^{f/f}$ *MMTV Cre*$^{-}$ (wildtype) mice. Mice of both genotypes were seen at the expected Mendelian frequency.

To examine the effect of the mutation on ductal branching, the fourth inguinal mammary gland was dissected at 10 to 12 weeks postpartum, when wildtype ductal branching is complete. Whole mounts were prepared and stained with hematoxylin, which revealed variable growth of the ductal network in the mutant. A scoring system was created to determine the extent of inhibition of growth (Fig 2-3A). Glands that exhibited an absence of ductal growth received a score of 1. Ductal trees that grew from the nipple but stopped prior to the lymph node was given a score of 2. A tree that progressed pass the lymph node but halted before the end of the fat pad distal to the nipple received a score of 3. Growth that completely filled the fat pad received a score of 4. Using this system, all wildtype (*Ext1*$^{f/f}$*MMTV Cre*$^{-}$, n = 10) mice and heterozygotes (*Ext1*$^{f/wt}$*MMTV Cre*$^{+}$, n = 36) had a score of 4 (Fig 2-3B and I), i.e. the fat pad was filled. In contrast, 31% of mutant mice (*Ext1*$^{f/f}$*MMTVCre*$^{+}$) were devoid of any ductal growth (n = 54, Fig 2-3C and I). About 2-3% of mutant mice had scores of 2 or 3. Thus, about 35% of the glands were affected, whereas 63% of mutant glands exhibited the wild type phenotype (Fig 2-3D). A comparison of tissue sections

prepared from wildtype of score 4 and a mutant with a score of 1) confirmed that the mutant lacked ductal structures (Fig 2-3E and 2-3F).

A defect in ductal branching can be caused by mistakes in terminal end bud (TEB) production and development. To take a closer look at the branching process, we examined mutant versus wildtype gland at 5 weeks postpartum, a period of rapid ductal expansion. *Ext1*$^{f/f}$ *MMTV Cre*$^{-}$ glands all exhibited a wildtype phenotype at 5 weeks (Fig. 2-3G). *Ext1*$^{f/f}$ *MMTV Cre*$^{+}$ glands showed a lack of ductal structures (Fig 2-3H) at a frequency similar to the 10 to 12 week analysis. These experiments show that ductal branching requires a mammary epithelial specific heparan sulfate chain.

Figure 2-3: Ext-1 deficient mammary glands show defects in branching morphogenesis. Whole mounts and sections of the fourth inguinal glands. **(A)** Schematic diagram of the fourth inguinal mouse mammary gland showing the nipple (N) and the lymph node (LN). Growth is measured from the nipple. Growth score of (1) is an abrogation of ductal epithelial growth, (2) is growth that stops before the lymph node, (3) is growth that is past the lymph node, but does not fill the entire gland, and (4) is a fully branched ductal epithelium. **(B)** Whole mount of *Ext1*$^{f/f}$ *MMTV cre*$^{-}$ gland at ten weeks. **(C)** Whole mount of *Ext1*$^{f/f}$ *MMTV cre*$^{+}$ gland at ten weeks (score of 1). **(D)** Whole mount of *Ext1*$^{f/f}$ *MMTV cre*$^{+}$ gland at ten weeks (score of 4). **(E)** Histological section of *Ext1*$^{f/f}$ *MMTV cre*$^{-}$ gland at ten weeks. Black arrows denote mammary epithelial ducts. **(F)** Histological section of *Ext1*$^{f/f}$ *MMTV cre*$^{+}$ gland at ten weeks (score of 1). **(G)** Whole mount of *Ext1*$^{f/f}$ *MMTV cre*$^{-}$ gland at 5 weeks. **(H)** Whole mount of *Ext1*$^{f/f}$ *MMTV cre*$^{+}$ gland at five weeks. **(I)** Table representing the number of *Ext1*$^{f/f}$ *MMTV cre*$^{-}$, *Ext1*$^{f/wt}$ *MMTV cre*$^{+}$ and *Ext1*$^{f/f}$ *MMTV cre*$^{+}$ glands and the respective growth scores.

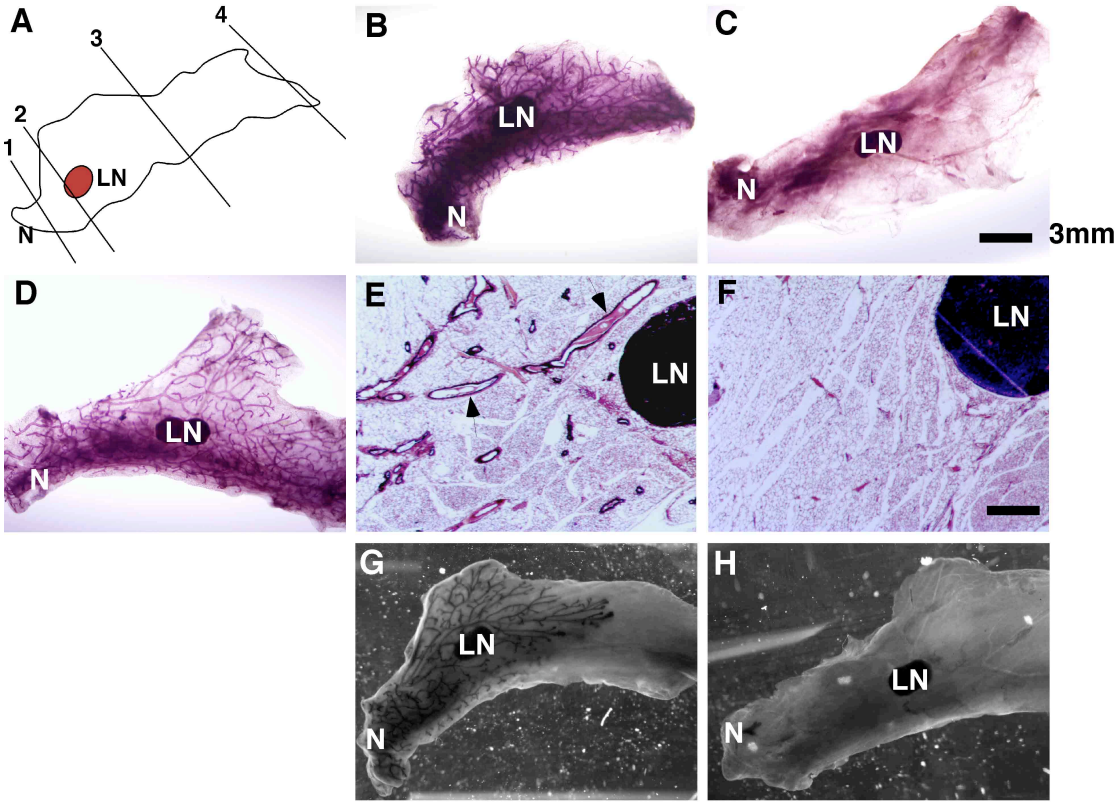

I

	Penetrance (%)			
Genotype	1	2	3	4 (distance)
Ext1 $^{f/f}$ *MMTV Cre* $^{-}$ (n=10)	0	0	0	100
Ext1 $^{f/wt}$ *MMTV Cre* $^{+}$ (n=36)	0	0	0	100
Ext1 $^{f/f}$ *MMTV Cre* $^{+}$ (n=54)	31	4	2	63

Cre inefficiency and *Ext1* inactivation. The previous data suggests that *Ext1* is critical for mammary ductal branching, but the variation in the phenotype (only 37% of animals displayed a growth phenotype) leads to some new questions. Are the *Ext1* deficient glands with a score of 4, able to participate in ductal branching without functional heparan sulfate, or are the *Ext1* deficient glands wildtype as a result of MMTV Cre inefficiency at the Ext1 locus? To study this problem, we took advantage of FGF-2 binding to heparan sulfate, to examine the cell surface heparan sulfate on isolated primary epithelia. *Ext1*$^{f/f}$ *MMTV Cre*$^{-}$ epithelia bind FGF-2 (Fig. 2-4A-C grey line) in a heparan sulfate specific manner. Treatment of isolated epithelia with heparin lyase, an enzyme that cleaves heparan sulfate chains, showed a two log reduction in FGF-2 binding (Fig 2-4A, black line). To test cre efficiency *in vitro*, *Ext1*$^{f/f}$ *MMTV Cre*$^{-}$ epithelia were treated with Adenovirus cre, which has previously shown to achieve 95% inactivation. *Ext1*$^{f/f}$ *MMTV Cre*$^{-}$ cells treated with Adenocre exhibited a similar reduction (Fig 2-4B, black line) in FGF-2 binding as compared to heparin lyase treatment. Finally, we examined the cell surface heparan sulfate in *Ext1*$^{f/f}$ *MMTV Cre*$^{+}$ mammary glands. Isolated epithelia from these animals necessarily had to come from glands that produced epithelia (a score of 2 or higher). *Ext1*$^{f/f}$ *MMTV Cre*$^{+}$ epithelia had a similar FGF-2 binding profile (Fig 2-4C) to wildtype. This signified that the variation in the phenotype was due to MMTV cre inefficiency and that *Ext1* is critical for ductal branching.

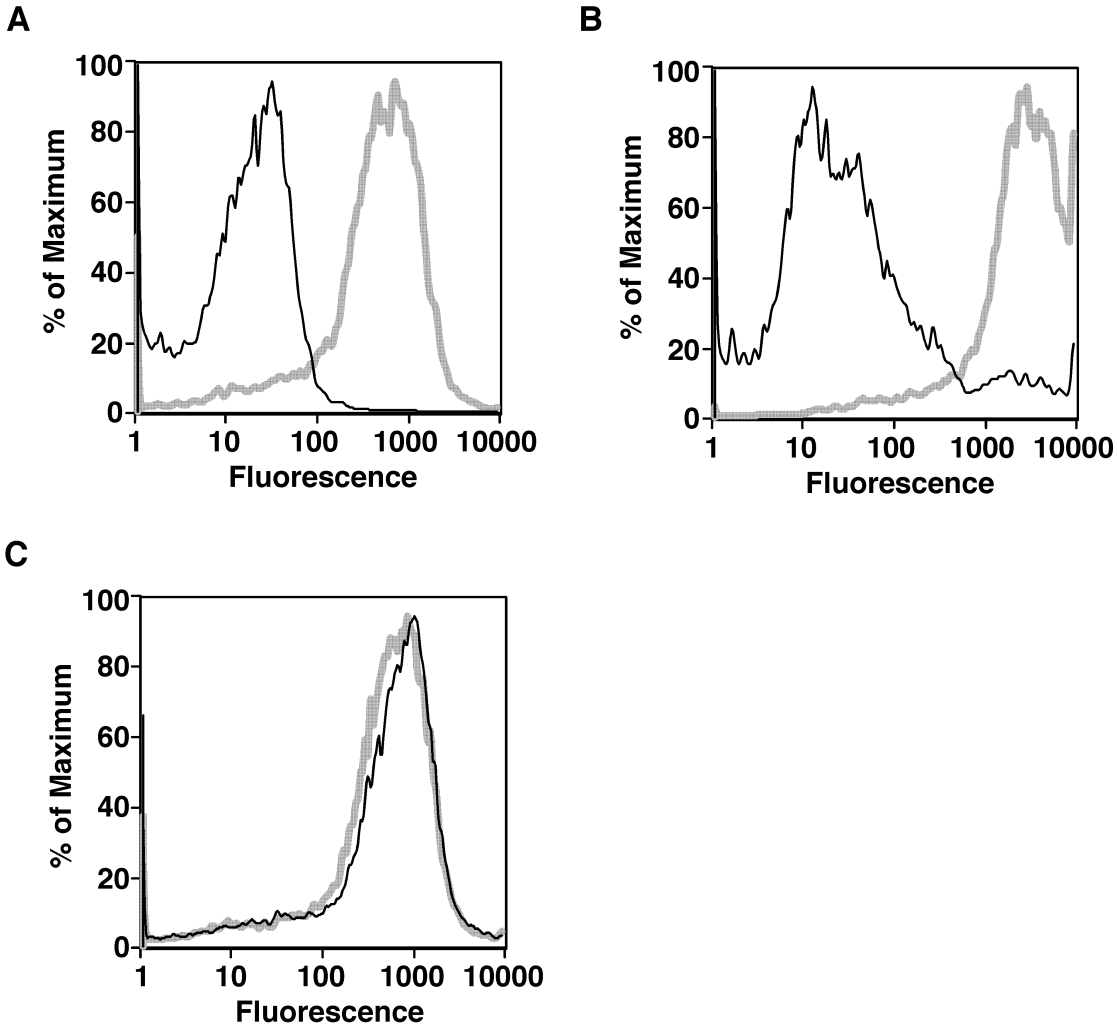

Figure 2-4: MMTV Cre expression is inefficient in *Ext1*$^{f/f}$ *MMTV cre*$^{+}$ glands. Isolated mammary epithelial cells were treated with FGF2 to measure cell surface heparan sulfate. **(A-C)** Grey line, *Ext1*$^{f/f}$ *MMTV cre*$^{-}$ epithelia treated with FGF2. **(A)** Black line, *Ext1*$^{f/f}$ *MMTV cre*$^{-}$ epithelia treated with heparan lyase and probed with FGF2. **(B)** Black line, *Ext1*$^{f/f}$ *MMTV cre*$^{-}$ epithelia treated with adenovirus Cre and probed with FGF2. **(C)** Black line, *Ext1*$^{f/f}$ *MMTV cre*$^{+}$ epithelia probed with FGF2

Mammary ductal epithelial branching depends on heparan sulfate chain modification. The *Ext1* gene encodes the heparan sulfate polymerase. Cell surface heparan sulfate on epithelia deficient in this gene, only contain the five linker sugar. This mutant brings up the question of whether the chain of repeating disaccharides is involved in morphogen interaction, or is the interaction mediated by the sulfation modification along the chains? To study the role of sulfation modification in mammary ductal branching we inactivated *Ndst1* selectively in mammary epithelial cells on an *Ndst2* deficient background. Singularly, neither *Ndst1* nor *Ndst2* deficiency has a role in pubertal branching. The knockout strategy will successfully eliminate chain sulfation by targeting the Ndst isoforms that are critical to all other sulfation modifications. The breeding resulted in littermate pairs of $Ndst1^{f/f}$ *MMTV* Cre^{+} $Ndst2^{-/-}$ (mutant) mice and $Ndst1^{f/f}$ *MMTV* Cre^{-} $Ndst2^{-/-}$ (wildtype) mice. Mice of both genotypes were seen at the expected Mendelian frequency. We followed the same model of growth as seen in Figure 2-3. $Ndst1^{f/f}$ *MMTV* Cre^{-} $Ndst2^{-/-}$ mice all exhibited a wildtype mammary ductal growth score (Fig 2-5B, and G). 18% of $Ndst1^{f/f}$ *MMTV* Cre^{+} $Ndst2^{-/-}$ mice were devoid of any ductal growth (Fig 2-5C, and G). 23% of $Ndst1^{f/f}$ *MMTV* Cre^{+} $Ndst2^{-/-}$ glands showed growth that stopped at a score of 2 or 3 (Fig 2-5D and E). Animals aged to 9 months showed a similar distribution of growth (data not shown) 59% of mutant glands exhibited the wild type phenotype (Fig 2-5F). These results are summarized in table form (Fig 2-5G). This experiment suggests that ductal branching is dependent on sulfation modification along the heparan sulfate chain.

Figure 2-5: Ndst deficient glands show defects in ductal branching. Whole mounts and sections of the fourth inguinal glands. **(A)** Schematic diagram of the fourth inguinal mouse mammary gland showing the nipple (N) and the lymph node (LN). **(B)** Whole mount of *Ndst1*$^{f/f}$ *MMTV Cre*$^{-}$ *Ndst2*$^{-/-}$ gland at ten weeks. **(C)** Whole mount of *Ndst1*$^{f/f}$ *MMTV Cre*$^{+}$ *Ndst2*$^{-/-}$ gland at ten weeks (score of 1). **(D)** Whole mount of *Ndst1*$^{f/f}$ *MMTV Cre*$^{+}$ *Ndst2*$^{-/-}$ gland at ten weeks (score of 2). **(E)** Whole mount of *Ndst1*$^{f/f}$ *MMTV Cre*$^{+}$ *Ndst2*$^{-/-}$ gland at ten weeks (score of 3). **(F)** Whole mount of *Ndst1*$^{f/f}$ *MMTV Cre*$^{+}$ *Ndst2*$^{-/-}$ gland at ten weeks (score of 4). **(G)** Table representing the number of *Ndst1*$^{f/f}$ *MMTV Cre*$^{-}$, *Ndst1*$^{f/f}$ *MMTV Cre*$^{-}$ *Ndst2*$^{-/-}$, and *Ndst1*$^{f/f}$ *MMTV Cre*$^{+}$ *Ndst2*$^{-/-}$ glands and the respective growth scores.

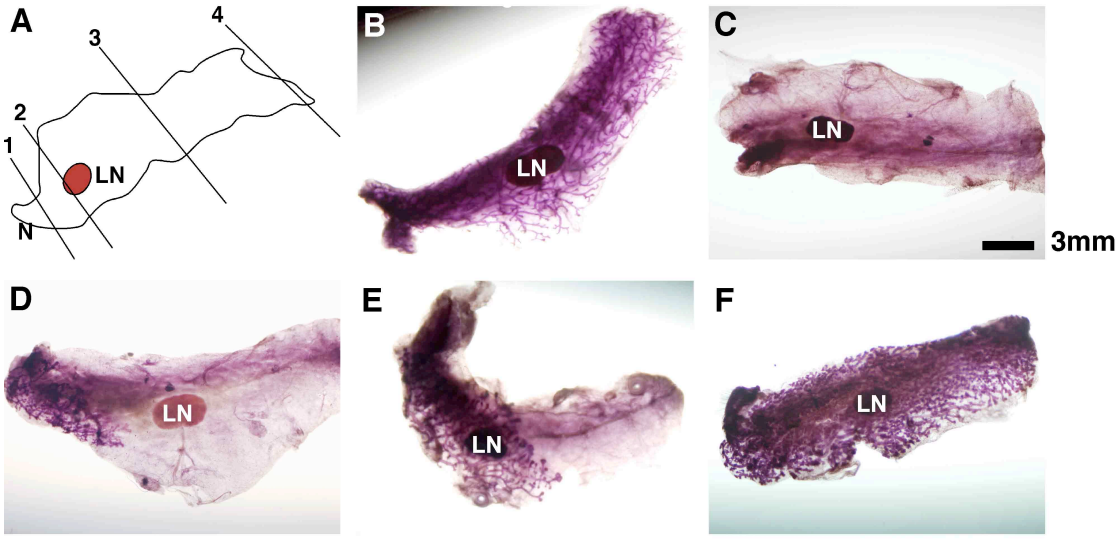

G

Genotype	Penetrance (%) 1	2	3	4 (distance)
Ndst1 $^{f/f}$ *MMTV Cre* $^{-}$ (n=11)	0	0	0	100
Ndst1 $^{f/f}$ *MMTV Cre* $^{-}$ *Ndst2* $^{-/-}$ (n=20)	0	0	0	100
Ndst1 $^{f/f}$ *MMTV Cre* $^{+}$ *Ndst2* $^{-/-}$ (n=79)	18	3	20	59

Ndst deficient ducts display hyperbranching and cellular chimerism in the level of sulfated cell surface heparan sulfate. A closer examination of *Ndst1*$^{f/f}$ *MMTV Cre*$^{+}$ *Ndst2*$^{-/-}$ mutant glands revealed pubertal hyperbranching. *Ndst1*$^{f/f}$ *MMTV Cre*$^{-}$ *Ndst2*$^{-/-}$ littermate pairs show regular spacing between ducts in a whole mount (Fig 2-6A) or histology section (Fig. 2-6C, black arrows point to ducts). *Ndst1*$^{f/f}$ *MMTV Cre*$^{+}$ *Ndst2*$^{-/-}$ glands show a marked increase in branching by whole mount (Fig. 2-6B) and histology section (Fig. 6D, black arrows point to ducts). This result was quantified by comparing total number of ducts in a section per area of the fat pad. The hyperbranching phenotype was seen in *Ndst1*$^{f/f}$ *MMTV Cre*$^{+}$ *Ndst2*$^{-/-}$ mutant glands, regardless of the growth score (Fig. 2-6D, E, and F). To examine the efficiency of MMTV cre inactivation, we looked at the cell surface heparan sulfate in *Ndst1*$^{f/f}$ *MMTV Cre*$^{+}$ *Ndst2*$^{-/-}$ glands (Fig. 2-6F black line) in comparison to *Ndst1*$^{f/f}$ *MMTV Cre*$^{-}$ *Ndst2*$^{-/-}$ glands (Fig. 2-6F, grey line). Isolated epithelia from these animals necessarily had to come from glands that produced epithelia (a score of 2 or higher). *Ndst1*$^{f/f}$ *MMTV Cre*$^{+}$ *Ndst2*$^{-/-}$ cells showed two distinct populations of FGF-2 binding cells. One bound at the level of *Ndst1*$^{f/f}$ *MMTV Cre*$^{-}$ *Ndst2*$^{-/-}$ cells while the other population showed a significant decrease in binding. This apperant chimerism may lead to the hyperbranching phenotype.

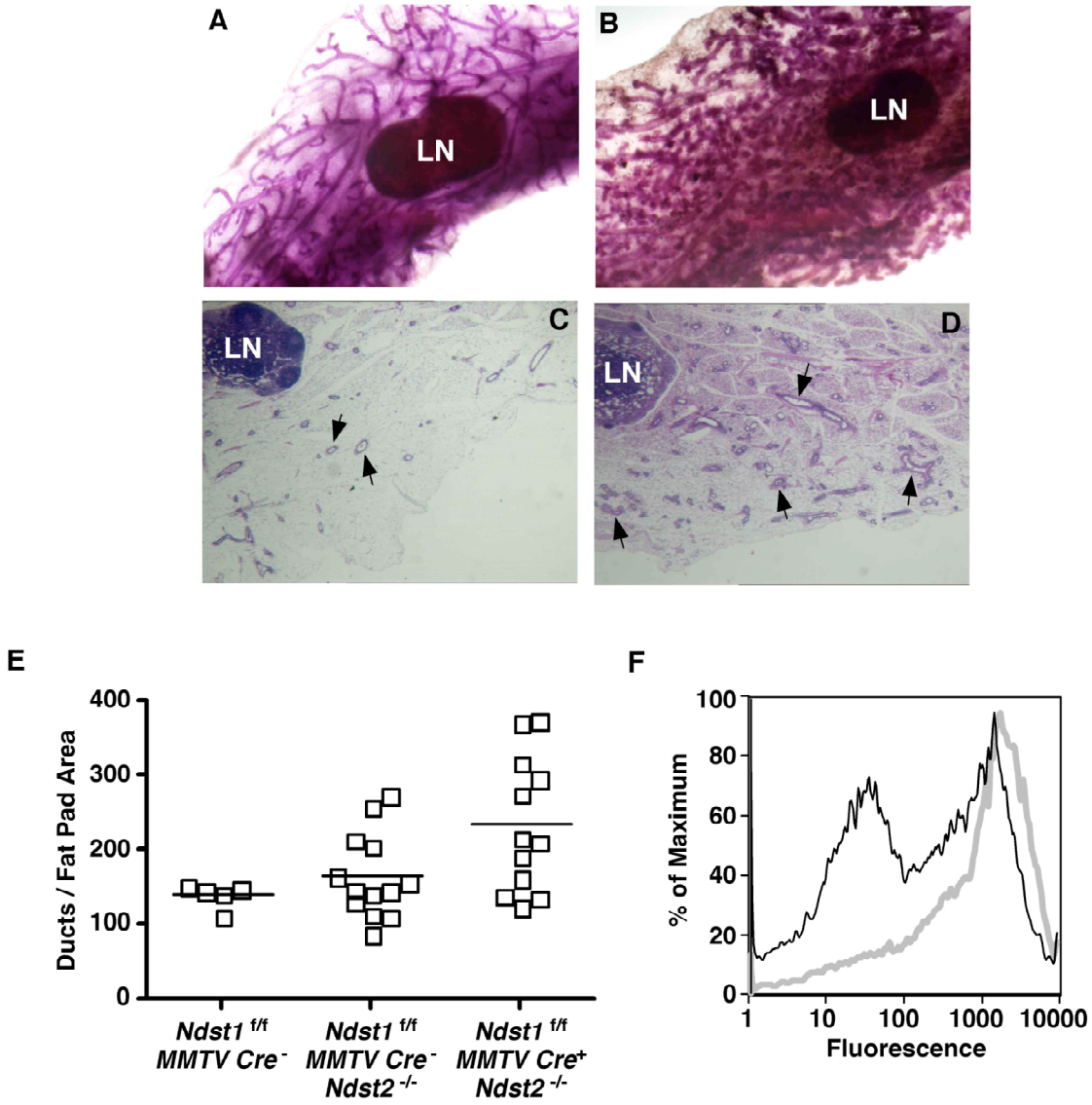

Figure 2-6: Ndst deficient glands show hyperbranched epithelial ducts Whole mounts and sections of the fourth inguinal glands. (**A**) Whole mount of *Ndst1*$^{f/f}$ *MMTV Cre*$^{-}$ *Ndst2*$^{-/-}$ gland at 10 weeks (**B**) Whole mount of *Ndst1*$^{f/f}$ *MMTV Cre*$^{+}$ *Ndst2*$^{-/-}$ (score of 4) gland at 10 weeks (**C**) Histology section of *Ndst1*$^{f/f}$ *MMTV Cre*$^{-}$ *Ndst2*$^{-/-}$ gland at 10 weeks (black arrows point to ducts) (**D**) Histology section of *Ndst1*$^{f/f}$ *MMTV Cre*$^{+}$ *Ndst2*$^{-/-}$ gland at 10 weeks (black arrows point to ducts) (**E**) Quantification of gland hyperbranching measured in number of ducts per area of fat pad (**F**) FGF2 binding to *Ndst1*$^{f/f}$ *MMTV Cre*$^{-}$ *Ndst2*$^{-/-}$ isolated epithelia (grey line) and *Ndst1*$^{f/f}$ *MMTV Cre*$^{+}$ *Ndst2*$^{-/-}$ isolated epithelia (black line).

***Hs2st* participates in primary and secondary branching.** *Ext-1* deficiency represents a drastic change to mammary epithelial cell heparan sulfate. To examine the affect of minor changes to the mammary epithelial cell heparan sulfate on ductal branching, we targeted the 2-O-sulfotransferase gene (*Hs2st*). The HS2ST enzyme transfers a sulfate to the 2 position of an iduronic acid of a heparan sulfate chain. This modification is crucial to the heparan sulfate binding of many growth factors found in mammary gland development including FGF-2. We inactivated *Hs2st* selectively in mammary epithelial cells by cross breeding mice with a conditional allele of *Hs2st* (*Hs2st*$^{f/f}$) to *MMTV Cre* mice. The breeding resulted in littermate pairs of *Hs2st*$^{f/f}$ *MMTV Cre*$^{+}$ (mutant) mice and *Hs2st*$^{f/f}$ *MMTV Cre*$^{-}$ (wildtype) mice. Mice of both genotypes were seen at the expected Mendelian frequency. *Hs2st*$^{f/f}$ *MMTV Cre*$^{-}$ glands at 10-12 weeks (Fig. 2-7A and C) appeared to have a wildtype amount of branching. *Hs2st*$^{f/f}$ *MMTV Cre*$^{+}$ glands showed a reduction in overall branching (Fig. 2-7B). There were long stretches of epithelial tube without any branch points (Fig. 2-7D). To statistically represent the loss of branching found in *Hs2st*$^{f/f}$ *MMTV Cre*$^{+}$ glands, we counted the total number of branch points per high powered field. The *Hs2st*$^{f/f}$ *MMTV Cre*$^{+}$ glands exhibited a three fold reduction in branching (Fig 2-7G).

Ductal branching is divided into two different mechanisms. Primary branching is facilitated by bifurcation and proliferation of the terminal end buds (TEBs). Secondary branching occurs from existing ductal structures. We examined glands from both wildtype and mutant mice at 5 weeks of age (during ductal branching). *Hs2st*$^{f/f}$ *MMTV Cre*$^{-}$ glands had a wildtype amount of TEBs and showed secondary

ductal branching (Fig. 2-7E). *Hs2st*$^{f/f}$ *MMTV Cre*$^{+}$ glands seemed to show a reduction in both TEB number and exhibited a complete lack of secondary ductal branching (Fig 2-7F).

To determine the extent of cell surface heparan sulfate alteration in *Hs2st*$^{f/f}$ *MMTV Cre*$^{+}$ glands, we isolated mammary epithelia and used FGF-2 as a heparan sulfate probe. FGF-2 binding is dependent on the 2-O-sulfate modification for binding to heparan sulfate. CHO-K1 cells bound FGF-2 (Fig. 2-7H, grey line) but CHO cells deficient in 2ost (pgsF17) exhibited a three log reduction in FGF-2 binding (Fig 2-7H, black line). Primary mammary epithelia isolated from *Hs2st*$^{f/f}$ *MMTV Cre*$^{-}$ glands bound FGF-2 (Fig. 2-7I, grey line), but cells isolated from *Hs2st*$^{f/f}$ *MMTV Cre*$^{+}$ glands had a reduction in FGF-2 binding (Fig. 2-7I, black line). These results suggested that the deficiency in branching seen in *Hs2st* deficient glands is due to a change in the cell surface heparan sulfate of the epithelial cells.

Figure 2-7. *Hs2st* deficient glands show decreased ductal branching. Whole mounts of the fourth inguinal mammary gland. **(A, C)** *Hs2st*$^{f/f}$ *MMTV cre*$^{-}$ gland at ten weeks. **(B, D)** *Hs2st*$^{f/f}$ *MMTV cre*$^{+}$ gland at ten weeks. **(E)** *Hs2st*$^{f/f}$ *MMTV cre*$^{-}$ gland at five weeks. **(F)** *Hs2st*$^{f/f}$ *MMTV cre*$^{+}$ gland at five weeks. **(G)** Graph that shows the number of branch points per 1mm^2 in a ten week gland in *Hs2st*$^{f/f}$ *MMTV cre*$^{-}$ versus *Hs2st*$^{f/f}$ *MMTV cre*$^{+}$ animals. **(H)** CHO cells reacted with biotinylated FGF-2, stained with PE-Cy5-streptavidin and analyzed by flow cytometry. Black line curve, 2ost deficient CHO with biotinylated FGF-2; grey line curve, Wildtype CHO cells with biotinylated FGF-2. (**I**) Black line curve, *Hs2st*$^{f/f}$ *MMTV cre*$^{+}$ mammary epithelial cells with biotinylated FGF-2; grey line curve, *Hs2st*$^{f/f}$ *MMTV cre*$^{-}$ mammary epithelial cells with biotinylated FGF-2.

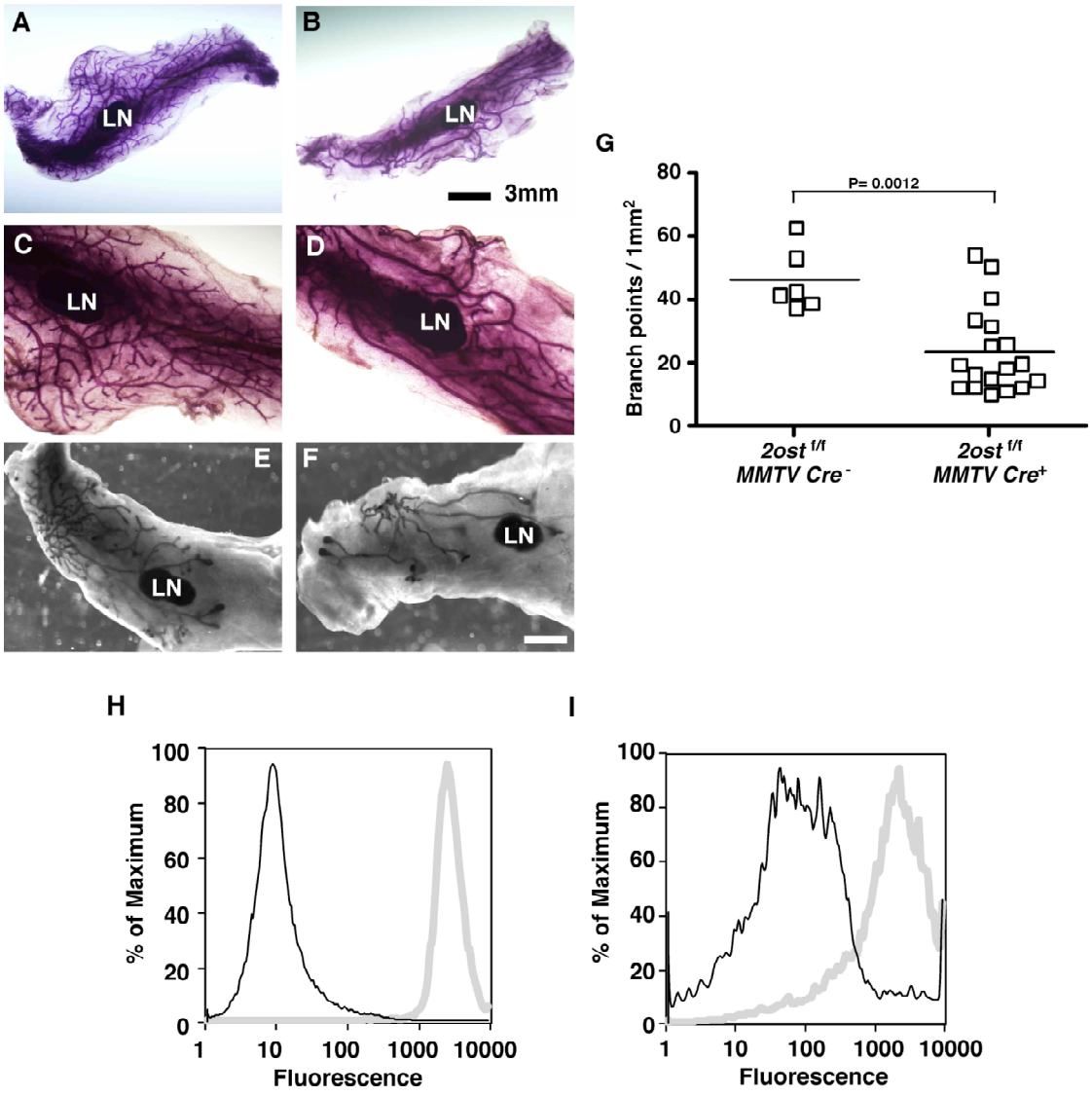
A
LN
B
LN
3mm
C
LN
D
LN
E
LN
F
LN
G
P= 0.0012
Branch points / 1mm²
80
60
40
20
0
2ost f/f MMTV Cre-
2ost f/f MMTV Cre+
H
% of Maximum
100
80
60
40
20
0
1
10
100
1000
10000
Fluorescence
I
% of Maximum
100
80
60
40
20
0
1
10
100
1000
10000
Fluorescence

2.4 Discussion

Previous work in the mammary field suggests that sulfated GAGs are present in growing mammary ducts, and that proteoglycans may have an effect on mammary ductal branching. To examine if these interactions are necessary for pubertal branching, we targeted mammary epithelial heparan sulfate production by inactivating the biosynthetic enzymes responsible for heparan sulfate polymerization and modification using the Cre recombinase under the control of the MMTV promoter. Altering heparan sulfate production had a striking effect on branching morphogenesis and the targeting of specific modifications along the chain led to aberrant phenotypes.

Mammary epithelia lacking EXT1 (heparan sulfate co-polymerase) fail to undergo ductal branching in response to pubertal hormones released at the onset of the estrous cycle. This phenotype is dramatic and highly penetrant and has not been observed in proteoglycan core protein gene knockouts. Some variability in the penetrance was observed due to inefficient Cre recombinase activity, but this seems like a minor shortcoming in the system. Since multiple heparin-binding growth factors are important to mammary ductal branching (Jackson et al., 1997; Luetteke et al., 1999; Yant et al., 1998), the complete loss of heparan sulfate chains probably affects multiple steps. It could also alter ECM formation and tissue organization. A major effort needs to be devoted to defining the specific growth factors and matrix molecules affected in this system.

The *Ext1* mutant defines a role for the heparan sulfate chain in mammary epithelial ductal branching, but does not address the importance of chain modification. To look at the role of sulfation, we produced mammary epithelia deficient in both NDST1 and NDST2. These isozymes initiate chain modification by creating the preferred substrate for all subsequent downstream modifications. Thus, an *Ndst*-deficient cell produces a chain devoid of any sulfate groups. Complete loss of both *Ndst1* and *Ndst2*, which occurs in 25% of mutant glands, blocked the ability of epithelia to form ducts and branch. This result implies that the chain by itself is not sufficient for epithelial duct formation.

Interestingly, inactivation of *Ndst1* and *Ndst2 in vivo* yielded a significant proportion of glands containing a mixture of $Ndst1^{-/-}Ndst2^{-/-}$ and $Ndst1^{+/+}Ndst2^{-/-}$ cells, likely due to inefficient Cre recombination and rescue of doubly mutant cells by cells expressing partially sulfated heparan sulfate. Examination of these glands revealed pubertal hyperbranching. A dramatic increase in both bifurcated end bud branching as well as side branching occurred. The hyperbranching phenotype is seen, regardless of the stage of growth arrest in the gland.

To further explore the role of specific sulfation events along the heparan sulfate chain in mammary epithelial ductal branching, we targeted HS2ST, which adds a 2-O-sulfate group to uronic acids. Mammary epithelia deficient in *Hs2st* show defects in the number and complexity of branched epithelia. Examination of mutant glands during ductal branching reveal a decrease in secondary branches and bifurcated terminal end buds. This result is very important, because it implies that a specific set

of growth factors and extracellular matrix components control secondary branching by interacting with the 2-O-sulfate groups on heparan sulfate chains. The importance of these studies is that (i) we have shown that MEC heparan sulfate has a cell autonomous effect on development; and (ii) the pattern of sulfation of the chain determines the extent of dichotomous branching, side branching, and formation of lobuloalveoli. We infer that that the way that this structural information is translated by cells is via binding and activation of different sets of heparin-binding growth factors and ECM components in the gland.

Many growth factors relevant to mammary gland development bind to heparan sulfate including FGF family members (Rapraeger et al., 1991), EGF family members (Aviezer and Yayon, 1994) and HGF (Zioncheck et al., 1995), To examine if heparan sulfate interacts with different growth factors during branching, we set up an *in vitro* system using Matrigel supplemented with growth factors. The results showed that *in vitro* mammary epithelial ductal branching can be induced by multiple members of the FGF family and HB-EGF, and this system depends on sulfation.

Single growth factor knockouts in the mammary gland rarely abrogate ductal growth. Compensation by different sets of growth factors could account for the mild phenotypes. Because many of these growth factors bind to heparan sulfate, altering its formation is equivalent to a combined mutation of multiple growth factors. Taking that into consideration, it is no surprise that heparan sulfate deficiency completely abrogates branching, and that small changes along the heparan sulfate chain have dramatic effects.

2.5 Materials and Methods

Transgenic Mice. All animals were handled in accordance with protocols for the humane treatment of animals approved by the IACUC and Animal Subjects Committee at the University of California San Diego. Mice bearing a loxP flanked allele of *Ext1* (*Ext1*$^{f/f}$) were obtained from Dr. Y. Yamaguchi (Burnham Institute, La Jolla, CA). Mice bearing a loxP flanked allele of *Hs2st* (*Hs2st*$^{f/f}$) were created in the Esko lab. The MMTV Cre line "A" mice in the 129 background was obtained from Dr. T. Wynshaw-Boris (University of California, San Diego) (Wagner et al., 1997) (Wagner et al., 2001). Cross breeding between the genotypes was initiated to obtain *Ext1* $^{f/f}$ *MMTV cre*$^{-}$ and *Ext1* $^{f/f}$ *MMTV cre*$^{+}$ littermates and *Hs2st* $^{f/f}$ *MMTV cre*$^{-}$ and *Hs2st* $^{f/f}$ *MMTV cre*$^{+}$ littermates. Only male mice carrying the MMTV Cre allele were used for breeding to avoid deletion of the conditional allele by Cre expression in oocytes. All the experiments were done with mice on a mixed background with littermate controls. Quantitative and qualitative aspects of phenotypes did not change with further crossing of *c-met* $^{f/f}$ *MMTV cre*$^{-}$ females and *c-met* $^{f/f}$ *MMTV cre*$^{+}$ females.

Cell Culture. Primary mammary epithelia were isolated and cultured following an established protocol (Pullan et al., 1996). Number 3 and 4 glands were excised and chopped with a razor blade, and digested with 0.2% trypsin and 0.2% collagenase A (Roche, Nutley, NJ). Cells were enriched by differential centrifugation. Tissue culture plates were precoated with 100ml/cm^2 of Ham's F12 (Invitrogen, Carlsbad, CA) medium containing 20% heat-inactivated fetal bovine serum (FBS)

(Atlanta Biologicals, Lawrenceville, GA) and 1mg/ml fetuin (Sigma, St. Louis, Mo). Cells were cultured in Ham's F12 medium containing 10% heat-inactivated FBS, 5mg/ml insulin, 1mg/ml hydrocortisone, 5ng/ml epidermal growth factor, 50mg/ml gentamycin, 100U/ml penicillin, and 100mg/ml streptomycin (all from Sigma). The medium was changed every day. In some experiments, cells were treated with heparan lyase (Ibex, Montreal, Quebec), in others they were treated with sodium chlorate.

bFGF Binding. The binding of basic Fibroblast Growth Factor (bFGF) was determined using flow cytometry. Isolated mammary epithelial cells were incubated with biotinylated bFGF in Hams F12 medium (Invitrogen, Carlsbad, CA) with 0.5 % BSA (Sigma, St. Louis, MO) for 1 hour with shaking at 4ºC. Cells were washed twice in PBS and incubated in PBS containing streptavidin-APC for 20 minutes with shaking at 4ºC. Samples where bFGF was omitted were included as negative controls. To show that bFGF binding was related to heparan sulfate expression, controls were also performed after pre-treatment of mammary epithelial cells with heparin lyases for 4 hours at 37 ºC.

Mammary Gland Histology. Histological analyses were performed by the Cancer Center Histology Core at the University of California, San Diego. Whole mounts were stained with hematoxylin (Fisher, Pittsburgh, PA) as described (Ip and Asch, 2000). Hematoxylin and eosin staining of sections was performed by standard procedures.

Mammary organoids culture. Mammary organoids were cultured according to a previously established protocol (Sternlicht et al., 2005). Briefly, adult ductal trees from glands 3 and 4 were excised and chopped with a razor blade, and digested with 0.2% trypsin and 0.2% collagenase A. The suspension was centrifuged at 300 g for 5 minutes and the pellets were gently agitated at room temperature for 2 minutes in DMEM/F12 with 40 U/ml TURBO Dnase (Ambion, Austin, TX). Cell clusters and dissociated single cells were pelleted at 300 g, washed with DMEM/F12, recentrifuged and resuspended in growth factor reduced Matirgel (Becton Dickinson, Franklin Lakes, NJ). The suspended organoids were transferred to 48-well plates over a thin cell free layer of Matirgel and allowed to gel at 37C. Following gel formation, 400ml of basal medium (ITS liquid media supplement (Sigma, St. Louis, MO) 100U/ml penicillin G in Hams F12) was added with or without growth factor and or 45mM sodium chlorate, and the organoids were cultured in a 5% CO2 incubator at 37C. Growth was observed over 7 days in the presence or absence of: FGF-2 (300ng/ml), FGF-10 (300ng/ml) (Sigma, St Louis, MO); FGF-7 (300ng/ml) (Reseach Diagnostics Inc., Concord, MA); and HB-EGF (60ng/ml) (R&D Systems, Minneapolis, MN).

2.6 References

Affolter, M., Bellusci, S., Itoh, N., Shilo, B., Thiery, J. P., and Werb, Z. (2003). Tube or not tube: remodeling epithelial tissues by branching morphogenesis. Dev Cell *4*, 11-18.

Aviezer, D., and Yayon, A. (1994). Heparin-dependent binding and autophosphorylation of epidermal growth factor (EGF) receptor by heparin-binding EGF-like growth factor but not by EGF. ProcNatlAcadSciUSA *91*, 12173-12177.

Bullock, S. L., Fletcher, J. M., Beddington, R. S., and Wilson, V. A. (1998). Renal agenesis in mice homozygous for a gene trap mutation in the gene encoding heparan sulfate 2-sulfotransferase. Genes Dev *12*, 1894-1906.

Fan, G., Xiao, L., Cheng, L., Wang, X., Sun, B., and Hu, G. (2000). Targeted disruption of NDST-1 gene leads to pulmonary hypoplasia and neonatal respiratory distress in mice. FEBS Lett *467*, 7-11.

Gordon, J. R., and Bernfield, M. R. (1980). The basal lamina of the postnatal mammary epithelium contains glycosaminoglycans in a precise ultrastructural organization. Dev Biol *74*, 118-135.

Grobe, K., Inatani, M., Pallerla, S. R., Castagnola, J., Yamaguchi, Y., and Esko, J. D. (2005). Cerebral hypoplasia and craniofacial defects in mice lacking heparan sulfate Ndst1 gene function. Development *132*, 3777-3786.

Howlin, J., McBryan, J., and Martin, F. (2006). Pubertal mammary gland development: insights from mouse models. J Mammary Gland Biol Neoplasia *11*, 283-297.

Ip, M. M., and Asch, B. B. (2000). Methods in mammary gland biology and breast cancer (New York: Kluwer Academic/Plenum Publishers).

Jackson, D., Bresnick, J., Rosewell, I., Crafton, T., Poulsom, R., Stamp, G., and Dickson, C. (1997). Fibroblast growth factor receptor signalling has a role in lobuloalveolar development of the mammary gland. J Cell Sci *110 (Pt 11)*, 1261-1268.

Li, J. P., Gong, F., Hagner-McWhirter, A., Forsberg, E., Abrink, M., Kisilevsky, R., Zhang, X., and Lindahl, U. (2003). Targeted disruption of a murine glucuronyl C5-epimerase gene results in heparan sulfate lacking L-iduronic acid and in neonatal lethality. J Biol Chem *278*, 28363-28366.

Lin, X., Wei, G., Shi, Z. Z., Dryer, L., Esko, J. D., Wells, D. E., and Matzuk, M. M. (2000). Disruption of gastrulation and heparan sulfate biosynthesis in EXT1-deficient mice. Dev Biol *224*, 299-311.

Liu, B. Y., McDermott, S. P., Khwaja, S. S., and Alexander, C. M. (2004). The transforming activity of Wnt effectors correlates with their ability to induce the accumulation of mammary progenitor cells. Proc Natl Acad Sci U S A *101*, 4158-4163.

Luetteke, N. C., Qiu, T. H., Fenton, S. E., Troyer, K. L., Riedel, R. F., Chang, A., and Lee, D. C. (1999). Targeted inactivation of the EGF and amphiregulin genes reveals distinct roles for EGF receptor ligands in mouse mammary gland development. Development *126*, 2739-2750.

Merry, C. L. R., Bullock, S. L., Swan, D. C., Backen, A. C., Lyon, M., Beddington, R. S. P., Wilson, V. A., and Gallagher, J. T. (2001). The molecular phenotype of heparan sulfate in the *Hs2st*$^{-/-}$ mutant mouse. J Biol Chem *276*, 35429-35434.

Pullan, S., Wilson, J., Metcalfe, A., Edwards, G. M., Goberdhan, N., Tilly, J., Hickman, J. A., Dive, C., and Streuli, C. H. (1996). Requirement of basement membrane for the suppression of programmed cell death in mammary epithelium. J Cell Sci *109 (Pt 3)*, 631-642.

Rapraeger, A. C., Krufka, A., and Olwin, B. B. (1991). Requirement of heparan sulfate for bFGF-mediated fibroblast growth and myoblast differentiation. Science *252*, 1705-1708.

Ringvall, M., Ledin, J., Holmborn, K., Van Kuppevelt, T., Ellin, F., Eriksson, I., Olofsson, A. M., Kjellén, L., and Forsberg, E. (2000). Defective heparan sulfate biosynthesis and neonatal lethality in mice lacking N-deacetylase/N-sulfotransferase-1. J Biol Chem *275*, 25926-25930.

Ruan, W., and Kleinberg, D. L. (1999). Insulin-like growth factor I is essential for terminal end bud formation and ductal morphogenesis during mammary development. Endocrinology *140*, 5075-5081.

Silberstein, G. B., and Daniel, C. W. (1982). Glycosaminoglycans in the basal lamina and extracellular matrix of the developing mouse mammary duct. Dev Biol *90*, 215-222.

Sternlicht, M. D., Sunnarborg, S. W., Kouros-Mehr, H., Yu, Y., Lee, D. C., and Werb, Z. (2005). Mammary ductal morphogenesis requires paracrine activation of stromal EGFR via ADAM17-dependent shedding of epithelial amphiregulin. Development *132*, 3923-3933.

Stickens, D., Zak, B. M., Rougier, N., Esko, J. D., and Werb, Z. (2005). Mice deficient in Ext2 lack heparan sulfate and develop exostoses. Development *132*, 5055-5068.

Wagner, K. U., McAllister, K., Ward, T., Davis, B., Wiseman, R., and Hennighausen, L. (2001). Spatial and temporal expression of the Cre gene under the control of the MMTV-LTR in different lines of transgenic mice. Transgenic Res *10*, 545-553.

Wagner, K. U., Wall, R. J., St-Onge, L., Gruss, P., Wynshaw-Boris, A., Garrett, L., Li, M., Furth, P. A., and Hennighausen, L. (1997). Cre-mediated gene deletion in the mammary gland. Nucleic Acids Res *25. 25*, 4323-4330.

Yant, J., Buluwela, L., Niranjan, B., Gusterson, B., and Kamalati, T. (1998). In vivo effects of hepatocyte growth factor/scatter factor on mouse mammary gland development. Exp Cell Res *241*, 476-481.

Zcharia, E., Metzger, S., Chajek-Shaul, T., Friedmann, Y., Pappo, O., Aviv, A., Elkin, M., Pecker, I., Peretz, T., and Vlodavsky, I. (2001). Molecular properties and involvement of heparanase in cancer progression and mammary gland morphogenesis. J Mammary Gland Biol Neoplasia *6*, 311-322.

Zioncheck, T. F., Richardson, L., Liu, J., Chang, L., King, K. L., Bennett, G. L., Fügedi, P., Chamow, S. M., Schwall, R. H., and Stack, R. J. (1995). Sulfated oligosaccharides promote hepatocyte growth factor association and govern its mitogenic activity. JBiolChem *270*, 16871-16878.

2.7 Acknowledgements

Chapter 2 is a reprint of material intended to be submitted for publication by Garner, B. Omai; Crawford E. Brett; and Esko D. Jeffrey. The dissertation author was the primary researcher and author of this paper.

Chapter 3: The Tyrosine Kinase Receptor Met is not Required for Mammary Epithelial Ductal Branching

3.1 Summary

Branching morphogenesis in the mammary gland depends on a large number of growth factors, many of which bind to heparan sulfate. HGF-Met signaling in primary mammary epithelia is dependent on heparan sulfate. To test the physiological relevance of HGF-Met signaling in mammary gland branching morphogenesis, we inactivated of the Met tyrosine kinase receptor gene *cmet* in mammary epithelial cells. To our surprise, tissue specific inactivation of *cmet* in the mammary epithelia does not affect branching morphogenesis. Furthermore, HGF is not able to efficiently induce branching in an *in vitro* model of branching morphogenesis as compared to other growth factors. Although we cannot exclude the possibility of compensation by other growth factors, these findings demonstrate that the HGF-Met interaction is not critical for branching morphogenesis in the mammary gland.

3.2 Introduction

Hepatocyte growth factor (HGF) is a 82kDa protein produced by mesenchymal cells and acts on surrounding epithelia. HGF can elicit a diverse range of responses including cell division, motility, and ductal branching. It is made as an inactive precursor that is cleaved into an active heterodimer. (Lyon et al., 1994). HGF

facilitates its biological activity through interactions with a single high affinity tyrosine kinase receptor; Met. Met is a 190 kDa transmembrane glycoprotein that is cleaved into a heterodimer. It is encoded by the gene *cmet.* Activation of Met by HGF results in receptor dimerization and tyrosine phosphorylation. This creates a unique docking site intracellularly, for downstream signaling that gives rise to the aforementioned range of biological activities (Kemp et al., 2006).

The interaction of HGF and Met may be facilitated by heparan sulfate (HS) proteoglycans. Heparan sulfate proteoglycans are known to play a role in growth factor/ tyrosine kinase interactions. It is clear that heparan sulfate can enhance the stability of the FGF (fibroblast growth factor) -FGFR complex. Heparan sulfate can also increase the local concentration growth factor at the cell surface. Heparan sulfate has not been shown to be required for the interaction between HGF and Met *in vivo*, but *in vitro*, heparin (a highly sulfated form of heparan sulfate) increases the mitogenic action of HGF and causes the oligermization of HGF (Zioncheck et al., 1995), which may facilitate interaction with Met. Basic clusters found in HGF facilitate the interaction between HGF and heparin (Mizuno et al., 1994). HGF also interacts with heparan sulfate, and the interaction between them requires a HS sequence containing iduronic acid and 6-o-sulfate modifications, differentiating it from the FGF-HS interaction (Lyon et al., 1994). Addition of heparin to HS-deficient CHO cells restored HGF signaling through Met tyrosine phosphorylation (Sakata et al., 1997). Met has also been found to interact with heparan sulfate (Rubin et al., 2001). Chlorate (sulfation inhibitor) treatment of renal epithelia inhibits HGF binding to the cell

surface and diminishes HGF dependent downstream signaling (Deakin and Lyon, 1999). Taken cumulatively, this data suggests heparan sulfate facilitates the interaction between HGF and Met.

The HGF-Met interaction has been implicated to play an important role in mammary epithelial morphogenesis. In early embryonic studies, HGF was found expressed by mesenchymal cells, and Met was found in the proximal epithelia (Sonnenberg et al., 1993). HGF and Met were also found to be expressed in mouse mammary tissue. Their expression was temporally regulated; the genes were expressed during virgin branching morphogenesis (6 weeks) and during the process of ductal hyperbranching found in the early stages of pregnancy (Niranjan et al., 1995). Mouse mammary fibroblasts produced HGF, while c-met was expressed on both luminal and myoepithelia.

In vitro branching models have shown that HGF-Met may be able to facilitate ductal branching. HGF was able to induce a tubular branching morphogenesis in TAC-2 clonal human mammary epithelia cells plated in a collagen matrix (Soriano et al., 1998) and EpH4 clonal mouse mammary epithelial cells plated in Matrigel (Niemann et al., 1998), (Berdichevsky et al., 1994). HGF treatment of primary mouse mammary epithelia induced tube formation in collagen gels (Kamalati et al., 1999). Finally, organ culture showed that HGF treatment was able to induce intensified growth resulting in numerous main ducts. Expression of antisense oligonucleotides to HGF blocked ductal branching of the glands (Yang et al., 1995).

In vivo overexpression studies of HGF induced a range of alterations in the virgin mammary gland. Transgenic overexpression of HGF in the whole animal induced a broad range of epithelial tumors including mammary (Takayama et al., 1997). Transplanted epithelia, virally overexpressing HGF, affected the structure and multiplicity of terminal end buds, resulting in a more highly branched gland (Yant et al., 1998). These results suggest that HGF plays an *in vivo* role in ductal branching.

Whole animal knockout models have not been informative for the role of the HGF-Met interaction in mammary epithelial branching. Systemic HGF knockout animals exhibit incomplete development and die in utero. The mutants show a reduced liver size and impairment in development of the placenta. (Schmidt et al., 1995). Met knockout animals exhibit the exact same phenotype in addition to defects in myogenesis of limb buds, diaphragm, and tip of the tongue (Bladt et al., 1995).

To study the role of HGF-Met in the mammary gland, we have used a conditional allele of *c-met* with the Cre-loxP recombination system to delete *c-met* in a tissue specific manner, in mammary epithelia.

Here, we show that signaling by HGF in primary mammary epithelia is dependent on heparan sulfate. Tissue specific inactivation of *cmet* in the mammary epithelia does not affect ductal branching. HGF is not able to efficiently induce branching in an *in vitro* model of branching morphogenesis; as compared to other heparan sulfate binding growth factors that are present *in vivo* during ductal branching. Thus, the HGF-Met interaction is not critical to branching morphogenesis in the mammary gland.

3.3 Results

Mammary epithelial signaling is dependent on heparan sulfate. There is a well established interaction between HGF-Met and heparan sulfate in both in vitro binding studies and in renal epithelial cells. We wanted to explore the role of heparan sulfate in HGF-Met interactions in primary mammary epithelia. HGF induces Met dimerization and trans-auto-tyrosine phosphorylation. This creates a docking site for signaling mediators including Src tyrosine kinase, PI3 Kinase, and various adaptor proteins including Grb2. Many of these signals converge on the MAP kinase pathway and lead to Erk phosphorylation (Rosario and Birchmeier, 2003). To study this effect, we treated wild type primary mammary epithelia with increasing concentrations of HGF (0-10ng/ml) for 20 minutes in the presence of heparan lyase, an enzyme that cleaves cell surface heparan sulfate (Fig 3-1). Without enzyme treatment, increasing concentrations of HGF elicited an increasing pErk signal. Upon treatment with heparan lyase, there was a marked decrease in pErk signaling at 1 and 3ng/ml HGF treatment. Downstream signaling mediated by HGF was partially dependent on cell surface heparan sulfate.

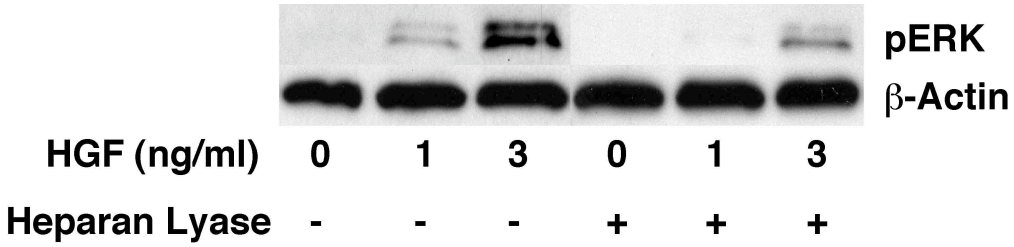

Figure 3-1: Heparan sulfate dependent signaling in primary mammary epithelial cells. Isolated primary mammary epithelial cells were treated with increasing concentrations of HGF (0-10ng/ml) for 20 minutes in the presence or absence of heparan lyase. Western blots determined intracellular signal intensity for pErk and B-Actin.

Normal branching morphogenesis in the absence of *cmet*. In wildtype mice, branching morphogenesis of the mammary ductal epithelia occurs from 4 to 10 weeks, concurrent with the beginiing of the estrous cycle. We asked whether the HGF-Met interaction was crucial for branching morphgenesis by conditionally inactivating the gene *cmet*, that codes for the tyrosine kinase receptor Met. Analysis of whole mount glands stained with hematoxylin from 12 week old *cmet* $^{f/f}$ *MMTVcre*$^{+}$ (mutant) animals (Fig. 3-2B and D) showed wild types amounts of branched epithelia and all fat pads were full, compared to *cmet* $^{f/f}$ *MMTVcre*$^{-}$ (wildtype) littermate controls (Fig 3-2A and C). To make sure the *cmet* $^{f/f}$ *MMTVcre*$^{+}$ glands were deficient in Met, we isolated epithelia from mutant and wildtype glands and analyzed protein expression of Met, along with downstream signals affected by the presence of Met. The *cmet* $^{f/f}$ *MMTVcre*$^{+}$ gland showed a reduction in Met protein as compared to the wildtype epithelia (Fig 3-2E). Previous work (Beviglia and Kramer, 1999) had shown that breast carcinoma cells phosphorylated FAK (focal adhesion kinase) in response to HGF treatment. We looked at the resting state of pFAK state and saw a reduction in pFAK with total FAK levels as a control. To confirm that HGF signaling had been abolished in *cmet* $^{f/f}$ *MMTVcre*$^{+}$ glands, we isolated mammary epithelia from both mutant and wildtype glands, and treated them with HGF. HGF has been shown to induce a strong pErk signal in mammary epithelia (Fig 3-1). *Cmet* $^{f/f}$ *MMTVcre*$^{-}$ epithelia showed a strong pErk signal upon treatment with 10ng/ml HGF for 20 minutes. *Cmet* $^{f/f}$ *MMTVcre*$^{+}$ epithelia showed no pErk response to HGF. These results suggests that the HGF-Met interaction is not critical to mammary ductal branching.

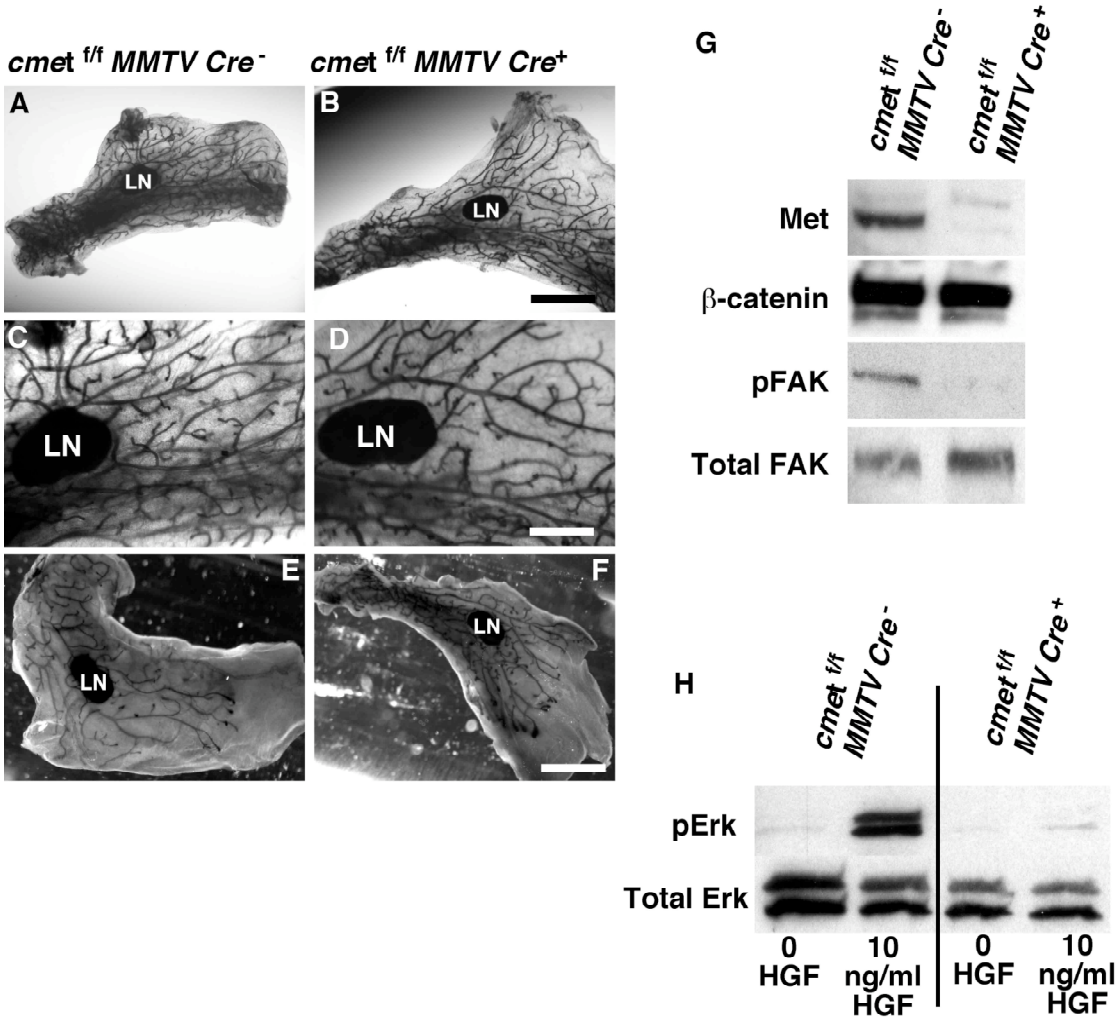

Figure 3-2. Mammary glands deficient in the C-met tyrosine kinase receptor. Whole mounts of mammary glands at 10 weeks. *c-met* $^{f/f}$ *MMTV Cre*$^{-}$ (**A** and **C**) and *c-met* $^{f/f}$ *MMTV Cre*$^{+}$ (**B** and **D**). Bar = 3mm in top panels, .7mm in bottom panels. Western blots of lysates from isolated primary epithelial cells of *c-met* $^{f/f}$ *MMTV Cre*$^{-}$ (wildtype) and *c-met* $^{f/f}$ *MMTV Cre*$^{+}$ (mutant) show intracellular signal intensity for c-met, B-catenin, pFAK and total FAK (**E**). Western blots of lysates from isolated primary epithelial cells of *c-met* $^{f/f}$ *MMTV Cre*$^{-}$ (wildtype) and *c-met* $^{f/f}$ *MMTV Cre*$^{+}$ (mutant) treated with HGF (10ng/ml for 20 minutes)(**F**). Intracellular signal intensity shown for pErk and total Erk.

HGF and *in vitro* branching morphogenesis. Previous data suggests that HGF can induce ductal branching in a number of in vitro branching models. This data conflicts with our reported mouse results. We wanted to revisit the branching model systems and look at the role of HGF. Many heparan sulfate binding growth factors are found spatially and temporally regulated during mammary gland development including FGFs, EGF family members and HGF. Many of these growth factors have been shown to induce branching in *in vitro* branching models. Taking advantage of a new system of mammary epithelial ductal branching (Sternlicht et al., 2005), we wanted to test the role of HGF-Met in ductal branching. Primary mammary epithelial cells plated into growth factor reduced Matrigel form a sphere of cells with a lumen on the inside (Fig. 3-3A black arrow). Upon treatment with a single growth factor e.g. FGF2, a complicated organoid structure of branches and end buds grow (Fig 3-3B). Previous experiments (Sternlicht et al., 2005)have shown that with varying efficiency, different growth factors can produce this effect. We tested the ability of HGF to form branched organoids from a sphere of primary epithelia and compared that to other growth factors found in the mammary gland. Branching was quantified by the percent of spheroids that achieved the branched state after seven days of treatment. Untreated spheroids did not branch. Spheroids treated with FGF-2 (300ng/ml) for 7 days showed 80% branching. FGF-7 (300ng/ml), FGF-10 (300ng/ml), EGF (30ng/ml) and HBEGF (60ng/ml) treatment all induced branching from 50% to 80% (Fig 3-3C). Treatment with HGF at 300ng/ml for seven days was not able to induce branching. Doubling the

concentration of HGF (600ng/ml) (HGF 2x) was only minimally able to induce branching. In this model system, HGF was not as efficient at inducing ductal branching (*in vitro*) as other growth factors relevant to mammary gland morphogenesis suggesting that HGF may not be important to *in vivo* ductal branching and correlating with the reported mouse data.

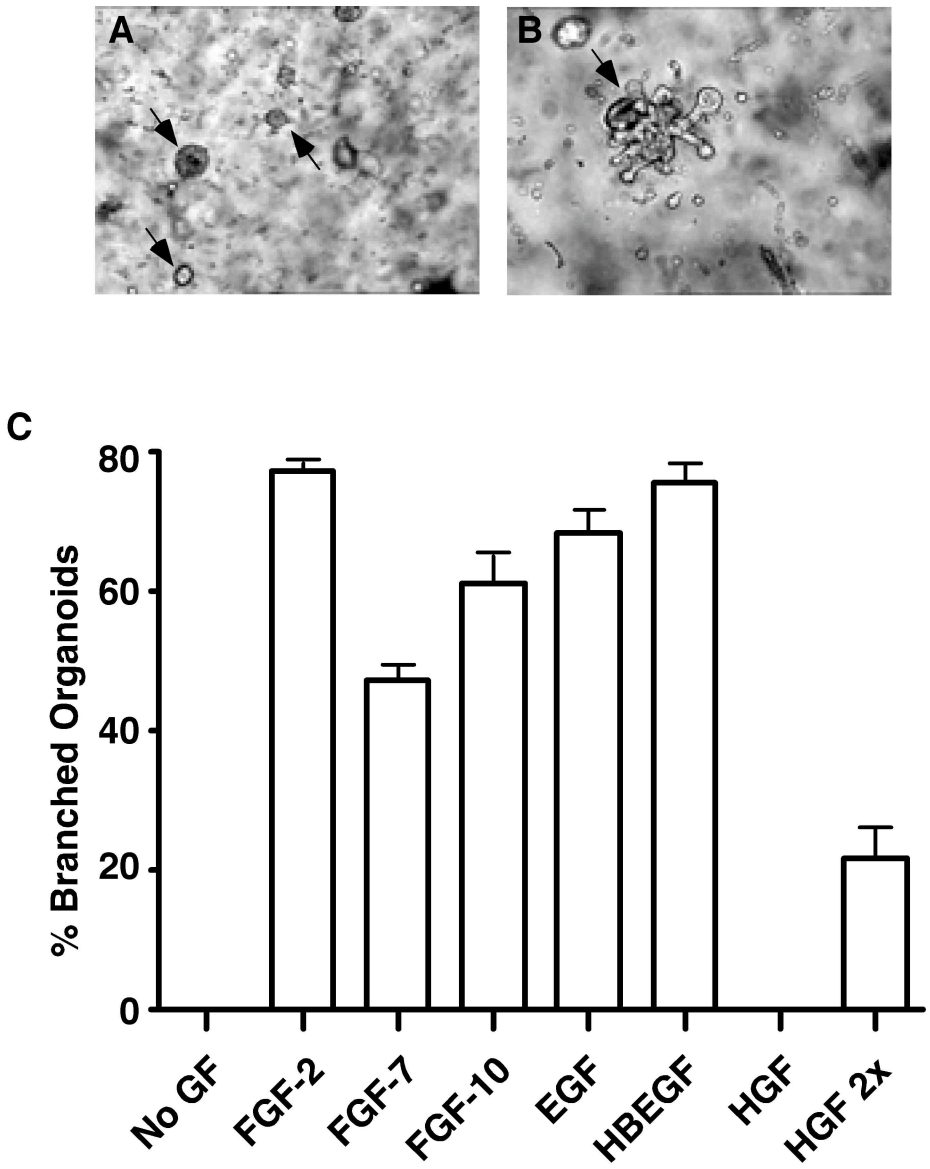

Figure 3-3. *In vitro* branching of primary mammary epithelial organoids in response to different growth factors. Isolated primary mammary epithelial cells were plated into growth factor reduced Matrigel in Hams F12, ITS buffer, and Penn. Spheroids formed within 24 hours (**A**). Upon treatment with FGF2 (300ng/ml) for 7 days, spheroids formed branched organoids structures (**B**). The number of spheroids that branched in response to no stimulation, FGF-2 (300ng/ml), HGF (300ng/ml), HGF 2x (600ng/ml), FGF-7 (300ng/ml), EGF (30ng/ml), FGF-10 (300ng/ml) and HB-EGF (60ng/ml) was calculated (**B**). Each bar represents the average of 3 isolations with three high powered fields counted per isoation +/- sd.

3.4 Discussion

Mammary epithelial branching morphogenesis coincides with the beginning of the mouse estrous cycle. Systemic hormones released during puberty facilitate the rapid growth of the ductal tree. Estrogen is the primary hormone that triggers growth in the gland. Removal of the ovaries abrogates ductal branching, which could be restored by the addition of estrogen. Subsequently, other steroid hormones including progesterone, glucocorticoid, and growth hormone have been shown to play a role in ductal branching, though they are not absolutely required; like estrogen (Howlin et al., 2006).

Terminal end buds (TEB) are the cellular structures responsible for proliferation and duct formation. It was found that the steroid receptor-expressing cells were not the cells facilitating proliferation but were often found adjacent to those cells. The effects of systemic hormones on proliferating cells are thought to be paracrine in nature. Systemic hormones induce stromal cells to release local growth factors that act on the proliferating cells of the terminal end bud. We wanted to explore whether these local growth factors are singularly necessary for ductal branching.

Many of these growth factors facilitate signaling through interactions with high affinity tyrosine kinase receptors. Both the growth factors and the receptors are found to be spatially and temporally regulated during ductal branching. One of these growth factor-receptor pairs is HGF and the tyrosine kinase receptor Met. HGF causes Met

dimerization, phosphorylation and signaling that leads to proliferation and cell migration. These processes may be vital to mammary ductal branching. Some of these interactions are mediated by low affinity interactions with heparan sulfate proteoglycans. Previous data suggests that HGF interacts with heparan sulfate to increase affinity for Met. Heparan sulfate deficiency in the mammary gland produces severe defects in branching morphogenesis and lobuloalveolar development (B. Crawford, O. Garner, J. Esko unpublished results) We wanted to test this interaction in primary mammary epithelia. Heparan lyase treated epithelia showed a reduction in Erk phosphorylation in response to HGF treatment. This implies that the interactions between HGF and heparan sulfate and Met is important in mammary epithelial signaling.

In vivo overexpression data suggests that HGF is involved in ductal epithelial branching. HGF transgenic animals showed overbranching of ductal epithelia. Systemic knockouts of HGF or Met were not informative because they died in utero of liver failure and placental defects. To explore the role of HGF-Met in mammary epithelial branching, we used a conditional knockout strategy to eliminate Met from ductal epithelia. These Met deficient glands showed no deficiency in pubertal ductal branching. This implies that the HGF-Met interaction is not necessary for ductal epithelial branching.

There are a variety of *in vitro* mammary branching morphogenesis assays that attempt to answer the question of growth factor relevance in the mammary gland. Most of them showed that HGF was able to initiate ductal epithelial. One weakness of

these assays, was that they were performed in a collagen matrix. While this is a defined extracellular matrix component, it does not convey the complexity found in the stroma and fat pad of the mammary gland. An additional weakness is the use of immortal mammary epithelial cell lines instead of primary cells. Finally, the branched organoids from these older assays did not accurately resemble branching in the mammary gland. A new assay of mammary epithelial ductal branching (Sternlicht et al., 2005), using primary mammary epithelia plated into Matrigel, was used to determine if HGF could facilitate ductal branching, compared to other growth factors found in the mammary gland. HGF was not able to induce the formation of branched organoids as compared to any of the FGFs (2,7, or 10), EGF, or HBEGF. This suggests that contrary to previous experiments, HGF may not be able to induce epithelial ductal branching.

These results correlate well with other single growth factor/ receptor knock outs in the mammary gland. FGF-2 and FGF-7 (Dono et al., 1998) deficient mice are able to nurse pups to weaning, implying that there are no major alterations in branching morphogenesis. There may be minor changes that have yet to be examined. A kinase negative form of FGFR1 (IIIc) or FGFR2 (IIIb) had no discernible affects on branching morphogenesis (Jackson et al., 1997). EGFR deficiency is expendable on the surface of the epithelium but is essential in the stroma (Wiesen et al., 1999). Targeted inactivation of EGF or TGFa had no effect on branching whereas targeted deletion of amphiregulin caused severely stunted ductal outgrowth (Luetteke et al.,

1999). Finally IGF-1 or IGF1R knockouts showed impaired ductal outgrowth, reduced TEBs and reduced duct number, but some branching still occurred.

These findings, combined with the new Met deficient results, suggest that the mammary gland may express more growth factors than is absolutely required for branching. This flexibility may allow the gland to sustain a single mutation, but still appropriately develop and function. It is possible that Met deficiency sensitizes the gland, so that an additional mutation may show dramatic phenotypes. We combined mutants of Met deficiency with heparan sulfate deficiency but saw no increase in severity in branching defects. One might predict that combining other growth factor mutations such as FGFs or EGFs with a Met deficiency may show dramatic alterations in ductal branching.

3.5 Materials and Methods

Transgenic Mice. All animals were handled in accordance with protocols for the humane treatment of animals approved by the IACUC and Animal Subjects Committee at the University of California San Diego. Mice bearing a loxP flanked allele of *c-met* (cmet$^{f/f}$) were obtained from Dr. S.S. Thorgeirsson (NIH, Maryland) (Huh et al., 2004). The MMTV Cre line "A" mice in the 129 background was obtained from Dr. T. Wynshaw-Boris (University of California, San Diego) (Wagner et al., 1997) (Wagner et al., 2001). Cross breeding between the two genotypes was initiated to obtain *c-met* $^{f/f}$ *MMTV cre*$^{-}$ and *c-met* $^{f/f}$ *MMTV cre*$^{+}$ littermates. Only male mice carrying the MMTV Cre allele were used for breeding to avoid deletion of the conditional allele by Cre expression in oocytes. All the experiments were done with mice on a mixed background with littermate controls. Quantitative and qualitative aspects of phenotypes did not change with further crossing of *c-met* $^{f/f}$ *MMTV cre*$^{-}$ females and *c-met* $^{f/f}$ *MMTV cre*$^{+}$ females.

Cell Culture. Primary mammary epithelia were isolated and cultured following an established protocol (Pullan et al., 1996). Number 3 and 4 glands were excised and chopped with a razor blade, and digested with 0.2% trypsin and 0.2% collagenase A (Roche, Nutley, NJ). Cells were enriched by differential centrifugation. Tissue culture plates were precoated with 100ml/cm^2 of Ham's F12 (Invitrogen, Carlsbad, CA) medium containing 20% heat-inactivated fetal bovine serum (FBS)

(Atlanta Biologicals, Lawrenceville, GA) and 1mg/ml fetuin (Sigma, St. Louis, Mo). Cells were cultured in Ham's F12 medium containing 10% heat-inactivated FBS, 5mg/ml insulin, 1mg/ml hydrocortisone, 5ng/ml epidermal growth factor, 50mg/ml gentamycin, 100U/ml penicillin, and 100mg/ml streptomycin (all from Sigma). The medium was changed every day. In some experiments, cells were treated with heparan lyase (Ibex, Montreal, Quebec).

Mammary Gland Histology. Histological analyses were performed by the Cancer Center Histology Core at the University of California, San Diego. Whole mounts were stained with hematoxylin (Fisher, Pittsburgh, PA) as described (Ip and Asch, 2000). Hematoxylin and eosin staining of sections was performed by standard procedures.

Western Blotting. Primary mammary epithelial cells were grown in 100cm tissue culture dishes. Some plates were treated with 10ng/ml HGF (Sigma, St. Louis, MO) for 20 minutes. Cells were lysed in 1%NP-40 buffer. Protein content was determined with the Bradford assay (BioRads, Hercules, CA) using BSA as a standard. Ten micrograms of protein from cultured cells was electrophoresed on BioRad precast Ready gels and transferred to nitrocellulose with a semidry blotting apparatus. The following antibodies were used: phospho-Erk1/2 (p44/42, Thr202/Tyr204), p44/p42, phosphoAkt/PKB (Ser308) (Cell Signaling Technology, Beverly, MA); phosphoFAK (pY397), FAK (Invitrogen, Carlsbad, CA); b-Actin

(Santa Cruz Biotechnology, Santa Cruz, CA); b-catenin (Abcam, Cambridge, MA). HRP-conjugated anti-rabbit were obtained from Biorad (Hercules, CA). HRP-conjugated anti-mouse IgG were obtained form Amersham Biosciences (Piscataway, NJ). HRP was detected using the SuperSignal West Pico chemiluminescent substrate (Pierce, Rockford, IL).

Mammary organoids culture. Mammary organoids were cultured according to a previously established protocol (Sternlicht et al., 2005). Briefly, adult ductal trees from glands 3 and 4 were excised and chopped with a razor blade, and digested with 0.2% trypsin and 0.2% collagenase A. The suspension was centrifuged at 300 g for 5 minutes and the pellets were gently agitated at room temperature for 2 minutes in DMEM/F12 with 40 U/ml TURBO Dnase (Ambion, Austin, TX). Cell clusters and dissociated single cells were pelleted at 300 g, washed with DMEM/F12, recentrifuged and resuspended in growth factor reduced Matirgel (Becton Dickinson, Franklin Lakes, NJ). The suspended organoids were transferred to 48-well plates over a thin cell free layer of Matirgel and allowed to gel at 37C. Following gel formation, 400ml of basal medium (ITS liquid media supplement (Sigma, St. Louis, MO) 100U/ml penicillin G in Hams F12) was added with or without growth factor, and the organoids were cultured in a 5% CO2 incubator at 37C. Growth was observed over 7 days in the presence or absence of: FGF-2 (300ng/ml), EGF (30ng/ml) (Invitrogen, Carlsbad, CA); HGF (300ng/ml or 600ng/ml), FGF-10 (300ng/ml) (Sigma, St Louis, MO); FGF-

7 (300ng/ml) (Reseach Diagnostics Inc., Concord, MA); and HB-EGF (60ng/ml) (R&D Systems, Minneapolis, MN).

3.6 References

Berdichevsky, F., Alford, D., D'Souza, B., and Taylor-Papadimitriou, J. (1994). Branching morphogenesis of human mammary epithelial cells in collagen gels. J Cell Sci *107 (Pt 12)*, 3557-3568.

Beviglia, L., and Kramer, R. H. (1999). HGF induces FAK activation and integrin-mediated adhesion in MTLn3 breast carcinoma cells. Int J Cancer *83*, 640-649.

Bladt, F., Riethmacher, D., Isenmann, S., Aguzzi, A., and Birchmeier, C. (1995). Essential role for the c-met receptor in the migration of myogenic precursor cells into the limb bud. Nature *376*, 768-771.

Deakin, J. A., and Lyon, M. (1999). Differential regulation of hepatocyte growth factor scatter factor by cell surface proteoglycans and free glycosaminoglycan chains. JCell Sci *112*, 1999-2009.

Dono, R., Texido, G., Dussel, R., Ehmke, H., and Zeller, R. (1998). Impaired cerebral cortex development and blood pressure regulation in FGF-2-deficient mice. Embo J *17*, 4213-4225.

Howlin, J., McBryan, J., and Martin, F. (2006). Pubertal mammary gland development: insights from mouse models. J Mammary Gland Biol Neoplasia *11*, 283-297.

Huh, C. G., Factor, V. M., Sanchez, A., Uchida, K., Conner, E. A., and Thorgeirsson, S. S. (2004). Hepatocyte growth factor/c-met signaling pathway is required for efficient liver regeneration and repair. Proc Natl Acad Sci U S A *101*, 4477-4482.

Ip, M. M., and Asch, B. B. (2000). Methods in mammary gland biology and breast cancer (New York: Kluwer Academic/Plenum Publishers).

Jackson, D., Bresnick, J., Rosewell, I., Crafton, T., Poulsom, R., Stamp, G., and Dickson, C. (1997). Fibroblast growth factor receptor signalling has a role in lobuloalveolar development of the mammary gland. J Cell Sci *110 (Pt 11)*, 1261-1268.

Kamalati, T., Niranjan, B., Yant, J., and Buluwela, L. (1999). HGF/SF in mammary epithelial growth and morphogenesis: in vitro and in vivo models. J Mammary Gland Biol Neoplasia *4*, 69-77.

Kemp, L. E., Mulloy, B., and Gherardi, E. (2006). Signalling by HGF/SF and Met: the role of heparan sulphate co-receptors. Biochem Soc Trans *34*, 414-417.

Luetteke, N. C., Qiu, T. H., Fenton, S. E., Troyer, K. L., Riedel, R. F., Chang, A., and Lee, D. C. (1999). Targeted inactivation of the EGF and amphiregulin genes reveals distinct roles for EGF receptor ligands in mouse mammary gland development. Development *126*, 2739-2750.

Lyon, M., Deakin, J. A., and Gallagher, J. T. (1994). Liver heparan sulfate structure. A novel molecular design. J Biol Chem *269*, 11208-11215.

Mizuno, K., Inoue, H., Hagiya, M., Shimizu, S., Nose, T., Shimohigashi, Y., and Nakamura, T. (1994). Hairpin loop and second kringle domain are essential sites for heparin binding and biological activity of hepatocyte growth factor. J Biol Chem *269*, 1131-1136.

Niemann, C., Brinkmann, V., Spitzer, E., Hartmann, G., Sachs, M., Naundorf, H., and Birchmeier, W. (1998). Reconstitution of mammary gland development in vitro: requirement of c-met and c-erbB2 signaling for branching and alveolar morphogenesis. J Cell Biol *143*, 533-545.

Niranjan, B., Buluwela, L., Yant, J., Perusinghe, N., Atherton, A., Phippard, D., Dale, T., Gusterson, B., and Kamalati, T. (1995). HGF/SF: a potent cytokine for mammary growth, morphogenesis and development. Development *121*, 2897-2908.

Pullan, S., Wilson, J., Metcalfe, A., Edwards, G. M., Goberdhan, N., Tilly, J., Hickman, J. A., Dive, C., and Streuli, C. H. (1996). Requirement of basement membrane for the suppression of programmed cell death in mammary epithelium. J Cell Sci *109 (Pt 3)*, 631-642.

Rosario, M., and Birchmeier, W. (2003). How to make tubes: signaling by the Met receptor tyrosine kinase. Trends Cell Biol *13*, 328-335.

Rubin, J. S., Day, R. M., Breckenridge, D., Atabey, N., Taylor, W. G., Stahl, S. J., Wingfield, P. T., Kaufman, J. D., Schwall, R., and Bottaro, D. P. (2001). Dissociation of heparan sulfate and receptor binding domains of hepatocyte growth factor reveals that heparan sulfate-c-met interaction facilitates signaling. J Biol Chem *276*, 32977-32983.

Sakata, H., Stahl, S. J., Taylor, W. G., Rosenberg, J. M., Sakaguchi, R., Wingfield, P. T., and Rubin, J. S. (1997). Heparin binding and oligomerization of hepatocyte growth factor scatter factor isoforms - Heparan sulfate glycosaminoglycan requirement for Met binding and signalling. JBiolChem *272*, 9457-9463.

Schmidt, C., Bladt, F., Goedecke, S., Brinkmann, V., Zschiesche, W., Sharpe, M., Gherardi, E., and Birchmeier, C. (1995). Scatter factor/hepatocyte growth factor is essential for liver development. Nature *373*, 699-702.

Sonnenberg, E., Meyer, D., Weidner, K. M., and Birchmeier, C. (1993). Scatter factor/hepatocyte growth factor and its receptor, the c-met tyrosine kinase, can mediate a signal exchange between mesenchyme and epithelia during mouse development. J Cell Biol *123*, 223-235.

Soriano, J. V., Pepper, M. S., Orci, L., and Montesano, R. (1998). Roles of hepatocyte growth factor/scatter factor and transforming growth factor-beta1 in mammary gland ductal morphogenesis. J Mammary Gland Biol Neoplasia *3*, 133-150.

Sternlicht, M. D., Sunnarborg, S. W., Kouros-Mehr, H., Yu, Y., Lee, D. C., and Werb, Z. (2005). Mammary ductal morphogenesis requires paracrine activation of stromal EGFR via ADAM17-dependent shedding of epithelial amphiregulin. Development *132*, 3923-3933.

Takayama, H., LaRochelle, W. J., Sharp, R., Otsuka, T., Kriebel, P., Anver, M., Aaronson, S. A., and Merlino, G. (1997). Diverse tumorigenesis associated with aberrant development in mice overexpressing hepatocyte growth factor/scatter factor. Proc Natl Acad Sci U S A *94*, 701-706.

Wagner, K. U., McAllister, K., Ward, T., Davis, B., Wiseman, R., and Hennighausen, L. (2001). Spatial and temporal expression of the Cre gene under the control of the MMTV-LTR in different lines of transgenic mice. Transgenic Res *10*, 545-553.

Wagner, K. U., Wall, R. J., St-Onge, L., Gruss, P., Wynshaw-Boris, A., Garrett, L., Li, M., Furth, P. A., and Hennighausen, L. (1997). Cre-mediated gene deletion in the mammary gland. Nucleic Acids Res *25. 25*, 4323-4330.

Wiesen, J. F., Young, P., Werb, Z., and Cunha, G. R. (1999). Signaling through the stromal epidermal growth factor receptor is necessary for mammary ductal development. Development *126*, 335-344.

Yang, Y., Spitzer, E., Meyer, D., Sachs, M., Niemann, C., Hartmann, G., Weidner, K. M., Birchmeier, C., and Birchmeier, W. (1995). Sequential requirement of hepatocyte growth factor and neuregulin in the morphogenesis and differentiation of the mammary gland. J Cell Biol *131*, 215-226.

Yant, J., Buluwela, L., Niranjan, B., Gusterson, B., and Kamalati, T. (1998). In vivo effects of hepatocyte growth factor/scatter factor on mouse mammary gland development. Exp Cell Res *241*, 476-481.

Zioncheck, T. F., Richardson, L., Liu, J., Chang, L., King, K. L., Bennett, G. L., Fügedi, P., Chamow, S. M., Schwall, R. H., and Stack, R. J. (1995). Sulfated oligosaccharides promote hepatocyte growth factor association and govern its mitogenic activity. JBiolChem *270*, 16871-16878.

3.7 Acknowledgements

Chapter 3 is a reprint of material intended to be submitted for publication by Garner, B. Omai; and Esko D. Jeffrey. The dissertation author was the primary researcher and author of this paper.

Chapter 4: Defective Lobuloalveolar Development in Mice Containing a Mammary Epithelial Cell-Specific Inactivation of a Heparan Sulfate Sulfotransferase

4.1 Summary

We have examined the participation of heparan sulfate in mammary gland branching morphogenesis and lactation by inactivation of heparan sulfate GlcNAc *N*-deacetylase/*N*-sulfotransferase genes (*Ndst*) in mammary epithelial cells. Ndst1-deficiency resulted in a 2.3 fold reduction in glucosamine *N*-sulfation and decreased binding of FGF to mammary epithelial cells *in vitro* and *in vivo*. Mammary epithelia lacking either *Ndst1* or *Ndst2* underwent branching morphogenesis normally, filling the gland with ductal tissue by sexual maturity to the same extent as wildtype epithelia. *Ndst2*$^{-/-}$ animals also underwent normal lobuloalveolar expansion and lactation during pregnancy. In contrast, lobuloalveolar expansion did not occur in Ndst1-deficient glands, resulting in insufficient milk production to nurture newly born pups. Lactational differentiation of isolated mammary epithelial cells occurred normally via Stat5 activation, suggesting that the lack of milk production was due to insufficient expansion of the lobuloalveoli. Ndst1-deficient glands exhibited reduced phosphorylation of Akt/PKB and cyclin D1 expression, leading to extensive apoptosis at day 1 of lactation. These findings demonstrate a highly penetrant and mammary

epithelial cell-autonomous effect of altering heparan sulfate on lobuloalveolar development.

4.2 Introduction

Mammary gland development occurs in multiple stages: (i) fetal development of the rudimentary mammary buds, (ii) branching morphogenesis in immature animals, (iii) formation of lobular alveoli during pregnancy, (iv) differentiation of milk producing epithelia and lactation, and (v) involution after weaning. The classical endocrine hormones (estrogen, progesterone, growth hormone, and prolactin) regulate these developmental processes by acting on the mammary stroma to induce the local expression of soluble growth factors (Hovey et al., 2002). Based on genetic studies, a large family of growth factors participate, including fibroblast growth factors (FGFs) (Mailleux et al., 2002), Wnts (Brisken et al., 2000; Humphreys et al., 1997), parathyroid hormone-related protein (PTHrP) (Dunbar et al., 2001), Hedgehog proteins (Hh and Ihh) (Lewis et al., 2001; Lewis et al., 1999), transforming growth factor beta (TGFβ) (Forrester et al., 2005; Joseph et al., 1999) and inhibin-βb (Robinson and Hennighausen, 1997), insulin-like growth factors (IGF) 1 and 2 (Brisken et al., 2002; Ruan and Kleinberg, 1999) and IGF-binding protein-5 (IGFBP-5) (Chapman et al., 1999; Grimm et al., 2002), hepatocyte growth factor (HGF) (Yang et al., 1995), amphiregulin (Luetteke et al., 1999), EGF (Luetteke et al., 1999; Wiesen et al., 1999) and EGF receptors (Xie et al., 1997), and heregulin (HRG) (Li et al., 2002) and ERBB4 receptors (Long et al., 2003; Tidcombe et al., 2003). Nearly all of

these factors bind to heparan sulfate, a glycosaminoglycan present on extracellular matrix and cell surface proteoglycans. Interaction with heparan sulfate is hypothesized to protect growth factors against degradation, to create a storage depot for later release, to facilitate assembly of signaling complexes (co-receptor activity), to enable clearance by endocytosis, and to regulate their diffusion through the tissue (Bernfield et al., 1999; Delehedde et al., 2001; Lander et al., 2002). Heparan sulfate also can act indirectly in the system, e.g. by modulating the processing of growth factor precursors by matrix metalloproteases (Yu and Woessner, 2000; Yu et al., 2002).

Evidence supporting a role for heparan sulfate in mammary development derives from studies of genetically altered mouse strains. Hyperbranching occurs in the mammary epithelia of transgenic mice expressing human heparanase, a degradative enzyme secreted by cells (Zcharia et al., 2004). Mice deficient in syndecan-1, a cell surface heparan sulfate proteoglycan expressed by mammary epithelial cells, exhibit normal primary mammary duct formation, but have a mild reduction in secondary and tertiary branching (Alexander et al., 2000; Liu et al., 2003). Mice lacking the heparan sulfate bearing form of CD44 display defective lobuloalveolar expansion (Yu et al., 2002). However, one cannot discriminate if the effects on development were due to altering interactions dependent on the core protein versus reduction in heparan sulfate content, or whther the effects were cell-autonomous with respect to the mammary epithelia *versus* the stroma since the mutations were systemic. Mutants lacking other proteoglycans involved in heparan sulfate biosynthesis either succumb embryonically (Arikawa-Hirasawa et al., 1999),

obviating further studies of the mammary gland, or have no reported defects in mammary gland development or function (Cano-Gauci et al., 1999; Echtermeyer et al., 2001; Ishiguro et al., 2001; Zhou et al., 2004).

The essential nature of heparan sulfate has made it difficult to study the effect of altering its biosynthesis in the mammary gland. Systemic deletion of *Ext1* or *Ext2* (heparan sulfate copolymerase) results in early embryonic death (E6-7) due to failure to form mesoderm during gastrulation (Lin et al., 2000; Stickens et al., 2005). Deletion of the gene encoding heparan sulfate GlcNAc N-deacetylase/N-sulfotransferase-1 (*Ndst1*), one of a family of four enzymes involved in the initial sulfation of the heparan sulfate chains, leads to perinatal lethality with lung, brain and skeletal defects (Fan et al., 2000; Grobe et al., 2005; Ringvall et al., 2000). Similarly, deletion of two other modifying enzymes, uronyl 2-O-sulfotransferase and the glucuronyl C5 epimerase, causes perinatal death due to kidney agenesis (Bullock et al., 1998; Li et al., 2003; Merry et al., 2001). Therefore, to study the role of heparan sulfate in the mammary gland, we have created a conditional allele of *Ndst1* and used the Cre-*loxP* recombination system to delete *Ndst1* in a tissue-specific manner (Bishop and Esko, 2005; Grobe et al., 2005; Wang et al., 2005). Here, we show that tissue-specific inactivation of *Ndst1* in the mammary epithelia does not affect branching morphogenesis and lactational differentiation, but causes a striking defect in lobuloalveolar expansion leading to insufficient milk production for survival of offspring.

4.3 Results

Mammary gland epithelia express multiple proteoglycans. Analysis of RNA prepared from cultured mammary epithelial cells by quantitative reverse transcription polymerase chain reaction showed transcripts for multiple heparan sulfate proteoglycan core proteins (Fig. 4-1). Both secreted (agrin, perlecan, and collagen 18a) and membrane-bound proteoglycans (syndecans and glypicans) were present, with prominent expression of syndecan-4. The large repertoire of proteoglycans in the mammary gland suggested that ablating any single core protein gene might not lead to as dramatic a phenotype due to compensation (Alexander et al., 2000; Echtermeyer et al., 2001; Ishiguro et al., 2001; Liu et al., 2003). These observations prompted us to alter the biosynthesis of the chains, thereby affecting all heparan sulfate proteoglycans in the system.

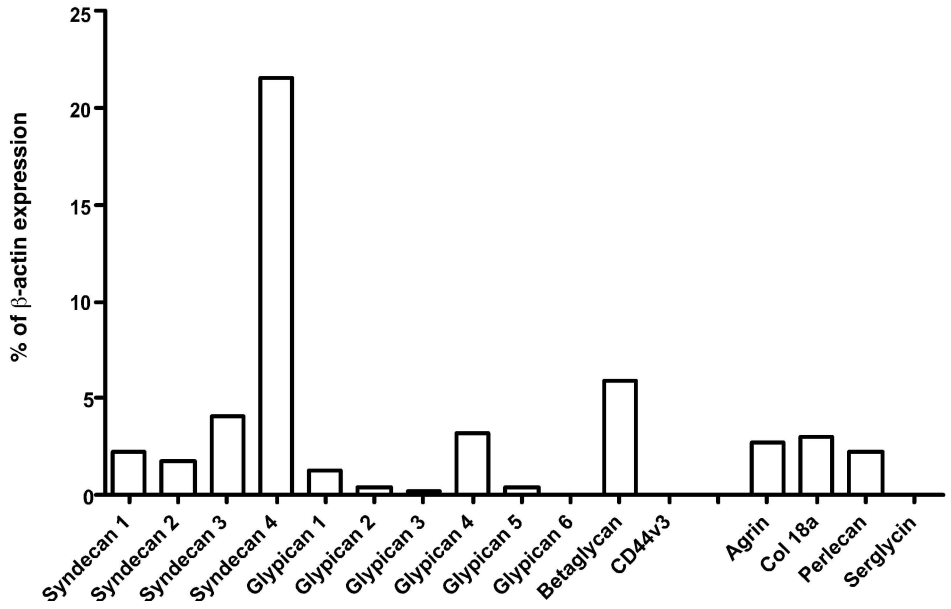

Figure 4-1: Quantitative RT-PCR analysis of mammary epithelial proteoglycan expression. RNA was isolated from mammary epithelial cells, reverse transcribed and amplified using gene specific primers to each proteoglycan (see Table S1). Quantitation was done by the $2^{-\Delta\Delta Ct}$ method using GAPDH as a control RNA. Final numbers represent % expression compared to β-actin (100%). Ct values from duplicate assays were used to calculate % expression. Error bars are not shown because they are factored into the final calculation.

Heparan sulfate assembly takes place by copolymerization of GlcNAc and GlcA residues, followed by a series of modification reactions in which segments of the chain undergo various sulfation reactions and a portion of the GlcA units are epimerized to iduronic acid (Esko and Lindahl, 2001). N-deacetylation and N-sulfation of subsets of GlcNAc residues represents the first committed step in modifying the chains and the other modifications depend on this reaction. A family of four dual function enzymes, designated GlcNAc N-deacetylase/N-sulfotransferases (NDSTs) exists in vertebrates (Grobe et al., 2002). RT-PCR analysis showed that mammary epithelia express high levels of *Ndst1* and *Ndst2*, a low level of *Ndst3*, and no *Ndst4* mRNAs (Fig. 4-2A). To alter the structure of the chains, we therefore examined mutants missing *Ndst1* and *Ndst2*.

Ndst2 null animals lack connective tissue-type mast cells but are otherwise normal (Forsberg et al., 1999; Humphries et al., 1999). In contrast, mice lacking *Ndst1* die perinatally due to lung insufficiency, and skeletal and forebrain defects (Fan et al., 2000; Grobe et al., 2005; Ringvall et al., 2000). Thus, to examine the participation of *Ndst1* in the mammary gland, we inactivated *Ndst1* selectively in mammary epithelial cells by cross breeding mice bearing a conditional allele ($Ndst1^{f/f}$, Fig. 4-2B) to *MMTVCre* mice, which express the bacteriophage Cre recombinase in mammary epithelia at day 6 postpartum (Wagner et al., 2001; Wagner et al., 1997). These mouse lines were bred to generate $Ndst1^{f/f}MMTVCre^{+}$ (mutant) and $Ndst1^{f/f}MMTVCre^{-}$

(wildtype) mice. Mice of both genotypes were obtained at the expected Mendelian frequency and appeared grossly normal.

Primary mammary epithelial cells were isolated from *Ndst1*$^{f/f}$*MMTVCre*$^{+}$ and *Ndst1*$^{f/f}$ *MMTVCre*$^{-}$ virgin and uniparous female mice and expanded in tissue culture. Evaluation of markers for epithelial keratin and milk proteins indicated >90% purity. DNA isolated from the cells was analyzed by HindIII/BamHI digestion and Southern blotting. The undeleted *Ndst1* allele generated a 2.7 kb band, whereas the deleted allele yielded a 3.2 kb band, based on analysis of clonal mammary epithelial cell lines derived from *Ndst1*$^{f/f}$ before and after Cre transfection in vitro (Fig. 4-2C). The intensities of the two bands indicated that deletion of *Ndst1* in *Ndst1*$^{f/f}$ *MMTVCre*$^{+}$ was ~60% in 3-month old virgin animals and ~80% in a uniparous female of the same age (Fig. 4-2C). The extent of recombination and deletion did not increase with multiple pregnancies, suggesting that some cells escape recombination.

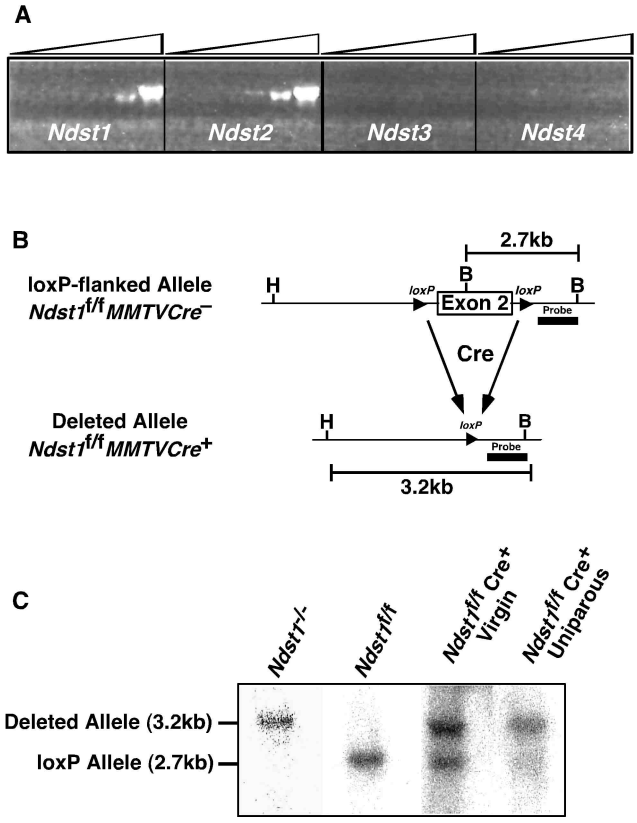

Figure 4-2: Inactivation of *Ndst1* in mammary epithelia. (**A**) RT-PCR analysis of Ndst expression in isolated epithelial cells. The ramp at top indicates increasing number of PCR amplification cycles. (**B**) The second exon of *Ndst1* was flanked with *loxP* recombinase recognition sites (triangles) (Grobe et al., 2005; Wang et al., 2005). Cre expression under the control of the *MMTV* promoter drives *loxP* recombination and deletion of the exon. Deletion of *Ndst1* exon 2 was verified by digestion of genomic DNA with Hind III (H) and Bgl II (B) followed by southern blotting with a probe (black bar) to the region between the recombination site and the Bgl II site. (**C**) Mammary epithelial cells were isolated from a virgin (lane 3) and a 3-month old uniparous female (lane 4) and analyzed by Southern blotting. For comparison, blots were performed on samples obtained from *Ndst1* deficient (lane 1) and *Ndst1*$^{f/f}$ (lane 2) mammary tumor cell lines. *Ndst1* deletion was approximately 60% complete in adult virgin mice and increased to >80% after one pregnancy.

***Ndst1* deficiency causes undersulfation of heparan sulfate in mammary ducts.** To determine how *Ndst1* deficiency affected mammary epithelia heparan sulfate, frozen sections of *Ndst1*$^{f/f}$*MMTVCre*$^{-}$ and *Ndst1*$^{f/f}$ *MMTVCre*$^{+}$ mammary glands were incubated with a biotinylated form of basic fibroblast growth factor (FGF-2) (Bai et al., 1999), which binds with high affinity to heparan sulfate in many tissues (Allen and Rapraeger, 2003). Staining with strepavidin-horseradish peroxidase yielded a distinct border of bound FGF-2 surrounding the luminal epithelia and myoepithelia, in a pattern characteristic of basement membranes (arrowheads, Fig. 4-3A). *Ndst1*$^{f/f}$*MMTVCre*$^{+}$ ducts displayed reduced binding of FGF-2 in the basement membrane. No change was observed in the staining of the mammary fat pad heparan sulfate (open arrowheads), consistent with the selective expression of Cre in the epithelial lineage. *Ndst2*$^{-/-}$ glands stained like wildtype (data not shown), consistent with the lack of effect of deleting this enzyme on heparan sulfate composition in most tissues (Ledin et al., 2004).

We next analyzed FGF-2 binding to heparan sulfate derived from mammary epithelial cell lines. Incubation of cells with biotinylated FGF-2 followed by flow cytometry showed that *Ndst1*$^{f/f}$*Ndst2*$^{-/-}$ cells bound FGF-2 like wildtype cells (Fig. 4-3B, curves **c** and **d**, respectively), whereas *Ndst1*$^{-/-}$*Ndst2*$^{+/+}$ cells bound ~5-fold less FGF-2 (curve **b**). Cells deficient in both *Ndst1* and *Ndst2* did not bind FGF-2 (data not shown), and behaved like wildtype cells incubated with phycoerythrin—Cy5-strepavidin alone (curve **a**). Heparan sulfate was also analyzed chemically from primary mammary epithelial cells from multiparous *Ndst1*$^{f/f}$*MMTVCre*$^{+}$ and

Ndst1$^{f/f}$*MMTVCre*$^{-}$ females. In these experiments, cells were labeled with [6-^{3}H]glucosamine in culture, and labeled heparan sulfate was purified and treated with nitrous acid at low pH, which cleaves the backbone of the polymer at each *N*-sulfated glucosamine unit (Shively and Conrad, 1976). The resulting oligosaccharides were then separated by gel filtration chromatography (Fig. 4-3C). Wildtype heparan sulfate was typically rich in *N*-sulfated glucosamine residues located in adjacent disaccharides (dp2) or separated by one or two *N*-acetylated disaccharides (dp4 and dp6, respectively), whereas mutant heparan sulfate contained fewer of these oligosaccharides and more extended structures rich in *N*-acetylated disaccharides that eluted as dp>18. The areas under the peaks can be used to estimate the extent of *N*-sulfation of the chains (Bame and Esko, 1989). Using this technique, we determined that heparan sulfate synthesized in cells derived from *Ndst1*$^{f/f}$*MMTVCre*$^{+}$ cells displayed a ~2-fold reduction in *N*-sulfation (~45% GlcNS in *Ndst1*$^{f/f}$*MMTVCre*$^{-}$ cells *vs*. ~25% in *Ndst1*$^{f/f}$*MMTVCre*$^{+}$ cells). This decrease in GlcNAc N-deacetylation/N-sulfation is comparable to effects seen in mutant CHO cells lacking *Ndst1* (Bame and Esko, 1989; Bame et al., 1991) and in tissues derived from mice bearing a systemic null allele of *Ndst1* (Grobe et al., 2005; Ledin et al., 2004). The residual sulfation of the chains reflects the expression of Ndst2 as observed in other cell types (Wang et al., 2005). The FGF-2 binding data and the chemical analysis indicate that Ndst1-deficiency reduced the overall level of *N*-sulfation.

Figure 4-3: Altered expression of heparan sulfate in *Ndst1$^{f/f}$MMTVCre^{+}* mammary epithelia. (A) Frozen sections of mammary glands were incubated with biotinylated FGF-2, which binds to heparan sulfate (Bai et al., 1999). Binding of FGF-2 was detected with streptavidin-HRP (brown stain). In wildtype *Ndst1$^{f/f}$MMTVCre^{-}* glands FGF-2 binds to the basement membrane surrounding the epithelial ducts (arrowheads). The upper right panel magnifies the boxed region, revealing the sharp staining of the basement membrane underlying the epithelial cells. FGF-2 also binds to the matrix surrounding the fat pad adipocytes (white arrowheads). Mutant *Ndst1$^{f/f}$MMTVCre^{+}* glands retain FGF-2 binding around fat pad adipocytes, but binding to the basement membrane was greatly reduced. The lower right panel magnifies the boxed region. Bar = 50 μm in the left panels, 12.5 μm in the right panels. (**B**) Mammary epithelial cells of different genotypes were reacted with biotinylated FGF-2, stained with PE-Cy5-strepavidin and analyzed by flow cytometry. Curve a, Wildtype cells without biotinylated FGF-2; curve b, *Ndst1$^{-/-}$Ndst2$^{+/+}$* cells; curve c, *Ndst1$^{f/f}$Ndst2$^{-/-}$ MMTVCre^{-}* cells; curve d, Wildtype cells with biotinylated FGF-2. **(C)** Heparan sulfate was isolated from [6-^{3}H]glucosamine labeled mammary epithelial cells derived from *Ndst1$^{f/f}$MMTVCre^{-}* and *Ndst1$^{f/f}$MMTVCre^{+}* mice and degraded with nitrous acid (Shively and Conrad, 1976). The individual oligosaccharides were separated by gel filtration chromatography and the area under the peaks was used to determine the extent of N-sulfation of the chains (Bame and Esko, 1989). dp, degree of polymerization.

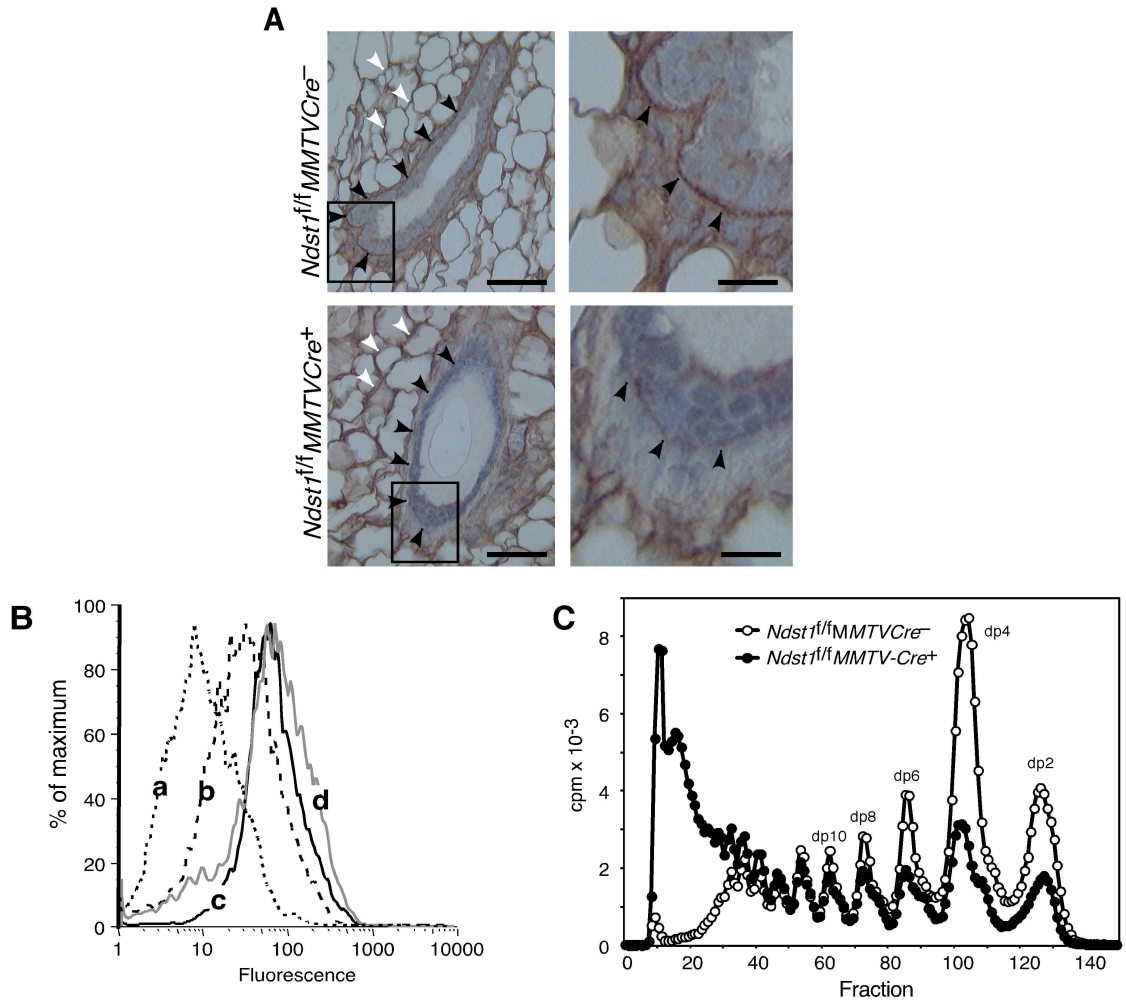
A
Ndst1f/fMMTVCre−
Ndst1f/fMMTVCre+
B
% of maximum
Fluorescence
a
b
c
d
C
Ndst1f/fMMTVCre−
Ndst1f/fMMTV-Cre+
cpm x 10-3
Fraction
dp4
dp6
dp8
dp10
dp2

Normal branching morphogenesis but defective lobuloalveolar development in absence of *Ndst1*. In wildtype mice, branching morphogenesis in the mammary gland occurs from birth to sexual maturity. By one month of age extensive branching has taken place, but the glands have not filled completely. Analysis of whole mount glands from one month old Ndst1- or Ndst2-deficient mice appeared normal with respect to the extent of fat pad colonization, overall branching, and the presence of terminal end buds (Fig. 4-4A-C). Sections stained with hematoxylin/eosin showed similar ductal density and similar gross arrangement of the surrounding connective tissue cells (Fig. 4-4D-F). Comparable results were observed in 3 month-old sexually mature animals as well, when the fat pad is filled completely and branching has ceased (Fig. 4-4G-I). We analyzed many glands from animals randomized with respect to the estrus cycle and do not see any consistent differences in branching, although minor differences in side branching could be present. (The most extreme case is shown in Fig. 4-4I). Thus, altering Ndst1 or Ndst2 expression in glands had minimal effects on branching morphogenesis.

Ndst1-deficient mice gave birth to normal size litters, but less than 30% of the offspring from Ndst1-deficient females survived more than ~1.5 days after birth and the surviving pups were small and developmentally runted. The pups suckled normally and fostering them with lactating female ICR mice allowed normal development. In contrast, ICR pups fostered to $Ndst1^{f/f}MMTVCre^{+}$ females perished shortly after transfer. Autopsy of the pups showed empty stomachs, suggesting that Ndst1-deficient

mothers did not produce sufficient milk. Ndst2-deficient females had pups that thrived normally.

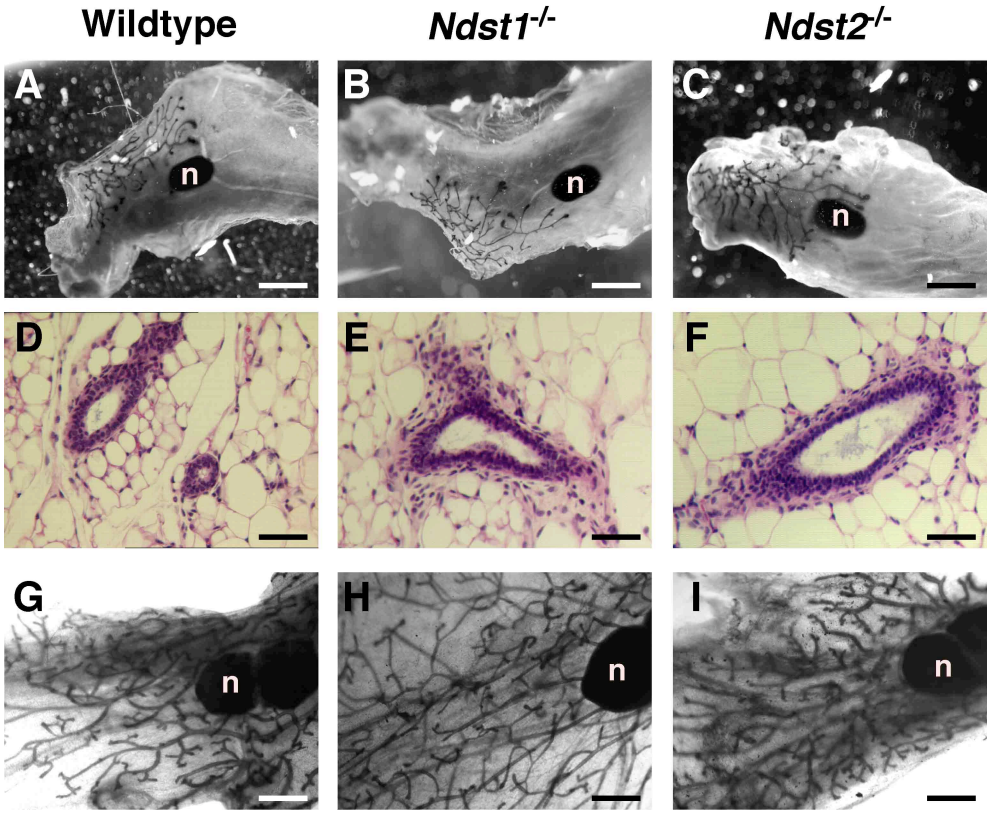

Figure 4-4: Branching morphogenesis is normal in NDST deficient epithelial cells. Whole mounts of the inguinal mammary glands were used to examine branching morphogenesis of one-month old *Ndst1*$^{f/f}$*Ndst2*$^{+/+}$*MMTVCre*$^{-}$ (Wildtype, **A**), *Ndst1*$^{f/f}$*Ndst2*$^{+/+}$*MMTVCre*$^{+}$ (*Ndst1*$^{-/-}$, **B**), and *Ndst1*$^{f/f}$*Ndst2*$^{-/-}$*MMTVCre*$^{-}$ (*Ndst2*$^{-/-}$, **C**) females. Deficiency of *Ndst1* or *Ndst2* has no effect on branching morphogenesis. Histological analysis of glands from one-month old animals showed normal organization of ductal epithelium (**D-F**). Whole mounts of 3 month-old glands also show normal branching (**G-I**). Bar = 1.5 mm in the upper panels, 100 μm in the middle panels, and 1 mm in the lower panels. n, lymph node.

Whole mounts of day 1 lactating (d1L) mammary glands from multiparous *Ndst1*$^{f/f}$*MMTVCre*$^{+}$ females showed dramatically retarded lobuloalveolar expansion compare to lactating glands from wildtype animals (Fig. 4-5M vs. 4-5O). Hematoxylin/eosin stained sections at d1L showed that the cellular architecture of the mammary ducts was normal, but lobuloalveoli were reduced in size and number (compare low magnification images in Fig. 4-5C to 4-5I and higher magnification images in Fig. 4-5F to 4-5L). Further analysis of stained sections at earlier time points revealed that the disruption in lobuloalveolar expansion found in *Ndst1*$^{f/f}$*MMTVCre*$^{+}$ females was not apparent at day 8 of pregnancy (d8P; Fig. 4-5A vs. 4-5G, and Fig. 4-5D vs. 4-5J), but was already manifest by day 15 of pregnancy (d15P; Fig. 4-5B vs. 4-5H and Fig. 4-5E vs. 4-5K) as shown by a 45% reduction in lobuloalveolar number in the *Ndst1*$^{f/f}$*MMTVCre*$^{+}$ females. In order to confirm the epithelial autonomy of this phenotype, *Ndst1*$^{f/f}$*MMTVCre*$^{+}$ epithelia were transplanted into the wild type fat pad from an inguinal gland cleared of epithelia. The host animals were bred two months later and whole mounts of the glands were analyzed at d1L. Control wild type fat pads receiving no epithelia remained devoid of ductal structures (data not shown), whereas those that received wildtype epithelia were histologically normal (Fig. 4-5N). Glands receiving *Ndst1*$^{f/f}$*MMTVCre*$^{+}$ epithelia (Fig. 4-5P) underwent ductal branching normally but exhibited the same reduced alveolar expansion seen in *Ndst1*$^{f/f}$*MMTVCre*$^{+}$ females (Fig. 4-5O). This finding confirmed that the lactation defect was due to the deletion of Ndst1 specifically in the mammary epithelia. No effect on lobuloalveolar expansion or lactation was observed in *Ndst2*$^{-/-}$ females (data

not shown). Whole mounts of multiparous non-pregnant *Ndst1*$^{f/f}$*MMTVCre*$^{+}$ females appeared normal (data not shown).

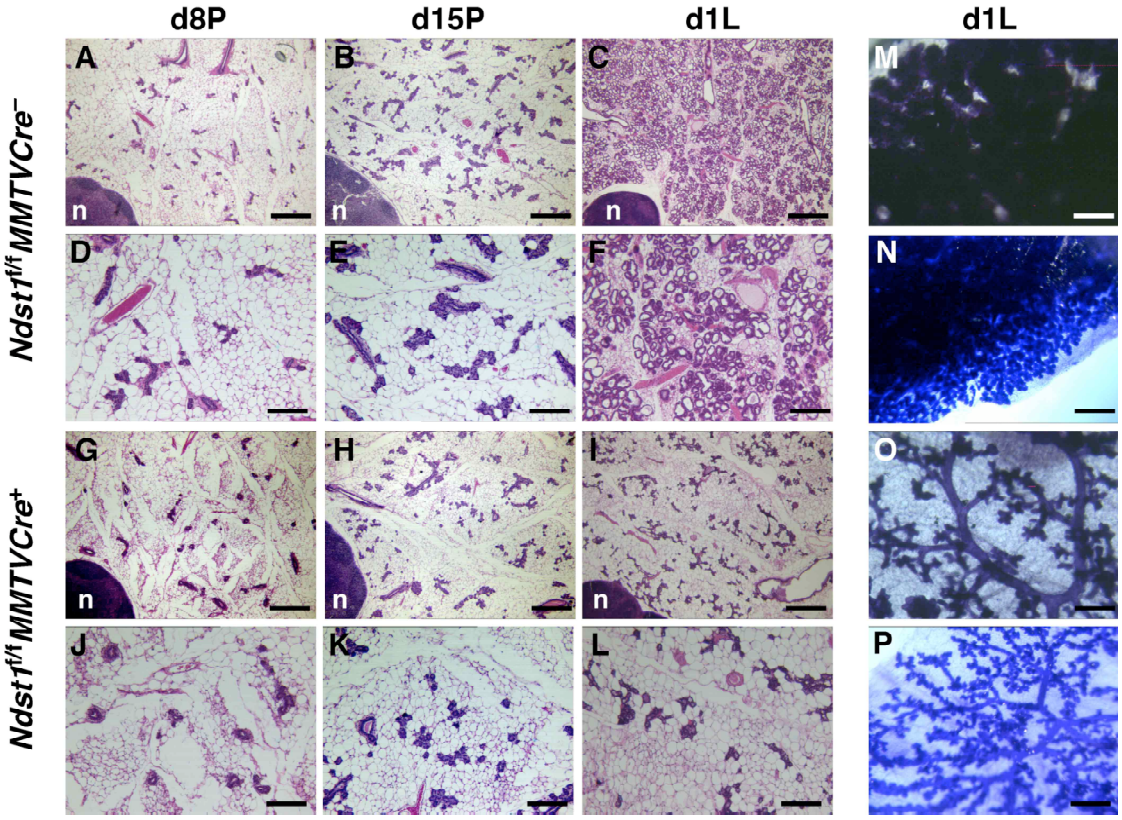

Figure 4-5: *Ndst1*$^{f/f}$*MMTVCre*$^{+}$ mammary glands do not form lobuloalveoli. Hematoxylin/eosin stained sections of d8P, d15P, and d1L mammary glands from *Ndst1*$^{f/f}$*MMTVCre*$^{-}$ (**A-F**) and *Ndst1*$^{f/f}$*MMTVCre*$^{+}$ (**G-L**) mice. (**A-C**, **G-I**): Bar = 500 μm; (**D-F**, **J-L**): Bar = 125 μm. No difference in glandular morphology was noted at d8P, but differences in ductal density occurred by d15P, increasing dramatically by d1L. (**M-P**), whole mounts of d1L inguinal mammary glands from *Ndst1*$^{f/f}$*MMTVCre*$^{-}$ (**M**) and *Ndst1*$^{f/f}$*MMTVCre*$^{+}$ (**O**). *Ndst1*–deficient glands are grossly underdeveloped. (**N**) Transplantation of *Ndst1*$^{f/f}$*MMTVCre*$^{-}$ epithelia into a cleared wildtype fat pad led to normal development at d1L. (**P**) Transplantation of *Ndst1*$^{f/f}$*MMTVCre*$^{+}$ epithelia showed a defect in lobuloalveoli development. (**M,O**): Bar = 100 μm; (**N,P**): Bar = 150 μm. n, lymph node.

Normal lactational differentiation in *Ndst1*$^{f/f}$*MMTVCre*$^{+}$ mice. To further characterize the defect in the *Ndst1*$^{f/f}$*MMTVCre*$^{+}$ females, casein and whey acidic protein (WAP) expression was analyzed. By quantitative PCR, the level of mRNAs of these proteins relative to GAPDH was dramatically reduced in d1L glands from *Ndst1*$^{f/f}$*MMTVCre*$^{+}$ mice compared to *Ndst1*$^{f/f}$*MMTVCre*$^{-}$ mice (Fig. 4-6A). However, the decrease in milk protein expression paralleled changes in keratin 18 mRNA (Fig. 4-6A) and keratin 7 protein expression (Fig. 4-6B), markers for mammary epithelial cells, suggesting that the reduced capacity to produce milk might have been related to the decrease in the number and size of lobuloalveoli rather than a defect in differentiation. Western blotting with antibodies to mouse milk from d1L glands showed that milk production was diminished in *Ndst1*$^{f/f}$*MMTVCre*$^{+}$ glands nearly to the same extent as keratin expression (Fig. 4-6C). Analysis of day 14 pregnant (d14P) glands showed that the antiserum was specific for milk proteins.

To confirm that differentiation was normal, primary mammary epithelial cells from mature *Ndst1*$^{f/f}$ females were plated on serum/fetuin coated plates and treated with adenoviral Cre (AdCre), which resulted in >95% deletion of *Ndst1*$^{f/f}$ allele. Passage of the cells in the presence of lactogenic hormones and Matrigel induced the epithelia to undergo differentiation into a lactational state in AdCre-treated cells and in cells infected with a control virus containing GFP (Fig. 4-6D). Normal lactation has been shown to require signaling through the prolactin receptor, which activates milk protein gene transcription through the phosphorylation of Stat5. Western blotting with anti-phospho-Stat5 antibodies confirmed that proper signaling had occurred (Fig. 4-

6E). Taken together, the data show that differentiation was normal in Ndst1-deficient glands and that the paucity of milk was due to a defect in the proliferation of the epithelial population required for lactation.

Figure 4-6: Characterization of the lactational defect in *Ndst1*-deficient mammary glands. Quantitative RT-PCR and Western blotting were used to characterize lactational capacity of *Ndst1*$^{f/f}$*MMTVCre*$^{+}$ females. (**A**) RNA isolated from d1L *Ndst1*$^{f/f}$*MMTVCre*$^{-}$ and *Ndst1*$^{f/f}$*MMTVCre*$^{+}$ mammary glands was analyzed by quantitative RT-PCR for the expression of whey acidic protein (WAP), β-casein, and keratin 18, genes specifically expressed by mammary epithelial cells. Data was normalized to the expression of GAPDH transcripts present in the sample. (**B**) Western blotting with antibodies to keratin 7 in d1L glands further confirmed that the *Ndst1*$^{f/f}$*MMTVCre*$^{+}$ mammary glands have a reduced population of epithelia. (**C**) Western blotting with antibodies to mouse milk from d1L glands shows that milk production was diminished in *Ndst1*$^{f/f}$*MMTVCre*$^{+}$ glands. Blotting of d14P extracts showed that the antibodies were selective for milk protein except for a minor band at 67 kDa. (**D, E**) Mammary epithelia from *Ndst1*$^{f/f}$ animals were treated with AdGFP or AdCre and cultured on Matrigel in the presence of lactogenic hormones. The lactational response was measured by Western blotting with antibodies to milk proteins (**D**) and phospho-Stat5 (**E**). No differences were observed between AdGFP and AdCre infected cells. Milk protein induction or Stat5 phosphorylation was not detected without the addition of lactogenic hormones.

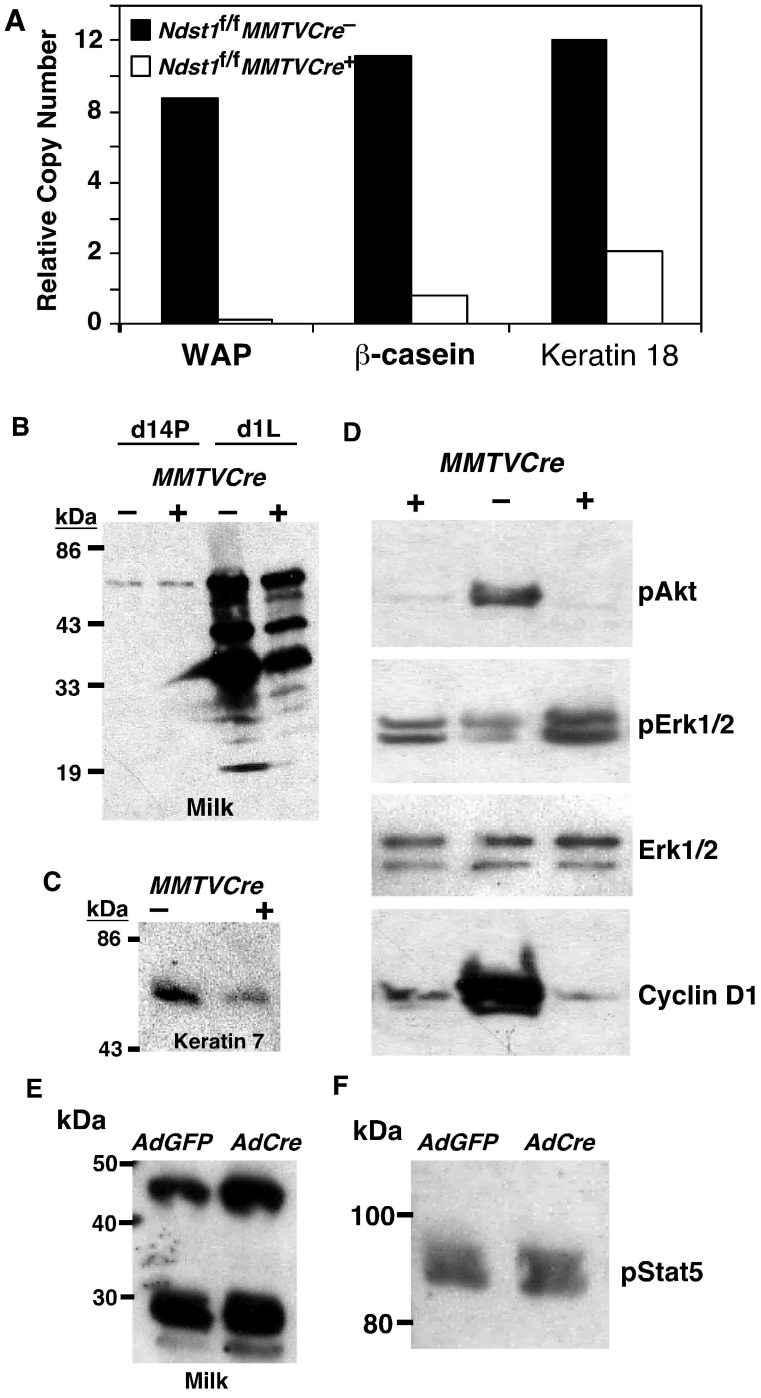
A
Ndst1f/f MMTVCre−
Ndst1f/f MMTVCre+
Relative Copy Number
12
8
4
2
0
WAP
β-casein
Keratin 18
B
d14P
d1L
MMTVCre
kDa
− + − +
86
43
33
19
Milk
C
MMTVCre
kDa
− +
86
43
Keratin 7
D
MMTVCre
+ − +
pAkt
pErk1/2
Erk1/2
Cyclin D1
E
kDa
AdGFP AdCre
50
40
30
Milk
F
kDa
AdGFP AdCre
100
80
pStat5

Altered cell proliferation and survival in *Ndst1* null mammary glands. To gain insight into the mechanism of altered expansion of the lobuloalveoli *in vivo*, extracts from mutant and wildtype glands at d1L were analyzed for factors involved in cell proliferation and survival. Ndst1-deficiency caused a dramatic diminution of Akt/PKB phosphorylation and cyclin D1 expression relative to total Erk1/2 and Erk phosphorylation (Fig. 4-7A, + lanes). When tissue sections from d1L glands were stained by TdT-mediated dUTP nick end-labeling (TUNEL), mutant glands exhibited a dramatic increase in apoptotic epithelial cells compared to wildtype glands (Fig. 4-7B) Taken together, these findings suggest that altering Ndst1 expression in mammary epithelia resulted in loss of signaling events required for proliferation and survival of the cells.

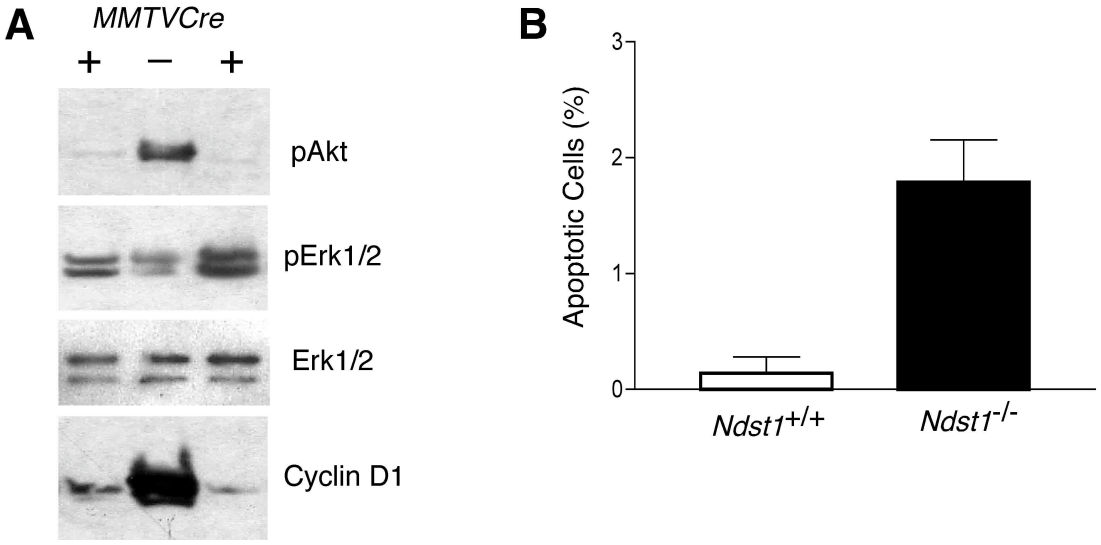

Figure 4-7: Signaling defects and apoptosis in *Ndst1*$^{f/f}$*MMTVCre*$^{+}$ glands. (A) In vivo signaling defects due to the deletion of *Ndst1* were revealed by probing d1L gland protein extracts with antibodies to specific signaling molecules. Two *Ndst1*$^{f/f}$*MMTVCre*$^{+}$ glands (+) and one *Ndst1*$^{f/f}$*MMTVCre*$^{-}$ gland (–) were analyzed by SDS-PAGE and Western blotted with antibodies to pAkt, pErk1/2, total Erk1/2 and Cyclin D1. Phosphorylation of Akt and expression of cyclin D1 was dramatically affected relative to total Erk and pErk (**B**) d1L mammary glands were examined for apoptosis by TUNEL assay and the number of positively stained epithelial cells was counted. Wild-type d1L glands show very little apoptosis, whereas Ndst1-deficient glands were highly apoptotic.

4.4 Discussion

Mouse mammary development proceeds through multiple well-defined steps. After birth, the epithelial placode undergoes branching morphogenesis from a rudimentary branched structure to a fully branched ductal tree that fills the fat pad. During pregnancy, further secondary and tertiary branching occurs and alveoli appear along the ducts, resulting eventually in the formation of lobuloalveoli that can differentiate into milk producing glands under the influence of lactogenic hormones. After weaning, the gland involutes by apoptosis of the epithelial cells, returning the gland to the virgin state. Each stage in this process depends on a series of growth factors, many of which can interact with heparan sulfate (Delehedde et al., 2001). To examine if these interactions are necessary for post-natal mammary development, we reduced the level of sulfation of the chains by inactivating *Ndst1* using the Cre recombinase under the control of the MMTV promoter. Because this system depends on hormonal activation during the estrous cycle, we cannot make any conclusions regarding the role of heparan sulfate on embryonic stages of differentiation. However, the alteration did not result in failure of the gland to undergo branching morphogenesis, suggesting that the residual level of sulfation of the chains mediated by Ndst2 was adequate for activation of relevant growth factors at this stage of glandular development. In contrast, altering heparan sulfate in this way had a striking and fully penetrant effect on lobuloalveolar expansion in female mice, leading to insufficient milk production to support their offspring.

During lobuloalveolar expansion, local growth factors released from the surrounding fat pad induce quiescent epithelia to undergo proliferation, resulting in alveolar budding, lobuloalveolar development and milk production. Lactogenic differentiation proceeds normally in Ndst1-deficient glands and isolated epithelia (Fig. 4-6), suggesting a discrete effect on budding and lobuloalveoli formation. The focal defect on alveolar development presumably arose from inefficient growth factor action due to failure to form appropriate complexes of ligands, signaling receptors and heparan sulfate (Delehedde et al., 2001). Relevant factors at this stage of development include one or more FGFs based on partial inhibition of lobuloalveoli in animals bearing a dominant-negative FGFR2IIIb construct (Jackson et al., 1997). Reduced binding of FGF-2 was observed in mutant glands (Fig. **3**), but the relevant FGF ligands active at this stage have not been identified (Dono et al., 1998; Guo et al., 1996; Mailleux et al., 2002; Ortega et al., 1998). Mutants altered in HRGα expression and ErbB4 receptors show reduced lobuloalveolar development (Gorska et al., 1998; Li et al., 2002). Since heparan sulfate interacts with these as well as other growth factors (e.g., Wnts, Hedgehog proteins, transforming growth factor beta, insulin-like growth factors, hepatocyte growth factor, heparin binding-epidermal growth factor, and amphiregulin) the defect observed in the mutant may arise from combined affects on multiple growth factors. Although we have not identified the factors affected by Ndst1-deficiency, the net effect is reduction in cyclin D1 expression, consistent with a proliferative defect, and decreased Akt/PKB phosphorylation, consistent with

increased apoptosis (Fig. 4-7). Thus, in this context Ndst1 and its product, heparan sulfate, can be viewed as a central regulatory molecule in the system.

Heparan sulfate does not occur as free chains in tissues, but rather as covalent complexes with proteoglycan core proteins. Over 17 different heparan sulfate proteoglycans are known (Bishop et al., 2007). Although mutants have not been made in all of these genes, inactivation of syndecans-1, -3, -4, glypican-3, and collagen XVIII have not been reported to exhibit lobuloalveolar defects (Alexander et al., 2000; Cano-Gauci et al., 1999; Echtermeyer et al., 2001; Ishiguro et al., 2001; Liu et al., 2003; Zcharia et al., 2004; Zhou et al., 2004). In contrast, mice lacking CD44 exhibit focal lobuloalveolar expansion, with a large number of condensed acini, but with sufficient milk production to allow 20-40% of the pups to survive (Yu et al., 2002). This finding suggests that altering Ndst1 probably affected sulfation of the chains on the heparan sulfate-bearing isoform of CD44. The more penetrant defect in Ndst1-deficient mice suggests that more than one type of proteoglycan may be required at this stage of development.

It would be interesting to extend the study of Ndst1 to other organ systems that undergo branching morphogenesis and alveolar development, e.g. the salivary gland (Patel et al., 2006), lung (Cardoso and Lu, 2006), kidney (Shah et al., 2004) and prostate gland (Thomson and Marker, 2006). Many of these systems appear to depend on heparan sulfate, but the array of growth factors differs significantly. Therefore, one might predict that altering sulfation by silencing Ndst1 or other sulfotransferases in the system could tease out different growth factor-heparan sulfate interactions required

during branching morphogenesis. Similarly, it will be interesting to examine how altering the formation of the entire chain or specific sulfation patterns mediated through the action of *O*-sulfotransferases affects mammary development.

4.5 Materials and Methods

Transgenic mice. All animals were handled in accordance with protocols for the humane treatment of animals approved by the IACUC and Animal Subjects Committee at the University of California, San Diego. Mice bearing a loxP flanked allele of *Ndst1* were described previously (Grobe et al., 2005; Wang et al., 2005). *Ndst2* deficient mice were obtained from Dr. L. Kjellen, University of Uppsala, Sweden (Forsberg et al., 1999). Cross breeding was initiated when the $Ndst1^{f/f}$ and $Ndst2^{-/-}$ mice were backcrossed to C57Bl/6 for 4 and 10 generations, respectively. The MMTV Cre line "A" mice in the 129 background was obtained from Dr. T. Wynshaw-Boris (University of California, San Diego) (Wagner et al., 2001; Wagner et al., 1997). Only male mice carrying the MMTV Cre allele were used for breeding to avoid deletion of the conditional allele by Cre expression in oocytes. All experiments were done with mice on a mixed background with littermate controls. Over the course of these studies, we did not note any qualitative and quantitative changes of phenotype with further backcrossing of $Ndst1^{f/f}$ with C57Bl/6 mice.

Cell culture. Primary mammary epithelia were isolated and cultured as described (Pullan and Streuli, 1996). Briefly, number 4 and 5 glands were excised and

chopped with a razor blade, and digested with 0.2% trypsin and 0.2% collagenase A. Cells and organoids were enriched by differential centrifugation. Multiwell tissue culture plates were precoated with 100 μl/cm^2 of Ham's F12 medium containing 20% heat-inactivated fetal bovine serum (FBS) and 1 mg/ml fetuin. Cells were cultured in Ham's F12 medium containing 10% heat-inactivated FBS, 5 μg/ml insulin, 1 μg/ml hydrocortisone, 5 ng/ml epidermal growth factor, 50 μg/ml gentamycin, 100 U/ml penicillin, and 100 μg/ml streptomycin. The medium was changed every two days.

Lactational differentiation was induced as described (Streuli et al., 1995). Briefly, first passage mammary epithelia were plated on serum/fetuin coated plates with Matrigel and cultured for 4 days in DMEM/F12 media containing 5 μg/ml insulin, 1 μg/ml hydrocortisone, 3 μg/ml prolactin, 50 μg/ml gentamycin, 100 U/ml penicillin, and 100 μg/ml streptomycin.

An adenovirus containing Cre recombinase (AdCre) was used to inactivate *Ndst1* in vitro, as described (Li et al., 2000). AdCre and adenovirus containing green fluorescent protein (AdGFP) were obtained from the Vector Core Development Lab at the University of California, San Diego. Cells were treated for 90 min twice over four days with 10^8 pfu/ml, washed with PBS and cultured in normal growth medium. Flow cytometry using biotinylated FGF and strepavidin phycoerythrin-Cy5 showed >10-fold decrease in fluorescence of ~99% of the cells (Wei et al., 2000).

Mammary gland histology. Histological analyses were performed by the Cancer Center Histology Core at the University of California, San Diego. Whole

mounts were stained with hematoxylin as described (Ip and Asch, 2000). Binding of FGF-2 to heparan sulfate was measured in frozen sections of the inguinal mammary gland using biotinylated FGF-2 and HRP-streptavidin (Wang et al., 2005). Hematoxylin and eosin staining of sections was performed by standard procedures. Lobuloalveolar number was determined by counting acini in 20 non-overlapping fields (200X magnification) located radially about the lymph node. Apoptotic cells were measured by TUNEL assay using the In Situ Cell Death Detection Kit from Roche (Mannheim, Germany).

Southern blotting and RT-PCR analysis. DNA was isolated from primary mammary epithelia from mice of various ages using the Qiagen DNeasy tissue kit (Qiagen, Valencia, CA). Samples (20 μg) was digested with Hind III and Bgl II overnight and analyzed by agarose gel (0.8%) electrophoresis. After transfer to a nylon membrane, the blot was probed with a genomic probe located outside of the deleted exon (Grobe et al., 2005).

RNA was isolated from purified mammary epithelial cells (TRIzol reagent), reverse transcribed (Superscript III, Invitrogen) and amplified using gene specific primers to each Ndst isoform (*Ndst1*, Forward: GGACATCTGGTCTAAG, Reverse: GATGCCTTTGTGATAG; *Ndst2*, Forward: GATGACAAGAGGCAC, Reverse: CAGTGCTGGCATTGG; *Ndst3*, Forward: CCACTGCCTTGTGTC, Reverse: GGAGTACGCTCGGTC; *Ndst4*, Forward: CTAACTACTTCCACTC, Reverse: ATGTGCACTGCATACC).

Q-PCR analysis of β-casein, whey acidic protein and keratin18 was done by the Genomics Core Facility at the University of California San Diego. The following primers were used: β-casein, Forward: AGGTGAATCTCATGGGACAGCT and Reverse: TGACTGGATGCTGGAGTGAACT; whey acidic protein, Forward: TGCCATGTGCTGTCCCG and Reverse: CCAGCTTTCGGAACACCAAT; keratin 18, Forward: CAGTATGAAGCGCTGGCTCA and Reverse: GTGGTACTCTCCTCAATCTGCTGA.

For qPCR analysis of individual proteoglycans, quantitation was done by the $2^{-\Delta\Delta Ct}$ method using GAPDH as a control RNA (supplementary Table S1) (Bishop and Esko, 2005). Final values represent relative expression compared to β-actin (100%). Ct values from duplicate assays were used to calculate expression data according to the Stratagene manual. Error bars are not shown because they are factored into the final calculation. Results were verified in two independent assays.

Western blotting. The lymph node from the number 4 mammary gland was removed and the gland was homogenized (Faraldo et al., 2001). Protein content was determined with the Bradford assay using BSA as a standard (BioRad, Hercules, CA). Ten micrograms of protein from whole glands or cultured cells was electrophoresed on BioRad precast Ready gels and transferred to nitrocellulose with a semi-dry blotting apparatus. The following antibodies were used: phospho-Akt/PKB (Ser308), phospho-Erk1/2 (p44/42, Thr202/Tyr204), p44/p42 (Cell Signaling Technology, Beverly, MA); anti-mouse milk antisera (Nordic Immunological Laboratories,

Tilburg); pStat5 (Tyr694), and cyclin D1 (H-295, Santa Cruz Biotechnology, Santa Cruz, CA); and keratan-7. HRP-conjugated anti-mouse and anti-goat IgG were obtained from BioRad (Hercules, CA). HRP was detected using the SuperSignal West Pico chemiluminescent substrate (Pierce, Rockford, Il).

Heparan sulfate analysis. Subconfluent primary mammary epithelial cells were cultured for 48 hr in DMEM containing 2 mM glucose, 10% dialyzed FBS, 5 μg/ml insulin, 1 μg/ml hydrocortisone, 5 ng/ml epidermal growth factor and 50 μCi/ml [6-^{3}H]glucosamine (New England Nuclear). Cell associated and secreted glycosaminoglycans were isolated, cleaved with nitrous acid pH 1.5 (Shively and Conrad, 1976), and fractionated by gel filtration chromatography as described (Bame and Esko, 1989).

4.6 References

Alexander, C. M., Reichsman, F., Hinkes, M. T., Lincecum, J., Becker, K. A., Cumberledge, S., and Bernfield, M. (2000). Syndecan-1 is required for Wnt-1-induced mammary tumorigenesis in mice. NatGenet *25*, 329-332.

Allen, B. L., and Rapraeger, A. C. (2003). Spatial and temporal expression of heparan sulfate in mouse development regulates FGF and FGF receptor assembly. J Cell Biol *163*, 637-648.

Arikawa-Hirasawa, E., Watanabe, H., Takami, H., Hassell, J. R., and Yamada, Y. (1999). Perlecan is essential for cartilage and cephalic development. Nat Genet *23*, 354-358.

Bai, X. M., Wei, G., Sinha, A., and Esko, J. D. (1999). Chinese hamster ovary cell mutants defective in glycosaminoglycan assembly and glucuronosyltransferase I. J Biol Chem *274*, 13017-13024.

Bame, K. J., and Esko, J. D. (1989). Undersulfated heparan sulfate in a Chinese hamster ovary cell mutant defective in heparan sulfate N-sulfotransferase. J Biol Chem *264*, 8059-8065.

Bame, K. J., Lidholt, K., Lindahl, U., and Esko, J. D. (1991). Biosynthesis of heparan sulfate. Coordination of polymer-modification reactions in a Chinese hamster ovary cell mutant defective in N-sulfotransferase. J Biol Chem *266*, 10287-10293.

Bernfield, M., Gotte, M., Park, P. W., Reizes, O., Fitzgerald, M. L., Lincecum, J., and Zako, M. (1999). Functions of cell surface heparan sulfate proteoglycans. Annu Rev Biochem *68*, 729-777.

Bishop, J. R., and Esko, J. D. (2005). The elusive role of heparan sulfate in Toxoplasma gondii infection. Mol Biochem Parasitol *139*, 267-269.

Bishop, J. R., Schuksz, M., and Esko, J. D. (2007). Heparan sulphate proteoglycans fine-tune mammalian physiology. Nature *446*, 1030-1037.

Brisken, C., Ayyannan, A., Nguyen, C., Heineman, A., Reinhardt, F., Tan, J., Dey, S. K., Dotto, G. P., and Weinberg, R. A. (2002). IGF-2 is a mediator of prolactin-induced morphogenesis in the breast. Dev Cell *3*, 877-887.

Brisken, C., Heineman, A., Chavarria, T., Elenbaas, B., Tan, J., Dey, S. K., McMahon, J. A., McMahon, A. P., and Weinberg, R. A. (2000). Essential function of Wnt-4 in

mammary gland development downstream of progesterone signaling. Genes Dev *14*, 650-654.

Bullock, S. L., Fletcher, J. M., Beddington, R. S., and Wilson, V. A. (1998). Renal agenesis in mice homozygous for a gene trap mutation in the gene encoding heparan sulfate 2-sulfotransferase. Genes Dev *12*, 1894-1906.

Cano-Gauci, D. F., Song, H. H., Yang, H., McKerlie, C., Choo, B., Shi, W., Pullano, R., Piscione, T. D., Grisaru, S., Soon, S.*, et al.* (1999). Glypican-3-deficient mice exhibit developmental overgrowth and some of the abnormalities typical of Simpson-Golabi-Behmel syndrome. JCell Biol *146*, 255-264.

Cardoso, W. V., and Lu, J. (2006). Regulation of early lung morphogenesis: questions, facts and controversies. Development *133*, 1611-1624.

Chapman, R. S., Lourenco, P. C., Tonner, E., Flint, D. J., Selbert, S., Takeda, K., Akira, S., Clarke, A. R., and Watson, C. J. (1999). Suppression of epithelial apoptosis and delayed mammary gland involution in mice with a conditional knockout of Stat3. Genes Dev *13*, 2604-2616.

Delehedde, M., Lyon, M., Sergeant, N., Rahmoune, H., and Fernig, D. G. (2001). Proteoglycans: pericellular and cell surface multireceptors external stimuli in the mammary gland. J Mammary Gland Biol Neoplasia *6*, 253-273.

Dono, R., Texido, G., Dussel, R., Ehmke, H., and Zeller, R. (1998). Impaired cerebral cortex development and blood pressure regulation in FGF-2-deficient mice. Embo J *17*, 4213-4225.

Dunbar, M. E., Dann, P., Brown, C. W., Van Houton, J., Dreyer, B., Philbrick, W. P., and Wysolmerski, J. J. (2001). Temporally regulated overexpression of parathyroid hormone-related protein in the mammary gland reveals distinct fetal and pubertal phenotypes. J Endocrinol *171*, 403-416.

Echtermeyer, F., Streit, M., Wilcox-Adelman, S., Saoncella, S., Denhez, F., Detmar, M., and Goetinck, P. (2001). Delayed wound repair and impaired angiogenesis in mice lacking syndecan-4. J Clin Invest *107*, 9-14.

Esko, J. D., and Lindahl, U. (2001). Molecular diversity of heparan sulfate. JClinInvest *108*, 169-173.

Fan, G., Xiao, L., Cheng, L., Wang, X., Sun, B., and Hu, G. (2000). Targeted disruption of NDST-1 gene leads to pulmonary hypoplasia and neonatal respiratory distress in mice. FEBS Lett *467*, 7-11.

Faraldo, M. M., Deugnier, M. A., Thiery, J. P., and Glukhova, M. A. (2001). Growth defects induced by perturbation of beta1-integrin function in the mammary gland epithelium result from a lack of MAPK activation via the Shc and Akt pathways. EMBO Rep *2*, 431-437.

Forrester, E., Chytil, A., Bierie, B., Aakre, M., Gorska, A. E., Sharif-Afshar, A. R., Muller, W. J., and Moses, H. L. (2005). Effect of conditional knockout of the type II TGF-beta receptor gene in mammary epithelia on mammary gland development and polyomavirus middle T antigen induced tumor formation and metastasis. Cancer Res *65*, 2296-2302.

Forsberg, E., Pejler, G., Ringvall, M., Lunderius, C., Tomasini-Johansson, B., Kusche-Gullberg, M., Eriksson, I., Ledin, J., Hellman, L., and Kjellén, L. (1999). Abnormal mast cells in mice deficient in a heparin-synthesizing enzyme. Nature *400*, 773-776.

Gorska, A. E., Joseph, H., Derynck, R., Moses, H. L., and Serra, R. (1998). Dominant-negative interference of the transforming growth factor beta type II receptor in mammary gland epithelium results in alveolar hyperplasia and differentiation in virgin mice. Cell Growth Differ *9*, 229-238.

Grimm, S. L., Seagroves, T. N., Kabotyanski, E. B., Hovey, R. C., Vonderhaar, B. K., Lydon, J. P., Miyoshi, K., Hennighausen, L., Ormandy, C. J., Lee, A. V.*, et al.* (2002). Disruption of steroid and prolactin receptor patterning in the mammary gland correlates with a block in lobuloalveolar development. Mol Endocrinol *16*, 2675-2691.

Grobe, K., Inatani, M., Pallerla, S. R., Castagnola, J., Yamaguchi, Y., and Esko, J. D. (2005). Cerebral hypoplasia and craniofacial defects in mice lacking heparan sulfate Ndst1 gene function. Development *132*, 3777-3786.

Grobe, K., Ledin, J., Ringvall, M., Holmborn, K., Forsberg, E., Esko, J. D., and Kjellén, L. (2002). Heparan sulfate and development: Differential roles of the N-acetylglucosamine N-deacetylase/N-sulfotransferase isozymes. Biochim Biophys Acta Gen Subj *1573*, 209-215.

Guo, L., Degenstein, L., and Fuchs, E. (1996). Keratinocyte growth factor is required for hair development but not for wound healing. Genes Dev *10*, 165-175.

Hovey, R. C., Trott, J. F., and Vonderhaar, B. K. (2002). Establishing a framework for the functional mammary gland: from endocrinology to morphology. J Mammary Gland Biol Neoplasia *7*, 17-38.

Humphreys, R. C., Lydon, J., O'Malley, B. W., and Rosen, J. M. (1997). Mammary gland development is mediated by both stromal and epithelial progesterone receptors. Mol Endocrinol *11*, 801-811.

Humphries, D. E., Wong, G. W., Friend, D. S., Gurish, M. F., Qiu, W. T., Huang, C. F., Sharpe, A. H., and Stevens, R. L. (1999). Heparin is essential for the storage of specific granule proteases in mast cells. Nature *400*, 769-772.

Ip, M. M., and Asch, B. B. (2000). Methods in mammary gland biology and breast cancer (New York: Kluwer Academic/Plenum Publishers).

Ishiguro, K., Kadomatsu, K., Kojima, T., Muramatsu, H., Matsuo, S., Kusugami, K., Saito, H., and Muramatsu, T. (2001). Syndecan-4 deficiency increases susceptibility to kappa-carrageenan-induced renal damage. Lab Invest *81*, 509-516.

Jackson, D., Bresnick, J., Rosewell, I., Crafton, T., Poulsom, R., Stamp, G., and Dickson, C. (1997). Fibroblast growth factor receptor signalling has a role in lobuloalveolar development of the mammary gland. J Cell Sci *110 (Pt 11)*, 1261-1268.

Joseph, H., Gorska, A. E., Sohn, P., Moses, H. L., and Serra, R. (1999). Overexpression of a kinase-deficient transforming growth factor-beta type II receptor in mouse mammary stroma results in increased epithelial branching. Mol Biol Cell *10*, 1221-1234.

Lander, A. D., Nie, Q., and Wan, F. Y. (2002). Do morphogen gradients arise by diffusion? Dev Cell *2*, 785-796.

Ledin, J., Staatz, W., Li, J. P., Gotte, M., Selleck, S., Kjellen, L., and Spillmann, D. (2004). Heparan sulfate structure in mice with genetically modified heparan sulfate production. J Biol Chem *279*, 42732-42741.

Lewis, M. T., Ross, S., Strickland, P. A., Sugnet, C. W., Jimenez, E., Hui, C., and Daniel, C. W. (2001). The Gli2 transcription factor is required for normal mouse mammary gland development. Dev Biol *238*, 133-144.

Lewis, M. T., Ross, S., Strickland, P. A., Sugnet, C. W., Jimenez, E., Scott, M. P., and Daniel, C. W. (1999). Defects in mouse mammary gland development caused by conditional haploinsufficiency of Patched-1. Development *126*, 5181-5193.

Li, J. P., Gong, F., Hagner-McWhirter, A., Forsberg, E., Abrink, M., Kisilevsky, R., Zhang, X., and Lindahl, U. (2003). Targeted disruption of a murine glucuronyl C5-epimerase gene results in heparan sulfate lacking L-iduronic acid and in neonatal lethality. J Biol Chem *278*, 28363-28366.

Li, L., Cleary, S., Mandarano, M. A., Long, W., Birchmeier, C., and Jones, F. E. (2002). The breast proto-oncogene, HRGalpha regulates epithelial proliferation and lobuloalveolar development in the mouse mammary gland. Oncogene *21*, 4900-4907.

Li, M., Wagner, K. U., and Furth, P. A. (2000). Transfection of Primary Mammary Epithelial Cells by Viral and Nonviral Methods, In Methods in Mammary Gland Biology and Breast Cancer Research, B. B. Asch, ed. (New York: Kluwer Academic / Plenum Publishers), pp. 233-244.

Lin, X., Wei, G., Shi, Z. Z., Dryer, L., Esko, J. D., Wells, D. E., and Matzuk, M. M. (2000). Disruption of gastrulation and heparan sulfate biosynthesis in EXT1-deficient mice. Dev Biol *224*, 299-311.

Liu, B. Y., Kim, Y. C., Leatherberry, V., Cowin, P., and Alexander, C. M. (2003). Mammary gland development requires syndecan-1 to create a beta-catenin/TCF-responsive mammary epithelial subpopulation. Oncogene *22*, 9243-9253.

Long, W., Wagner, K. U., Lloyd, K. C., Binart, N., Shillingford, J. M., Hennighausen, L., and Jones, F. E. (2003). Impaired differentiation and lactational failure of Erbb4-deficient mammary glands identify ERBB4 as an obligate mediator of STAT5. Development *130*, 5257-5268.

Luetteke, N. C., Qiu, T. H., Fenton, S. E., Troyer, K. L., Riedel, R. F., Chang, A., and Lee, D. C. (1999). Targeted inactivation of the EGF and amphiregulin genes reveals distinct roles for EGF receptor ligands in mouse mammary gland development. Development *126*, 2739-2750.

Mailleux, A. A., Spencer-Dene, B., Dillon, C., Ndiaye, D., Savona-Baron, C., Itoh, N., Kato, S., Dickson, C., Thiery, J. P., and Bellusci, S. (2002). Role of FGF10/FGFR2b signaling during mammary gland development in the mouse embryo. Development *129*, 53-60.

Merry, C. L. R., Bullock, S. L., Swan, D. C., Backen, A. C., Lyon, M., Beddington, R. S. P., Wilson, V. A., and Gallagher, J. T. (2001). The molecular phenotype of heparan sulfate in the *Hs2st*$^{-/-}$ mutant mouse. J Biol Chem *276*, 35429-35434.

Ortega, S., Ittmann, M., Tsang, S. H., Ehrlich, M., and Basilico, C. (1998). Neuronal defects and delayed wound healing in mice lacking fibroblast growth factor 2. ProcNatlAcadSciUSA *95*, 5672-5677.

Patel, V. N., Rebustini, I. T., and Hoffman, M. P. (2006). Salivary gland branching morphogenesis. Differentiation *74*, 349-364.

Pullan, S. E., and Streuli, C. H. (1996). The mammary gland epithelial cell, In Epithelial Cell Culture, A. Harris, ed. (Cambridge), pp. 97-121.

Ringvall, M., Ledin, J., Holmborn, K., Van Kuppevelt, T., Ellin, F., Eriksson, I., Olofsson, A. M., Kjellén, L., and Forsberg, E. (2000). Defective heparan sulfate

biosynthesis and neonatal lethality in mice lacking N-deacetylase/N-sulfotransferase-1. J Biol Chem *275*, 25926-25930.

Robinson, G. W., and Hennighausen, L. (1997). Inhibins and activins regulate mammary epithelial cell differentiation through mesenchymal-epithelial interactions. Development *124*, 2701-2708.

Ruan, W., and Kleinberg, D. L. (1999). Insulin-like growth factor I is essential for terminal end bud formation and ductal morphogenesis during mammary development. Endocrinology *140*, 5075-5081.

Shah, M. M., Sampogna, R. V., Sakurai, H., Bush, K. T., and Nigam, S. K. (2004). Branching morphogenesis and kidney disease. Development *131*, 1449-1462.

Shively, J. E., and Conrad, H. E. (1976). Formation of anhydrosugars in the chemical depolymerization of heparin. Biochemistry *15*, 3932-3942.

Stickens, D., Zak, B. M., Rougier, N., Esko, J. D., and Werb, Z. (2005). Mice deficient in Ext2 lack heparan sulfate and develop exostoses. Development *132*, 5055-5068.

Streuli, C. H., Schmidhauser, C., Bailey, N., Yurchenco, P., Skubitz, A. P., Roskelley, C., and Bissell, M. J. (1995). Laminin mediates tissue-specific gene expression in mammary epithelia. J Cell Biol *129*, 591-603.

Thomson, A. A., and Marker, P. C. (2006). Branching morphogenesis in the prostate gland and seminal vesicles. Differentiation *74*, 382-392.

Tidcombe, H., Jackson-Fisher, A., Mathers, K., Stern, D. F., Gassmann, M., and Golding, J. P. (2003). Neural and mammary gland defects in ErbB4 knockout mice genetically rescued from embryonic lethality. Proc Natl Acad Sci U S A *100*, 8281-8286.

Wagner, K. U., McAllister, K., Ward, T., Davis, B., Wiseman, R., and Hennighausen, L. (2001). Spatial and temporal expression of the Cre gene under the control of the MMTV-LTR in different lines of transgenic mice. Transgenic Res *10*, 545-553.

Wagner, K. U., Wall, R. J., St-Onge, L., Gruss, P., Wynshaw-Boris, A., Garrett, L., Li, M., Furth, P. A., and Hennighausen, L. (1997). Cre-mediated gene deletion in the mammary gland. Nucleic Acids Res *25. 25*, 4323-4330.

Wang, L., Fuster, M., Sriramarao, P., and Esko, J. D. (2005). Endothelial heparan sulfate deficiency impairs L-selectin- and chemokine-mediated neutrophil trafficking during inflammatory responses. Nat Immunol *6*, 902-910.

Wei, G., Bai, X. M., Gabb, M. M. G., Bame, K. J., Koshy, T. I., Spear, P. G., and Esko, J. D. (2000). Location of the glucuronosyltransferase domain in the heparan

sulfate copolymerase EXT1 by analysis of Chinese hamster ovary cell mutants. J Biol Chem *275*, 27733-27740.

Wiesen, J. F., Young, P., Werb, Z., and Cunha, G. R. (1999). Signaling through the stromal epidermal growth factor receptor is necessary for mammary ductal development. Development *126*, 335-344.

Xie, W., Paterson, A. J., Chin, E., Nabell, L. M., and Kudlow, J. E. (1997). Targeted expression of a dominant negative epidermal growth factor receptor in the mammary gland of transgenic mice inhibits pubertal mammary duct development. Mol Endocrinol *11*, 1766-1781.

Yang, Y., Spitzer, E., Meyer, D., Sachs, M., Niemann, C., Hartmann, G., Weidner, K. M., Birchmeier, C., and Birchmeier, W. (1995). Sequential requirement of hepatocyte growth factor and neuregulin in the morphogenesis and differentiation of the mammary gland. J Cell Biol *131*, 215-226.

Yu, W. H., and Woessner, J. F., Jr. (2000). Heparan sulfate proteoglycans as extracellular docking molecules for matrilysin (matrix metalloproteinase 7). J Biol Chem *275*, 4183-4191.

Yu, W. H., Woessner, J. F., Jr., McNeish, J. D., and Stamenkovic, I. (2002). CD44 anchors the assembly of matrilysin/MMP-7 with heparin-binding epidermal growth factor precursor and ErbB4 and regulates female reproductive organ remodeling. Genes Dev *16*, 307-323.

Zcharia, E., Metzger, S., Chajek-Shaul, T., Aingorn, H., Elkin, M., Friedmann, Y., Weinstein, T., Li, J. P., Lindahl, U., and Vlodavsky, I. (2004). Transgenic expression of mammalian heparanase uncovers physiological functions of heparan sulfate in tissue morphogenesis, vascularization, and feeding behavior. Faseb J *18*, 252-263.

Zhou, Z., Wang, J., Cao, R., Morita, H., Soininen, R., Chan, K. M., Liu, B., Cao, Y., and Tryggvason, K. (2004). Impaired angiogenesis, delayed wound healing and retarded tumor growth in perlecan heparan sulfate-deficient mice. Cancer Res *64*, 4699-4702.

4.7 Acknowledgements

We would like to acknowledge the kind assistance of Dr. T. Seagroves (UCSD) with mammary gland biology methods, Dr. L. Kjellen (Uppsala, Sweden) and Dr. Wynshaw-Boris (UCSD) for mice, Dr. R. Johnson (UCSD) for Cre adenovirus, the UCSD Cancer Center Histology Core for their assistance with histological analysis, Dr. S. Rought-Crawford (UCSD) for quantitative RT-PCR analysis, and Dr. B. Yu (UCSD) for help with imaging work. This work was supported by training grant CA67754 (B.E.C), NRSA Minority Predoctoral Fellowship AI58916 (O.B.G.), NRSA Fellowship AI52692 (J.R.B) and GM33063 and HL57345 (J.D.E) from the National Institutes of Health.

Chapter 4 is a reprint of material intended to be submitted for publication by Crawford, E. Brett; Garner, B. Omai; Bishop, R. Joseph; Zhang, Y. David; Castagnola, Jan; and Esko, D. Jeffery. The dissertation author was the co-primary researcher and author of this paper.

Chapter 5: Perspective and Conclusions

5.1 Heparan Sulfate Structure Determines Mammary Gland Development and Function

This thesis attempts to define the role of epithelial heparan sulfate in mammary gland branching by specifically targeting the biosynthetic machinery responsible for heparan sulfate polymerization and modification *in vivo*. The mammary gland was used as a model of branching because of advantages over other branched systems; (1) the gland undergoes development postnatally, (2) mammary epithelial cells (MECs) can be easily transplanted, and (3) transgenic mice bearing Cre recombinase are available enabling the inactivation of target genes specifically in mammary epithelia at different stages in mammary gland development. Biosynthetic enzymes were targeted because mammary epithelia express multiple proteoglycans. Compensation by expressed proteoglycans may explain the lack of strong phenotypes in mutants lacking individual proteoglycans (Liu et al., 2004). Tissue specific knockouts were used because systemic knockouts in heparan sulfate biosynthetic core proteins arrest before mammary development begins (Bullock et al., 1998; Lin et al., 2000; Ringvall et al., 2000).

Mammary epithelia lacking EXT1 (heparan sulfate co-polymerase) fail to undergo ductal branching in response to pubertal hormones released at the onset of the estrous cycle. This phenotype is dramatic and highly penetrant and has not been observed in proteoglycan core protein gene knockouts. Some variability in the

penetrance was observed due to inefficient Cre recombinase activity, but this seems like a minor shortcoming in the system. Since multiple heparin-binding growth factors are important to mammary ductal branching (Jackson et al., 1997; Luetteke et al., 1999; Yant et al., 1998), the complete loss of heparan sulfate chains probably affects multiple steps. It could also alter ECM formation and tissue organization. A major effort needs to be devoted to defining the specific growth factors and matrix molecules affected in this system.

The *Ext1* mutant defines a role for the heparan sulfate chain in mammary epithelial ductal branching, but does not address the importance of chain modification. To look at the role of sulfation, we produced mammary epithelia deficient in both NDST1 and NDST2. These isozymes initiate chain modification by creating the preferred substrate for all subsequent downstream modifications. Thus, an *Ndst*-deficient cell produces a chain devoid of any sulfate groups. Complete loss of both *Ndst1* and *Ndst2*, which occurs in 25% of mutant glands, blocked the ability of epithelia to form ducts and branch. This result implies that the chain by itself is not sufficient for epithelial duct formation.

Interestingly, inactivation of *Ndst1* and *Ndst2 in vivo* yielded a significant proportion of glands containing a mixture of $Ndst1^{-/-}Ndst2^{-/-}$ and $Ndst1^{+/+}Ndst2^{-/-}$ cells, likely due to inefficient Cre recombination and rescue of doubly mutant cells by cells expressing partially sulfated heparan sulfate. Examination of these glands revealed pubertal hyperbranching. A dramatic increase in both bifurcated end bud branching as

well as side branching occurred. The hyperbranching phenotype is seen, regardless of the stage of growth arrest in the gland.

To further elucidate the role of sulfation in mammary epithelial development, we looked at mutant glands deficient in either *Ndst1* or *Ndst2*. Neither gland exhibited a branching phenotype. However, *Ndst1*-deficient glands were incapable of producing lobuloalveolar structures during pregnancy, whereas *Ndst2*$^{-/-}$ glands were normal. Ndst1-deficieny led to insufficient milk production and the death of pups. Further experiments showed a lack of survival signals, an increase in apoptosis during pregnancy, and elevated stat3 expression, as though the gland was undergoing precocious involution. *In vitro* experiments suggested a deficiency in heregulin signaling, consistent with other knockout experiments.

To further explore the role of specific sulfation events along the heparan sulfate chain in mammary epithelial ductal branching, we targeted HS2ST, which adds a 2-O-sulfate group to uronic acids. Mammary epithelia deficient in *Hs2st* show defects in the number and complexity of branched epithelia. Examination of mutant glands during ductal branching reveal a decrease in secondary branches and bifurcated terminal end buds. This result is very important, because it implies that a specific set of growth factors and extracellular matrix components control secondary branching by interacting with the 2-O-sulfate groups on heparan sulfate chains. The importance of these studies is that (i) we have shown that MEC heparan sulfate has a cell autonomous effect on development; and (ii) the pattern of sulfation of the chain determines the extent of dichotomous branching, side branching, and formation of

lobuloalveoli. We infer that that the way that this structural information is translated by cells is via binding and activation of different sets of heparin-binding growth factors and ECM components in the gland.

To our knowledge, this is the first system that clearly defines separate roles for distinct modifications of heparan sulfate in a branched organ *in vivo*. Future experiments should focus on the role of other heparan sulfate modifying enzymes, including the HS6STs, HS3STs, and HSGLCE. Systemically, the mutations in *Hs6sts* and *Hsglce* show perinatal embryonic lethality (Li et al., 2003), but whether mammary buds exist in these animals is not known. If present, transplantation studies using an embryonic bud from these knock out animals, grown in a wildtype fat pad, might be able to help define the role of these heparan sulfate modifications in mammary gland development. Alternatively, animals containing conditional alleles of these genes might be generated and cross bred to *MMTV* cre mice. Other cre animals are available as well to study the role of heparan sulfate modifications at different stages of mammary gland development, such as *WAP* cre, which turns on at pregnancy. This system could be used to define the role of genes that arrest mammary gland development at earlier stages, such as *Ext1* and *Hs2st* (Lin et al., 2000; Merry et al., 2001).

5.2 Mammary Specific Growth Factors Bind to Heparan Sulfate

Many growth factors relevant to mammary gland development bind to heparan sulfate including FGF family members (Rapraeger et al., 1991), EGF family members

(Aviezer and Yayon, 1994) and HGF (Zioncheck et al., 1995), as outlined in Chapter 1. To examine if heparan sulfate interacts with different growth factors during branching, we set up an in vitro system using Matrigel supplemented with growth factors. The results showed that *in vitro* mammary epithelial ductal branching can be induced by multiple members of the FGF family and HB-EGF, and this system depends on sulfation.

An examination of single growth factor and receptor knockouts in the mammary gland (Table 5-1) reveals that they rarely show a complete abrogation of ductal branching.

Table 5-1: Single Growth Factor and Receptor Knockouts

Growth Factor/Receptor	Mammary Phenotype
HGF	Whole animal knockout – perinatal lethality due to placental defects – no data on mammary effects (Schmidt et al., 1995)
Met	Whole animal knockout – perinatal lethal (Bladt et al., 1995)
FGF-2	Whole animal knockout – viable, no mammary phenotype (slight brain defects) (Dono et al., 1998)
FGF-7	Whole animal knockout – viable, no mammary phenotype (Guo et al., 1996)
FGF-10	Whole animal knockout – Missing mammary placode 1, 2, 3 and 5. No further data due to animal death (multiple organ failure in development) (Mailleux et al., 2002)
FGFr2	Mammary targeted conditional ablation – severe delay in ductal development (Sternlicht et al., 2006)
FGFR2b	Whole animal knockout – exact same phenotype as FGF10 knockout (Mailleux et al., 2002)
FGFR2 (IIIb)	Whole animal knockout – do not develop discernible mammary primordial (Spencer-Dene et al., 2001)
FGFR2 (IIIb)	Dominant negative - Marked impairment of lobular alveolar development (Jackson et al., 1997)

Table 5-1: Continued

Growth Factor/Receptor	Mammary Phenotype
HB-EGF	Whole animal knockout – Die early due to heart defects, no data on mammary development (Jackson et al., 2003)
EGF	Whole animal knock out – no mammary phenotype in adult animal (Luetteke et al., 1999)
Amphiregulin	Whole animal knockout – Underdeveloped branching morphogenesis, TEBs form but don't progress through the gland, lactation still occurs upon pregnancy (able to nurse young) (Luetteke et al., 1999)
ErbB2	Whole animal knockout – delays in ductal penetration (Jackson-Fisher et al., 2004)
EGFR	EGFR -/- stroma can't support branching morphogenesis of wild type epithelia, EGFR-/- epithelia grows in wild type stroma (Wiesen et al., 1999)

Compensation by different sets of growth factor could account for the mild phenotypes. Because many of these growth factors bind to heparan sulfate, altering its formation is equivalent to a combined mutation of multiple growth factors. Taking that into consideration, it is no surprise that heparan sulfate deficiency completely abrogates branching, and that small changes along the heparan sulfate chain have dramatic effects.

To further explore the role of heparan sulfate and growth factor interactions in the mammary gland, we examined HGF and its tyrosine kinase receptor Met signaling (a heparan sulfate dependent process) in mammary gland development. Previous research described in Chapter 1, suggests that the HGF/Met interaction was central to mammary ductal branching (Yant et al., 1998), and that heparan sulfate may play an important regulatory role in this interaction (Lyon and Gallagher, 1994). Systemic knockouts in HGF or Met have been uninformative because they die before pubertal mammary branching (Bladt et al., 1995; Schmidt et al., 1995). Chapter 3 shows that a mammary epithelial specific knock out of the Met tyrosine kinase receptor does not exhibit a branching phenotype, contrary to previous *in vitro* evidence that proclaimed the HGF-Met interaction was necessary for mammary ductal branching. To explore whether the loss of Met sensitized the gland to a heparan sulfate deficiency, we crossed the *Ext1* heterozygote onto the Met deficient animal. This genetic cross yielded no synthetic phenotype, consistent with a lack of requirement for Met-HGF interaction for mammary ductal branching.

It might me possible to explore the role of growth factor/HS interactions in mammary development by crossing multiple growth factor knockout animals to animals with heparan sulfate deficiencies. For example, a triple cross with FGF2, FGF7 and *Ext1* (heterozygote) deficiencies may show a branching phenotype, while the absence of any single growth factor gene has no phenotype (Dono et al., 1998; Guo et al., 1996). Another way to explore growth factor/HS interactions is to implant beads into heparan sulfate deficient glands that locally release growth factors. Certain growth factors may be able to overcome the HS deficiency by raising the local concentration above a critical threshold. In this regard, a transgenic mouse overexpressing certain growth factors, crossed onto a mammary epithelial, heparan sulfate deficient, animal, might help to identify which growth factors are affected in heparan sulfate deficient glands.

There are also *in vitro* assays that will help to determine exactly which growth factors are involved in heparan sulfate regulation of mammary ductal branching. One method is to homogenize mammary tissue during different developmental stages, and examine binding to differentially sulfated oligosaccharides by column chromatography. For example, growth factors that facilitate bifurcation require 2-O-sulfate groups based on our studies of *Hs2st* knockouts. These factors presumably would bind to native heparin, but not to 2-O-desulfated heparin, which can be produced chemically from heparin in large quantities. An additional *in vitro* method is to expand the mammary branching assay to include epithelia isolated from the animal bearing a conditional (f/f) allele. Treatment with Adenoviral Cre and incubation in

Matrigel may demonstrate the requirement for an individual growth factor for branching.

A third approach to define the relevant growth factor signaling pathways affected in the heparan sulfate deficient mutants might utilize growth factor reporter strains that are available. For example, Wnt signaling has been shown to be involved in mammary ductal side branching because overexpression of Wnt4 leads to a hyperbranched phenotype during puberty (Bradbury et al., 1995). Wnt reporter mice containing a downstream signal of Wnt activation attached to a lacZ reporter, crossed to *Ndst*-deficient animals, might confirm misregulation of Wnt signaling during pubertal branching. Collectively, these experiments would help to determine which growth factor pathways are affected in the heparan sulfate deficient and modified animals.

5.3 Proteoglycans in Mammary Gland Development

The question of which proteoglycans are critical to mammary development, remains unanswered. Some systemic proteoglycan core protein mutants are viable and reproduce (Echtermeyer et al., 2001), but small changes in mammary gland development may have been overlooked. Some systemic proteoglycan knockout animals arrest before mammary development (Arikawa-Hirasawa et al., 1999), thus requiring the use of embryonic mammary bud transplantation or conditional knockouts to study their function. Other experiments could focus on the creation of compound mutants in proteoglycan core protein genes. Perhaps a double knockout of syndecan 1

and syndecan 4 would exhibit a very strong ductal branching phenotype, while a triple knockout of all the basement membrane heparan sulfate proteoglycans would only have an effect on pregnancy.

5.4 The Role of Stromal Cell Specific Heparan Sulfate

Heparan sulfate is found in both the epithelia and the stroma of the mammary gland (Gordon and Bernfield, 1980) (Silberstein and Daniel, 1982). The *in vivo* experiments in this thesis demonstrate the necessity for epithelial heparan sulfate in mammary gland development (Chapter 2 and 4). This result is consistent with the *in vitro* branching assay, which showed that cell surface sulfation is required for mammary epithelial branching. The stromal heparan sulfate that sits adjacent to the epithelia (in either assay system) apparently is not able to facilitate the heparan sulfate interactions required for branching and development. However, we cannot exclude the possibility that stromal proteoglycans produced by connective tissue cells or adipocytes do not play a role. Other tissue-specific Cre transgenic mice could provide some insight into this question. Alternatively, transplantation experiments involving fat pads from the *Ext1* heterozygotes or a mouse overexpressing human heparinases (Zcharia et al., 2001), implanted with wildtype epithelia, might yield information.

5.5 Heparan Sulfate, Other Branched Organs, and Disease

The work in this thesis clearly demonstrates a genetic role for heparan sulfate in mammary gland development. As described in Chapter 1, several mammalian branched organs rely on epithelial ductal morphogenesis including the lung, pancreas, kidney, and salivary glands. Thus, it is reasonable to assume that most of these systems will also depend on heparan sulfate. The kidney system has over nine different cre animals available to target genes at different times in development and different kidney cell types. I predict that heparan sulfate will be as critical to branching in these other organs, as it is in the mammary gland.

One reason to study the development of branched organs is to determine the contribution of heparan sulfate to pathophysiological conditions in these systems. Branched organs show a high preponderance towards the development of cancer, and carcinomas of the breast make up a large percentage of malignancies. Tumors rely on growth factor dependent signaling for primary growth and metastasis and often the same factors are involved in tumor growth and progression as in normal development. Syndecan-1 deficient animals are protected against Wnt-1 derived mammary tumors (Alexander et al., 2000). Thus, this data and the results presented here suggests that mammary epithelial heparan sulfate may be a chemotherapeutic target. To validate this hypothesis, future experiments could focus on mammary epithelial tumor models in the *Ndst1* deficient or *Hs2st* deficient glands. Positive results would make heparan sulfate a viable target for anti-tumor drugs.

5.6 References

Alexander, C. M., Reichsman, F., Hinkes, M. T., Lincecum, J., Becker, K. A., Cumberledge, S., and Bernfield, M. (2000). Syndecan-1 is required for Wnt-1-induced mammary tumorigenesis in mice. NatGenet *25*, 329-332.

Arikawa-Hirasawa, E., Watanabe, H., Takami, H., Hassell, J. R., and Yamada, Y. (1999). Perlecan is essential for cartilage and cephalic development. Nat Genet *23*, 354-358.

Aviezer, D., and Yayon, A. (1994). Heparin-dependent binding and autophosphorylation of epidermal growth factor (EGF) receptor by heparin-binding EGF-like growth factor but not by EGF. ProcNatlAcadSciUSA *91*, 12173-12177.

Bladt, F., Riethmacher, D., Isenmann, S., Aguzzi, A., and Birchmeier, C. (1995). Essential role for the c-met receptor in the migration of myogenic precursor cells into the limb bud. Nature *376*, 768-771.

Bradbury, J. M., Edwards, P. A., Niemeyer, C. C., and Dale, T. C. (1995). Wnt-4 expression induces a pregnancy-like growth pattern in reconstituted mammary glands in virgin mice. Dev Biol *170*, 553-563.

Bullock, S. L., Fletcher, J. M., Beddington, R. S., and Wilson, V. A. (1998). Renal agenesis in mice homozygous for a gene trap mutation in the gene encoding heparan sulfate 2-sulfotransferase. Genes Dev *12*, 1894-1906.

Dono, R., Texido, G., Dussel, R., Ehmke, H., and Zeller, R. (1998). Impaired cerebral cortex development and blood pressure regulation in FGF-2-deficient mice. Embo J *17*, 4213-4225.

Echtermeyer, F., Streit, M., Wilcox-Adelman, S., Saoncella, S., Denhez, F., Detmar, M., and Goetinck, P. (2001). Delayed wound repair and impaired angiogenesis in mice lacking syndecan-4. J Clin Invest *107*, 9-14.

Gordon, J. R., and Bernfield, M. R. (1980). The basal lamina of the postnatal mammary epithelium contains glycosaminoglycans in a precise ultrastructural organization. Dev Biol *74*, 118-135.

Guo, L., Degenstein, L., and Fuchs, E. (1996). Keratinocyte growth factor is required for hair development but not for wound healing. Genes Dev *10*, 165-175.

Jackson, D., Bresnick, J., Rosewell, I., Crafton, T., Poulsom, R., Stamp, G., and Dickson, C. (1997). Fibroblast growth factor receptor signalling has a role in

lobuloalveolar development of the mammary gland. J Cell Sci *110 (Pt 11)*, 1261-1268.

Jackson, L. F., Qiu, T. H., Sunnarborg, S. W., Chang, A., Zhang, C., Patterson, C., and Lee, D. C. (2003). Defective valvulogenesis in HB-EGF and TACE-null mice is associated with aberrant BMP signaling. Embo J *22*, 2704-2716.

Jackson-Fisher, A. J., Bellinger, G., Ramabhadran, R., Morris, J. K., Lee, K. F., and Stern, D. F. (2004). ErbB2 is required for ductal morphogenesis of the mammary gland. Proc Natl Acad Sci U S A *101*, 17138-17143.

Li, J. P., Gong, F., Hagner-McWhirter, A., Forsberg, E., Abrink, M., Kisilevsky, R., Zhang, X., and Lindahl, U. (2003). Targeted disruption of a murine glucuronyl C5-epimerase gene results in heparan sulfate lacking L-iduronic acid and in neonatal lethality. J Biol Chem *278*, 28363-28366.

Lin, X., Wei, G., Shi, Z. Z., Dryer, L., Esko, J. D., Wells, D. E., and Matzuk, M. M. (2000). Disruption of gastrulation and heparan sulfate biosynthesis in EXT1-deficient mice. Dev Biol *224*, 299-311.

Liu, B. Y., McDermott, S. P., Khwaja, S. S., and Alexander, C. M. (2004). The transforming activity of Wnt effectors correlates with their ability to induce the accumulation of mammary progenitor cells. Proc Natl Acad Sci U S A *101*, 4158-4163.

Luetteke, N. C., Qiu, T. H., Fenton, S. E., Troyer, K. L., Riedel, R. F., Chang, A., and Lee, D. C. (1999). Targeted inactivation of the EGF and amphiregulin genes reveals distinct roles for EGF receptor ligands in mouse mammary gland development. Development *126*, 2739-2750.

Lyon, M., and Gallagher, J. T. (1994). Hepatocyte growth factor/scatter factor: A heparan sulphate-binding pleiotropic growth factor. BiochemSocTransact *22*, 365-370.

Mailleux, A. A., Spencer-Dene, B., Dillon, C., Ndiaye, D., Savona-Baron, C., Itoh, N., Kato, S., Dickson, C., Thiery, J. P., and Bellusci, S. (2002). Role of FGF10/FGFR2b signaling during mammary gland development in the mouse embryo. Development *129*, 53-60.

Merry, C. L. R., Bullock, S. L., Swan, D. C., Backen, A. C., Lyon, M., Beddington, R. S. P., Wilson, V. A., and Gallagher, J. T. (2001). The molecular phenotype of heparan sulfate in the *Hs2st*$^{-/-}$ mutant mouse. J Biol Chem *276*, 35429-35434.

Rapraeger, A. C., Krufka, A., and Olwin, B. B. (1991). Requirement of heparan sulfate for bFGF-mediated fibroblast growth and myoblast differentiation. Science *252*, 1705-1708.

Ringvall, M., Ledin, J., Holmborn, K., Van Kuppevelt, T., Ellin, F., Eriksson, I., Olofsson, A. M., Kjellén, L., and Forsberg, E. (2000). Defective heparan sulfate biosynthesis and neonatal lethality in mice lacking N-deacetylase/N-sulfotransferase-1. J Biol Chem *275*, 25926-25930.

Schmidt, C., Bladt, F., Goedecke, S., Brinkmann, V., Zschiesche, W., Sharpe, M., Gherardi, E., and Birchmeier, C. (1995). Scatter factor/hepatocyte growth factor is essential for liver development. Nature *373*, 699-702.

Silberstein, G. B., and Daniel, C. W. (1982). Glycosaminoglycans in the basal lamina and extracellular matrix of the developing mouse mammary duct. Dev Biol *90*, 215-222.

Spencer-Dene, B., Dillon, C., Fantl, V., Kerr, K., Petiot, A., and Dickson, C. (2001). Fibroblast growth factor signalling in mouse mammary gland development. Endocr Relat Cancer *8*, 211-217.

Sternlicht, M. D., Kouros-Mehr, H., Lu, P., and Werb, Z. (2006). Hormonal and local control of mammary branching morphogenesis. Differentiation *74*, 365-381.

Wiesen, J. F., Young, P., Werb, Z., and Cunha, G. R. (1999). Signaling through the stromal epidermal growth factor receptor is necessary for mammary ductal development. Development *126*, 335-344.

Yant, J., Buluwela, L., Niranjan, B., Gusterson, B., and Kamalati, T. (1998). In vivo effects of hepatocyte growth factor/scatter factor on mouse mammary gland development. Exp Cell Res *241*, 476-481.

Zcharia, E., Metzger, S., Chajek-Shaul, T., Friedmann, Y., Pappo, O., Aviv, A., Elkin, M., Pecker, I., Peretz, T., and Vlodavsky, I. (2001). Molecular properties and involvement of heparanase in cancer progression and mammary gland morphogenesis. J Mammary Gland Biol Neoplasia *6*, 311-322.

Zioncheck, T. F., Richardson, L., Liu, J., Chang, L., King, K. L., Bennett, G. L., Fügedi, P., Chamow, S. M., Schwall, R. H., and Stack, R. J. (1995). Sulfated oligosaccharides promote hepatocyte growth factor association and govern its mitogenic activity. JBiolChem *270*, 16871-16878.

Appendix 1: Small Changes in Lymphocyte Development and Activation in Mice by Tissue-Specific Inactivation of Heparan Sulfate Biosynthetic Enzymes

1.1 Summary

We have examined the role of heparan sulfate in lymphocyte development and activation by inactivating heparan sulfate biosynthetic enzymes (N-deacetylase/N-sulfotransferase or the Ext1 co-polymerase) specifically in T cells and B cells. We found that while T cell and B cell surface heparan sulfate exists, it does not play a major role in development. *Ndst* deficient T cells showed normal ratios of CD4/CD8 positive cells in the blood, spleen and thymus. *Ext1* deficient B cells showed a slight change in the number of developing B cells, but these did not correlate with a change in antibody production. Heparan sulfate-deficient T cells were hyperresponsive to low-level activation, suggesting that cell surface heparan sulfate plays a role in the proliferation of activated T cells. This correlated well with an analysis of wild type T cell heparan sulfate, which showed a downregulation in cell surface heparan sulfate in response to activation. These findings demonstrate that cell surface heparan sulfate may not play a critical role in lymphocyte development, but does have some very defined roles in lymphocyte activation.

1.2 Introduction

Lymphocytes, i.e. T and B cells, are involved in the adaptive arm of the immune system. Proper cell-cell and cell-matrix interactions are crucial to T and B cell development as well as activation upon antigen challenge. In many contexts, such interactions are coordinated by heparan sulfate proteoglycans. Cell surface heparan sulfate proteoglycans also bind extracellular proteins including growth factors and cytokines, and form signaling complexes with receptors.

Structurally, heparan sulfate is a type of glycosaminoglycan characterized by alternating uronic acid and D-glucosamine units. The chains form covalent complexes with specific core proteins that constitute the families of heparan sulfate proteoglycans (Esko and Lindahl, 2001). The structure of heparan sulfate depends on the action of a family of specific enzymes. Synthesis begins with the assembly of a linkage tetrasaccharide on serine residues of the proteoglycan core protein. After addition of N-acetylglucosamine by a transferase, polymerization occurs by the alternating addition of glucuronic acid and N-acetylglucosamine residues under control of the Ext1/Ext2 co-polymerase. As the chain grows, it undergoes a series of enzymatically catalyzed modifications that include N-acetylglucosamine N-deacetylation and N-sulfation, uronic acid epimerization and variable O-sulfation (Esko and Lindahl, 2001). Four N-deacetylase/N-sulfotransferase isozymes (Ndst1-4) exist that vary in the relative ratios of N-deacetylase/N-sulfotransferase activity and expression across different tissues. The composition on the heparan sulfate chain can therefore vary

widely among different tissues giving rise to unique binding sites for various ligands such as growth factors, morphogens, and matrix proteins.

The importance of heparan sulfate on lymphocytes is only partly known, and the expression on T cells is debated. RT-PCR analysis showed that T cells express the Ndst1 and 2 enzymes from the heparan sulfate biosynthesis pathway. A number of studies indicate that T cells express heparan sulfate and the proteoglycan syndecan-1 (CD138) (Bobardt et al., 2003; Cladera et al., 2001) that mediates cell adhesion (Stanley et al., 1995). Other studies failed to demonstrate heparan sulfate and only very low levels of syndecan were registered (Jackson, 1997), and some claim very low levels of heparan sulfate but high levels of chondroitan sulfate (Hart, 1982). However, the cytokine interleukin (IL-) 2 that is critical to T cell activation and proliferation is known to bind to heparan sulfate (Wrenshall and Platt, 1999). Although chondroitan sulfate is the more abundant proteoglycan in B cells (Engelmann et al., 1995), they show transient expression of some heparan sulfate containing proteoglycans and constant expression of others. Syndecan-1 is found on pro-B cells and plasma cells (Sanderson et al., 1989). Syndecan-4, which may also mediate adhesion (Stanley et al., 1995) is found on B cell lines representing most developmental stages (Kim et al., 1994). Isoform v of CD44 (phagocytic glycoprotein-1, CD44-HS) is expressed on activated B cells where it enhances integrin-mediated adhesion (van der Voort et al., 2000). Through these or other proteoglycans, heparan sulfate may play a role in B cell differentiation and activation by antigens.

Systemic knockouts of heparan sulfate biosynthetic enzymes have not been informative about the role of heparan sulfate on lymphocytes. The *Ndst1* knockout mouse shows dramatically reduced N-sulfation of heparan sulfate on most parts of the body and the new born pups die shortly after birth due to lung failure (Ringvall et al., 2000). The *Ndst2* knockout mouse is viable and the only obvious defect is that of connective tissue-type mast cells (Forsberg et al., 1999). *Ext1* deficiency in the whole animal results in embryonic lethality at E7 from gastrulation defects (Lin et al., 2000). A recent publication surprisingly showed that CD44-deficient mice were normal with respect to B cell subsets and in vitro responses to B cell stimulation (Bradl et al., 2004), even if they show reduced T cell apoptosis in a model of hepatitis (Chen et al., 2001). Syndecan-1 deficient mice show defects in wound healing but are otherwise reported to be normal (Forsberg et al., 1999).

In order to study the effects of disrupting heparan sulfate biosynthesis only in lymphocytes, we used two *Cre-LoxP*-based models. To study the function of heparan sulfate in T cells, we bred mice with a conditional allele of *Ndst1* (*Ndst1*$^{f/f}$) onto an *Lck* (T cell specific) *Cre*$^{+}$ animal. These mice with T cells missing *Ndst1* were bred onto an *Ndst2* deficient background, creating an *Ndst1*$^{f/f}$ *Lck Cre*$^{+}$ *Ndst2*$^{-/-}$ animal whose T cells had missing sulfation on the heparan sulfate chains. To study the role of heparan sulfate in B cells, we bred mice with a conditional allele of *Ext1* (*Ext1*$^{f/f}$) onto a *CD19* (B cell specific) *Cre*$^{+}$ animal, creating mice with B cells with heparan sulfate only as a shortened five linker sugar and no further disaccharide backbone. This approach

permitted investigation of lymphocyte heparan sulfate functions in an otherwise normal environment.

1.2 Results

Conditional Inactivation of Biosynthetic Enzymes in Heparan Sulfate Biosynthesis. To establish the extent of inactivation of *Ndst1* in T cells and *Ext1* in B cells, we analyzed genomic DNA by Southern blotting and PCR. Gene eviction was substantial, but incomplete in both T and B cells, possibly due to variability in Lck Cre and CD19 Cre expression (data not shown). However, bFGF binding was abolished, suggesting that both T cells (Fig 1-1A) and B cells (Fig 1-1B) were devoid of any normally functioning heparan sulfate.

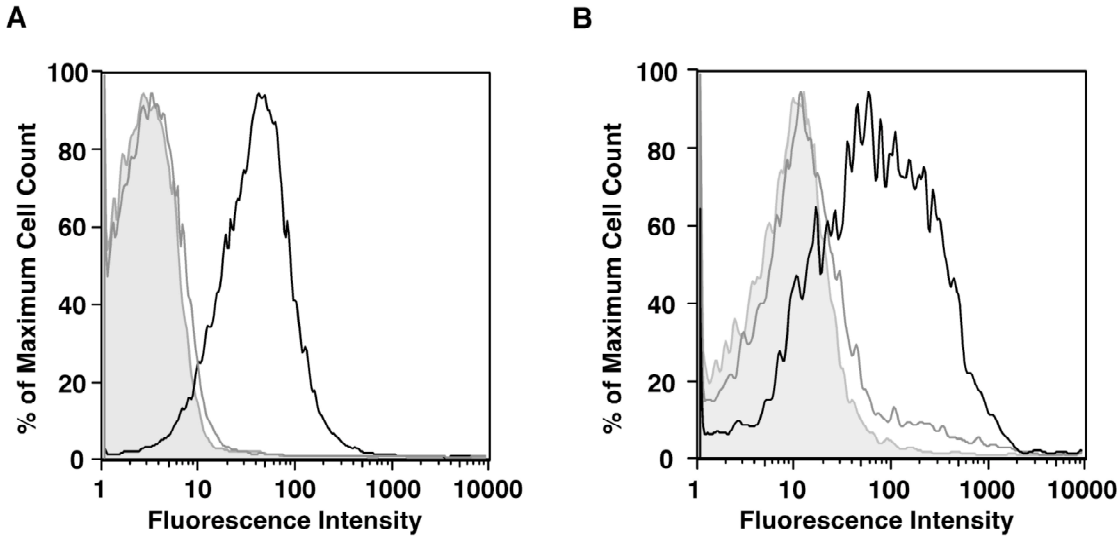

Figure 1-1: Disruption of heparan sulfate biosynthesis in T cells and B cells. Splenic lymphocytes of different genotypes were incubated with biotinylated basic Fibroblast Growth Factor (bFGF), stained with PE-Cy5-streptavidin and analyzed by flow cytometry. (**A**) T cells. Grey shaded curve, N*dst1*$^{f/f}$ *LckCre*$^{-}$*Ndst2*$^{-/-}$ T cells without bFGF; black line curve, *Ndst1*$^{f/f}$ *LckCre*$^{-}$ *Ndst2*$^{-/-}$ T cells with bFGF; grey line curve, *Ndst1*$^{f/f}$ *LckCre*$^{+}$ *Ndst2*$^{-/-}$ T cells with bFGF. (**B**) B cells. Grey shaded curve, *Ext1*$^{f/f}$ *CD19Cre*$^{-}$ B cells without bFGF; black line curve, *Ext1*$^{f/f}$ *CD19Cre*$^{-}$ B cells with bFGF; grey line curve, *Ext1*$^{f/f}$ *CD19Cre*$^{+}$ B cells with bFGF.

Alterations in T Cell Development. Even though there were no differences in T cell counts in the thymus, peripheral blood, or spleen between littermate pairs of *Ndst1* $^{f/f}$ *Lck Cre*$^{-}$ *Ndst2*$^{-/-}$ and *Ndst1* $^{f/f}$ *Lck Cre*$^{+}$ *Ndst2*$^{-/-}$ mice (Table 1.1), we examined spleen histology for structural abnormalities (n=3). The wild type spleens showed defined lymphoid follicles with B cells (Fig. 1-2C) and periarteriolar lymphoid sheath (PALS) containing T cells (Fig. 1-2B) surrounded by areas dense with macrophages (Fig 2A). The *Ndst1* $^{f/f}$ *Lck Cre*$^{+}$ *Ndst2*$^{-/-}$ spleens showed reduction in follicular size (Fig 2D), T cells were displaced into the B cell areas (Fig 1-2E), and the entire follicles appeared smaller (Fig 1-2F).

Table 1-1: T cell counts in *Ndst1* $^{f/f}$ *Lck Cre*$^{+}$ *Ndst2*$^{-/-}$ and *Ndst1* $^{f/f}$ *Lck Cre*$^{-}$ *Ndst2*$^{-/-}$ mice[1]

	Ndst1 $^{f/f}$ *Lck Cre*$^{+}$ *Ndst2*$^{-/-}$	*Ndst1* $^{f/f}$ *Lck Cre*$^{-}$ *Ndst2*$^{-/-}$	p-value
Thymus			
CD4-/CD8- cells	9.7 (6.1-13.3) %	9.6 (5.6-13.7) %	1.00
CD4+/CD8+ cells	76.9 (73.3-80.5) %	76.1 (73.6-78.7) %	1.00
CD4+ cells[2]	9.7 (9.4-10.1) %	10.0 (9.5-10.4) %	0.44
CD8+ cells[2]	3.7 (3.4-4.0) %	4.3 (3.3-5.3) %	1.00
CD4+/CD8+ ratio[2]	2.65 (2.32-2.97)	2.42 (1.96-2.89)	1.00
Peripheral blood			
CD4+ cells	12.5 (8.0-14.3) %	12.4 (9.5-15.1) %	1.00
CD8+ cells	6.8 (4.2-8.8) %	7.1 (4.7-8.2) %	0.83
CD4+/CD8+ ratio	1.81 (1.54-2.16)	1.89 (1.55-2.06)	0.83
Spleen			
CD4+ cells	10.6 (4.5-16.7) %	14.9 (9.6-20.1) %	0.44
CD8+ cells	5.5 (3.2-7.9) %	7.2 (5.3-9.1) %	0.44
CD4+/CD8+ ratio	1.76 (1.41-2.12)	2.01 (1.81-2.21)	1.00

[1]n= 10 littermate pairs
[2]single positive cells

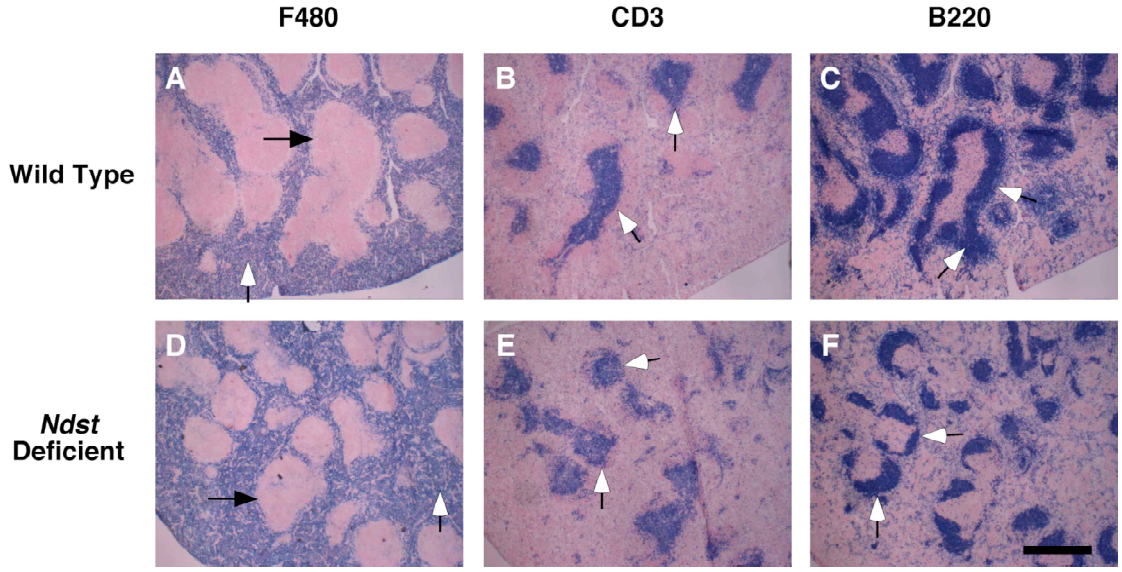

Figure 1-2: Splenic follicle architecture in *Ndst1*$^{f/f}$ *LckCre*$^{+}$ *Ndst2*$^{-/-}$ mice. Spleen sections from wild type and *Ndst* deficient mice. (**A, D**) white arrows, F480 macrophage stain; black arrows, splenic follicle. (**B, E**) white arrows, CD3 stain for T cells. (**C, F**) white arrows, B220 stain for B cells. Original magnification, 20x

Alterations in B Cell Development

The percentage of bone marrow pro-B cells was significantly higher and the percentage of splenic marginal and transitional B cells was significantly lower in the *Ext1*$^{f/f}$ *CD19 Cre*$^{+}$ mice than in their *Ext1*$^{f/f}$ *CD19 Cre*$^{-}$ littermates (Table 1-2). There were heparan sulfate alterations related to the B cell developmental stages (Figure 1-3A). Pro-B cells were unaffected, whereas there was a gradual loss of ability to bind bFGF through the remaining stages in the bone marrow. The B cells in peripheral blood bound more bFGF than the mature B cells in the bone marrow, and there was further loss of binding in the spleen. These differences in bFGF binding were not related to changes in one of the major core proteins of heparan sulfate-bearing proteoglycans found in B cells, as indicated by syndecan-1 expression (Figure 1-3B).

Table 1-2: B cell counts in *Ext1$^{f/f}$ CD19 Cre^{-} and Ext1$^{f/f}$ CD19 Cre^{+}* mice[1]

	EXT1 f/f CD19 Cre+	*EXT1 f/f CD19 Cre-*	p-val.
Bone Marrow			
Pro B	10.4 (8.9-15.3) %	8.4 (6.4-10.2) %	**0.018**
Pre B	25.2 (16.4-32.5) %	26.6 (19.3-31.8) %	0.50
Immature B	18.0 (14.5-21.4) %	19.6 (14.6-24.4) %	0.27
Mature B	7.8 (6.0-9.7) %	7.5 (5.2-10.1) %	0.67
Peripheral blood			
B cells	4.6 (3.8-5.2) x 10^9/L	5.2 (4.6–6.2) x 10^9/L	0.06
T cells	4.0 (3.1-4.8) x 10^9/L	4.1 (3.6-4.9) x 10^9/L	0.51
Spleen			
Marginal and Transitional B cells	6.1 (4.6-8.3) %	8.4 (6.0-11.3) %	0.04
Follicular B cells	21.7 (17.1-26.3) %	19.7 (17.3-23.1) %	0.24

[1]n=11 littermate pairs

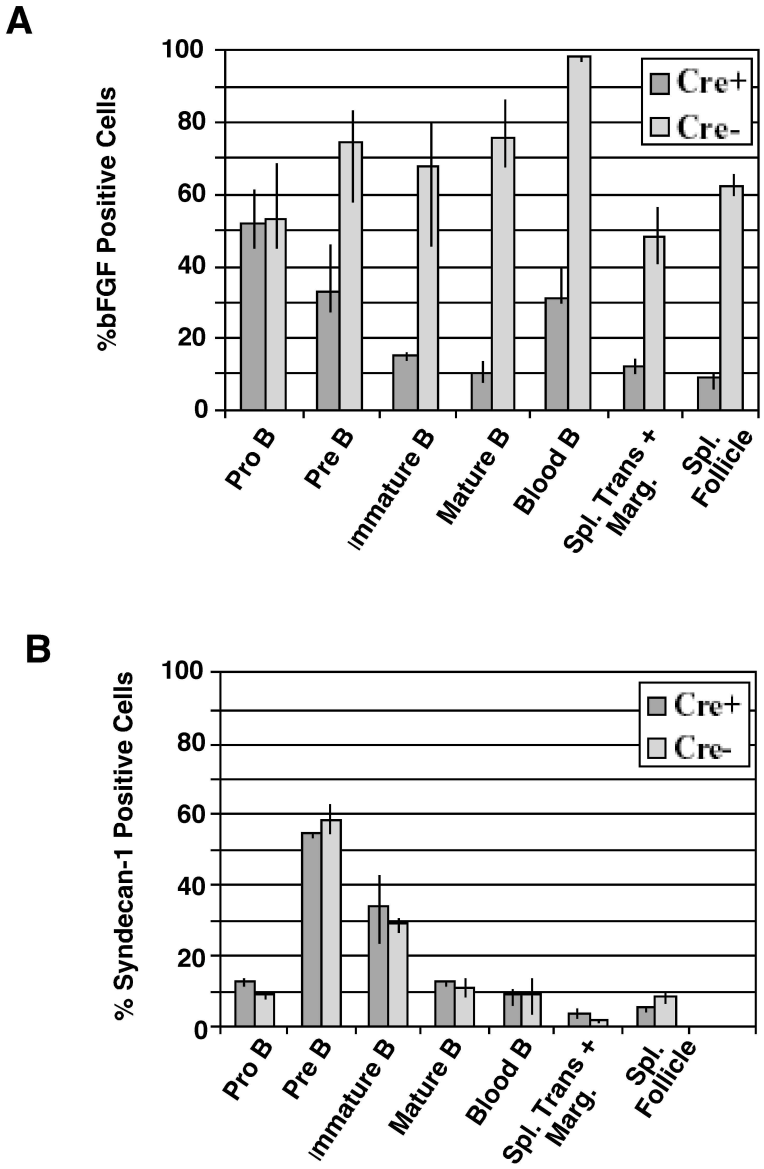

Figure 1-3: B cell bFGF binding and Syndecan-1 expression in Ext1$^{f/f}$ CD19Cre+ mice. (A) bFGF-binding B cells as percentages of total B cells at the similar developmental stage for bone marrow (pro-B, pre-B, immature B, and mature B cells), peripheral blood, and spleen (transitional and marginal B, and follicular B cells) in *Ext1*$^{f/f}$ *CD19Cre*$^{+}$ and *Ext1*$^{f/f}$ *CD19Cre*$^{-}$ mice (n=3 littermate pairs). **(B)** Syndecan-1 expressing B cells as percentages of total B cells at the similar developmental stage for bone marrow, peripheral blood, and spleen (n=2 littermate pairs).

B Cell Activation. After both subcutaneous and intraperitoneal injection of the T-dependent antigen DNP-KLH there was a significant increase in DNP-specific IgM and IgG1 ($p<0.001$) (Figure 1-4). There were no differences between the mice with B cell *Ext1* inactivation and their littermate controls ($p>0.27$). Subcutaneous immunization with the T-independent antigen DNP-ficoll gave very small responses (data not shown), but after intraperitoneal immunization there were significant increases in DNP-specific IgM and IgG3 ($p<0.001$). There were no differences between the groups ($p>0.60$).

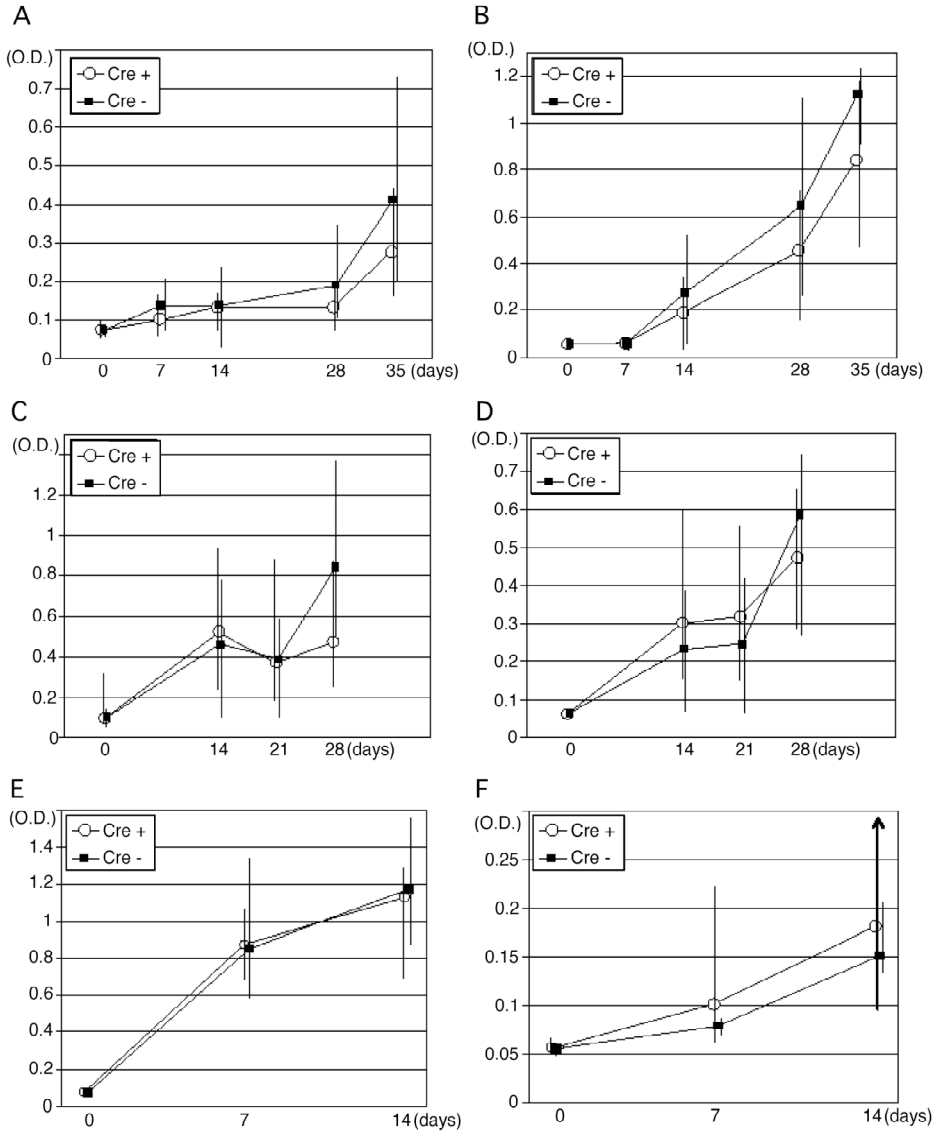

Figure 1-4: Antibody responses in Ext1$^{f/f}$ CD19Cre+ mice.
DNP-specific IgM (**A**) and IgG1 (**B**) antibody response after subcutaneous immunization with the T-dependent antigen DNP-KLH (n=7 littermate pairs, medians with 95 % confidence intervals). DNP-specific IgM (**C**) and IgG1 (**D**) antibody response after intraperitoneal immunization with DNP-KLH (n=5 littermate pairs, medians and range). DNP-specific IgM (**E**) and IgG3 (**F**) antibody response after intraperitoneal immunization with the T-independent antigen DNP-ficoll (n=5 littermate pairs, medians and range).

T Cell Proliferation and Activation. To examine the effect of T cell heparan sulfate on T cell proliferation, we first determined if there were changes in cell surface heparan sulfate in normal proliferating activated T cells. Unstimulated T cells contained high levels of CFSE (Fig 1-5A). After activation by anti-CD3, there were five different proliferative subsets, differentiated by decreasing amounts of CFSE. The entire population of activated T cells showed a reduced ability to bind to bFGF (Fig 1-5B) indicating down-regulation of cell surface heparan sulfate. The more they proliferated as indicated by the CFSE stain, the more the normal T cells down-regulated heparan sulfate as shown by an increasing reduction in bFGF binding (Fig 1-5C).

Figure 1-5: T cell heparan sulfate expression during *in vitro* activation. Isolated splenic T cells were stimulated with anti-CD3, and stained with CFSE and bFGF to measure proliferation and cell surface heparan sulfate. (**A**) Black line, isolated T cells stained with CFSE showing 5 different proliferative subsets; grey shaded area, CFSE stain in non-activated control T cells. (**B**) bFGF binding in entire activated T cell population (Grey shaded curve, N*dst1*$^{f/f}$ *LckCre*$^{-}$*Ndst2*$^{-/-}$ T cells without bFGF; black line curve, entire population of activated *Ndst1*$^{f/f}$ *LckCre*$^{-}$ *Ndst2*$^{-/-}$ T cells with bFGF). (**C**) bFGF binding in individual subsets of activated T cells as indicated by CFSE staining in panel A (Grey shaded curve, N*dst1*$^{f/f}$ *LckCre*$^{-}$*Ndst2*$^{-/-}$ T cells without bFGF; black line curve, individual populations of activated *Ndst1*$^{f/f}$ *LckCre*$^{-}$ *Ndst2*$^{-/-}$ T cells with bFGF).

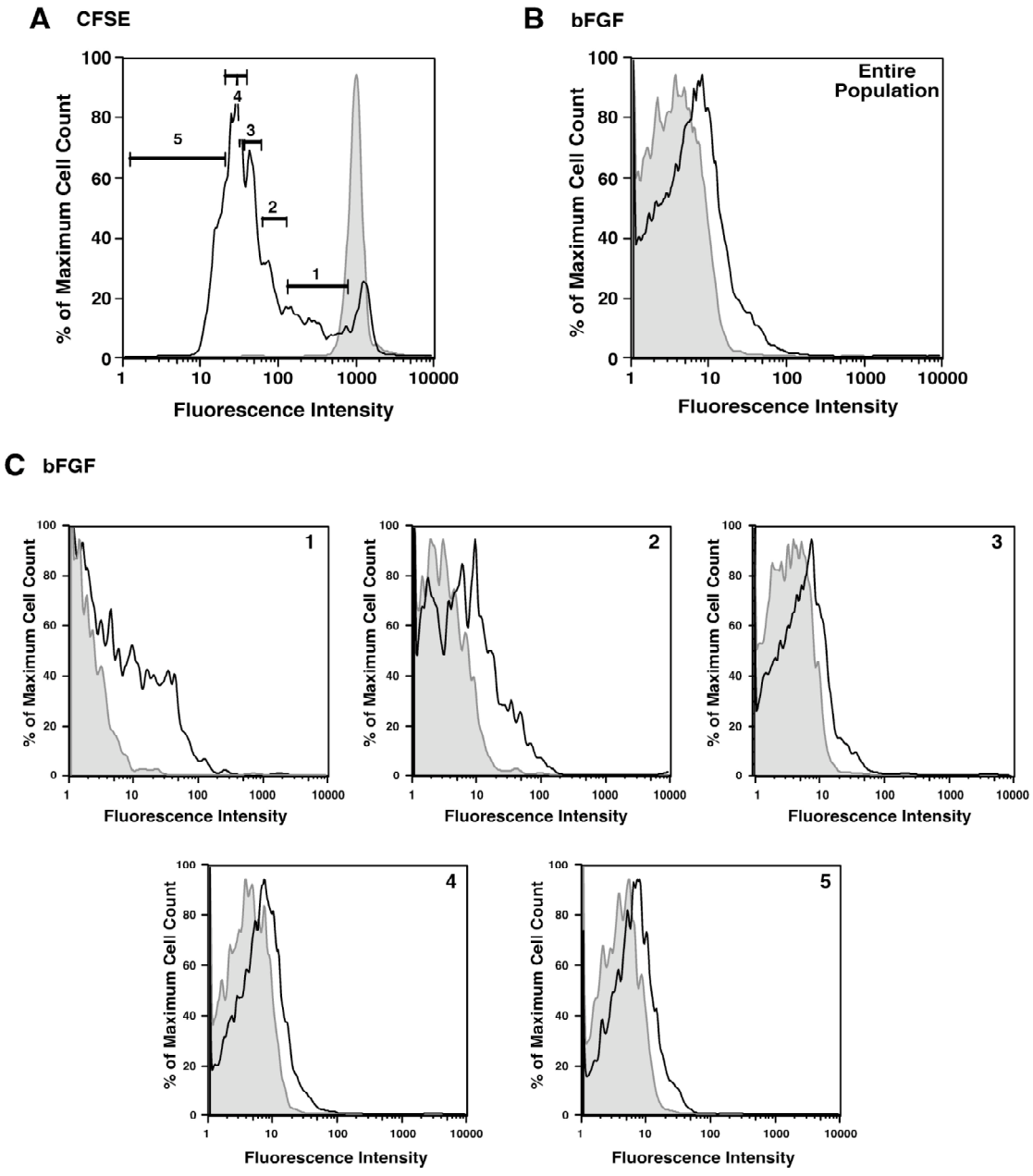
A CFSE
% of Maximum Cell Count
Fluorescence Intensity
1
2
3
4
5
B bFGF
Entire Population
% of Maximum Cell Count
Fluorescence Intensity
C bFGF
1
2
3
4
5
% of Maximum Cell Count
Fluorescence Intensity

The down-regulation of heparan sulfate during proliferation in wild type T cells would suggest that T cells deficient in heparan sulfate may be hypersensitive to T cell activation. Splenic T cells from wild type, *Ndst1* $^{f/f}$ *Lck Cre*$^{-}$ *Ndst2*$^{-/-}$ and *Ndst1* $^{f/f}$ *Lck Cre*$^{+}$ *Ndst2*$^{-/-}$ animals were activated by anti-CD3 and proliferation was measured by CFSE staining. At 0.8 mg/ml and 0.1 mg/ml anti-CD3, T cells from the genetically altered mice proliferated to the same extent as the wild type (Fig 1-6A,B). At lower antibody doses, however, the *Ndst* deficient T cells were more sensitive than the wild type cells, as shown by the increase in proliferation (Fig 1-6C,D). We examined IL-2 production during activation as a possible mechanism for this increased proliferation, but there were no differences in IL-2 concentrations (data not shown).

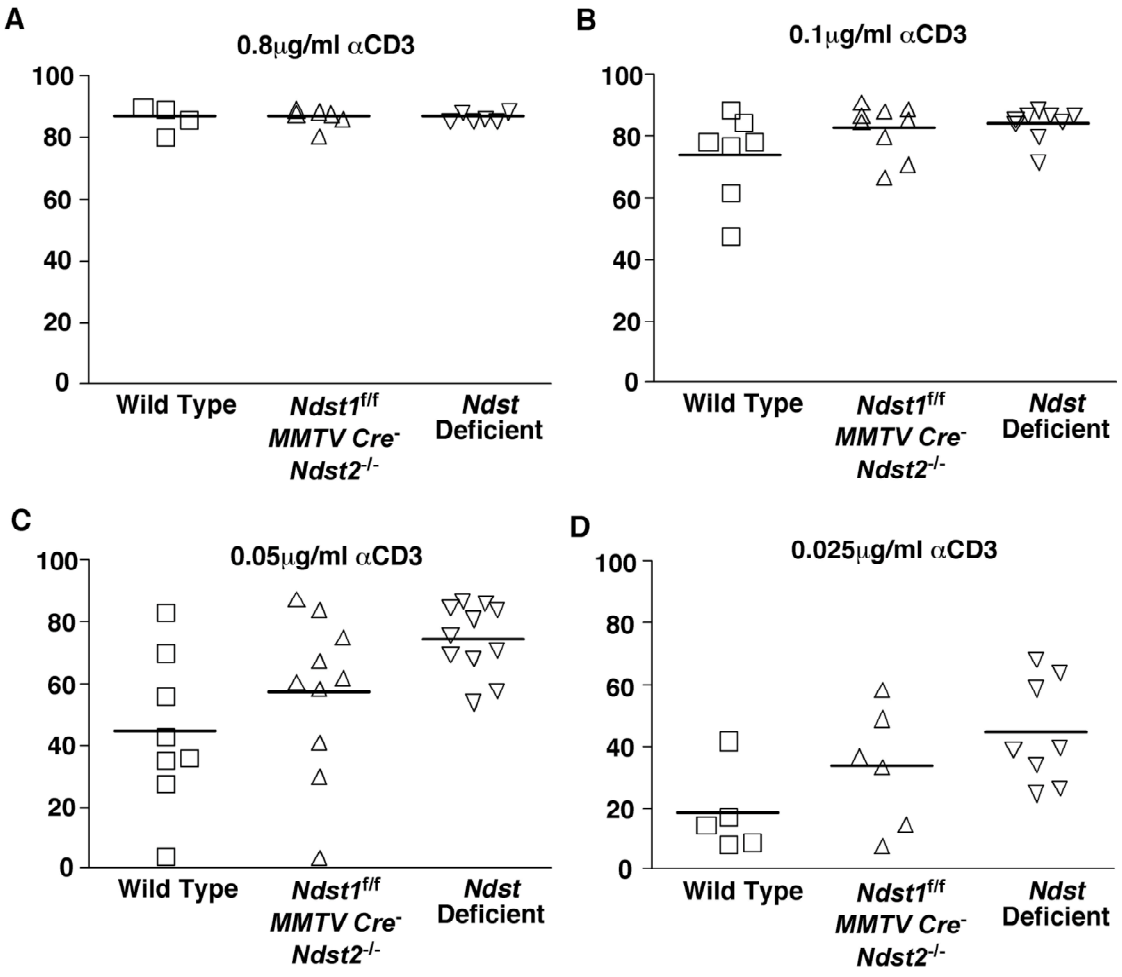

Figure 1-6: T cell activation by anti-CD3 in *Ndst1*$^{f/f}$ *LckCre*$^{+}$ *Ndst2*$^{-/-}$ mice . Isolated splenic T cells from wild type, *Ndst1*$^{f/f}$ *LckCre*$^{-}$ *Ndst2*$^{-/-}$, and *Ndst1*$^{f/f}$ *LckCre*$^{+}$ *Ndst2*$^{-/-}$ animals were stimulated with varying concentrations of anti-CD3 for 3 days, and proliferation was measured as a decrease in CFSE stain. Data are percentage proliferating cells of total cells. Square; wild type, Upward triangle; *Ndst1*$^{f/f}$ *LckCre*$^{-}$ *Ndst2*$^{-/-}$, Downward triangle; *Ndst1*$^{f/f}$ *LckCre*$^{+}$ *Ndst2*$^{-/-}$. (**A**) Isolated T cells stimulated with 800 ng/mL anti-CD3. (**B**) Isolated T cells stimulated with 100 ng/mL anti-CD3. (**C**) Isolated T cells treated with 50 ng/mL ant-CD3. (**D**) Isolated T cells treated with 25 ng/mL anti-CD3.

1.4 Discussion

In this study, we found that while T cell and B cell surface heparan sulfate exists, it does not play a major role in development. There were slight changes in the number of developing B cells, but these did not correlate with a change in antibody production. Heparan sulfate-deficient T cells were hyperresponsive to low-level activation, suggesting that cell surface heparan sulfate plays a role in the proliferation of activated T cells.

T cell changes

Despite incomplete *Ndst1* eviction, which is in accordance with previous findings employing Lck Cre (Gu et al., 1994), bFGF binding to T cells was abolished, indicating a complete loss of normally functioning heparan sulfate. This may indicate that *Ndst2* plays a large role in sulfation of T cells, since we used *Ndst2*$^{-/-}$ mice. In spite of the lack of bFGF binding, T cell development was normal in the *Ndst1* $^{f/f}$ *Lck Cre*$^{+}$ *Ndst2*$^{-/-}$ animals. Lck has an early expression profile in T cell development, and is subsequently found in all T cell lineages (Gu et al., 1994), so the results cannot be attributed to late Lck Cre expression. Since functional heparan sulfate ectodomains may be shed from cells, ~~the~~ heparan sulfate produced by the thymic stroma might render the T cell-specific heparan sulfate redundant in development.

T cells were found in B cell areas of splenic lymphoid follicles in the *Ndst1*$^{f/f}$ *Lck Cre*$^{+}$ *Ndst2*$^{-/-}$ mice. Thus, T cell heparan sulfate may play a critical role in defining

cellular compartments in splenic follicles by organizing growth factors and extracellular matrix proteins into trafficking regions. Cell surface integrins have been proposed to regulate the spatial organization of T cells within lymphoid organs (van den Berg et al., 1993), and integrins are known to interact with cell surface heparan sulfate (Diamond et al., 1995). Another possible role is the interaction between heparan sulfate and chemokines. CCL19 and CCL21 are involved in attracting and retaining naïve T cells into peripheral lymph node T cell areas (Ebert et al., 2005), and splenic follicles may use a similar mechanism. Almost all known chemokines bind heparin or heparan sulfate *in vitro* (Lortat-Jacob et al., 2002).

Genetically altered T cells showed a hyperresponsive proliferative response to low levels of activation. This could be due to the interaction between cell surface heparan sulfate and IL-2. Cell surface heparan sulfate may bind IL-2 and sequester this cytokine away from the IL-2 receptor as part of normal regulation of the immune response, and removal of cell surface heparan sulfate would make the T cells more sensitive to IL-2. Wild type T cells downregulated cell surface heparan sulfate in response to proliferative signals, which would facilitate ~~a~~ rapid clonal expansion. This proposed mechanism of heparan sulfate sequestration of a ligand from a receptor has been shown for the growth factor Wnt in fibroblasts (Ai et al., 2003).

The hypersensitivity of heparan sulfate-deficient T cells may implicate heparan sulfate in autoimmunity. Many autoimmune diseases arise from overactive, or especially sensitive T cells. Other T cell specific changes in cell surface glycosylation have led to autoimmune phenotypes. The Mgat5 (an enzyme involved in N-

acetylglucosamine transfer) deficient animal developed kidney autoimmune disease, possibly due to lowering T cell activation thresholds (Demetriou et al., 2001). Its possible that these T cell specific, heparan sulfate deficient animals may also show autoimmune phenotypes.

B cell changes

Even if there was efficient *Ext1* gene inactivation resulting in reduced and/or changed heparan sulfate expression in B cells in the present mouse model, there were only minor changes in B cell subpopulations and no significant changes in antibody responses to T-dependent or T-independent antigens. Various factors may have contributed to these results.

One possibility is that the timing or degree of *Ext1* inactivation may have been inappropriate. The B220 isoform of CD45 is the earliest B lineage marker, but CD19 is expressed from the next stage, the pro-B cell (Hardy and Hayakawa, 2001). A previous study showed that the deletion efficiency of another gene using the same CD19 Cre+ mouse strain was 75-80% in pre-B cells and 90-95% in splenic B cells, indicating that the Cre-mediated deletion is an ongoing process during B cell development (Rickert et al., 1997). These data are comparable to our findings, showing a progressive reduction in bFGF binding taking place after the pro-B cell stage in the Ext-1f/f CD19 Cre+ mouse (Fig. 2). Other investigations using CD19 Cre-mediated B cell gene alteration in the Pax5 (Horcher et al., 2001) and alpha 4 (Inui et al., 2002) genes have resulted in changes in B cell functions, indicating that this

approach may be effective for some genes. However, the *Ext1* gene inactivation did not result in total abolishment in bFGF binding at any stage. Thus the experimental animals may have had enough cells with functional heparan sulfate to be able to respond normally to differentiation signals.

It could be argued that heparan sulfate on the B cells might not be crucial to development during the stages after CD19 is expressed. The current literature does not support this view. In the mouse, the earliest B cell stages are dependent on stromal contact and cytokines, especially stem cell factor, interleukin (IL-) 7, and Flt-3 ligand for normal development (Hardy, 1991) (Kouro et al., 2001). Pro-B cells lacking plasma membrane heparan sulfate due to heparinase treatment show a 50-75% reduction in IL-7 driven proliferation in parallel with substantial reduction in their ability to bind biotinylated IL-7 (Borghesi et al., 1999).

It has been estimated that about 90% of the immature B cells produced in the bone marrow are lost due to selection against self-reactive cells (Rolink et al., 2001). It is not known whether heparan sulfate is involved in this selection, which is strongly dependent on the B cell receptor. This selection process may have favored the more normal B cells in our experimental mouse, since a larger proportion of the B cells in the peripheral blood were able to bind bFGF than of the immature or mature B cells in the bone marrow (Fig 3). Even so, there was a tendency towards lower B cell counts in peripheral blood of the mice with *Ext1* gene inactivation (Table 2). Since we did not measure bone marrow B cell turnover and apoptosis in our mice, it is not known whether there may have been a compensatory enhancement in the production of B-

committed precursor cells. The finding of an increased percentage of pro-B cells in the *Ext-1*$^{f/f}$ *CD19 Cre*$^{+}$ mice may support this hypothesis.

Antibody responses to immunizations were similar in the mice with *Ext1* gene inactivation and control littermates. There may have also been a selection of functional cells at this stage, where normally only a very limited number of activated cells are necessary to give rise to large clones of antibody-producing plasma cells. Upon antigen stimulation, human tonsillar B cells show a strong transient increase in the specific heparan sulfate-containing isoform of CD44 (van der Voort et al., 2000). This strongly promotes the binding of hepatocyte growth factor through a heparan sulfate dependent mechanism, which in turn may strengthen B cell adhesion e.g. to antigen presenting cells. Mice homozygous for CD44 gene inactivation have normal B cells and show no defects in response to type II collagen immunization (Stoop et al., 2001). However, their B cells show altered migration patterns during inflammation (Stoop et al., 2002), resulting in reduced responses in a model of autoimmune arthritis (Stoop et al., 2001). Since the *Ext1* gene-inactivated mice were only challenged by immunization, we cannot exclude that their responses to infection, perhaps with selected pathogens, may be altered.

In conclusion, we acknowledge that cell surface heparan sulfate may not play a critical role in lymphocyte development, but does have some very defined roles in lymphocyte activation. Further studies are needed to determine if selected pathogen response, or models of autoimmunity are affected by a change in lymphocyte cell surface heparan sulfate.

1.5 Materials and Methods

Mice C57BL/6 mice expressing Lck-Cre (J Marth, University of California, San Diego, CA), mice bearing a *LoxP* flanked allele of *Ndst1* (Grobe, 2005), and *Ndst2* deficient mice (L Kjellen, University of Uppsala, Sweden (Forsberg et al., 1999)) were crossed until *Ndst1*$^{f/f}$ *Lck Cre*$^{+}$ on an *Ndst2*$^{-/-}$ background mice were obtained. Littermates of Cre^{-} and Cre^{+} animals were matched in most experiments. Wild type C57BL/6 animals were ordered from Jackson Laboratories (Bar Habor, ME). C57BL/6 mice expressing CD19 Cre were crossed with mice homozygous for a *LoxP*-modified *Ext1* allele (Y Yamaguchi, Burnham Institute, San Diego, CA) generating heterozygous Cre-mediated deletion of the *Ext1* gene in B cells. Through further crossing, *Ext1*$^{f/f}$ *CD19 Cre*$^{+}$ and *Ext1*$^{f/f}$ *CD19 Cre*$^{-}$ littermates were bred. The mice were born healthy and grew normally, showing no obvious anatomical abnormalities. All animals were handled in accordance with protocols for the humane treatment of animals approved by the IACUC and Animal Subjects Committee at the University of California, San Diego. All experiments were approved by the Animal Care Facility.

T Cell Isolation Mice were killed by cervical traction while in isoflurane (Vedco, St. Joseph, MO) anesthesia. The spleen and thymus were removed and placed in phosphate-buffered saline (PBS) with 1% fetal calf serum (FCS) and 10 mM Hepes (Invitrogen, Carlsbad, CA). The organs were mashed between two sterile slides and

resuspended in ACK lysis buffer (Fisher Scientific, Pittsburgh, PA) for 2 minutes to eliminate red blood cells. The cells were filtered through a 40 mm cell strainer (BD Falcon, Franklin Lakes, NJ) and T cells were isolated using anti-CD90 antibody-coated paramagnetic beads (MACS, Miltenyil Biotec, Auburn, CA) as indicated by the manufacturer. T cells from blood were collected by tail vein incision and isolated similarly to the organ isolation protocol.

B Cell Isolation Mice were killed as described. Peritoneal lavage was performed using 10 mL sterile PBS and peripheral blood was obtained by cardiac puncture, using EDTA as an anticoagulant. Bone marrow was obtained by flushing the femurs, tibiae and humeri with sterile buffer (Hank's Balanced Salt Solution (HBSS) with 1% FCS and 10mM Hepes). The spleens were removed, and B cells from peritoneum, bone marrow, spleen, and blood were isolated by procedures similar to those described for T cells, using anti-B220 antibody-coated paramagnetic (MACS) beads.

Lymphocyte Subpopulations. B cells from bone marrow, peripheral blood, spleen, and peritoneal lavage were stained for flow cytometric analysis with various combinations of the following monoclonal antibodies (Pharmingen, BD Biosciences, San Diego, CA): anti-CD43-FITC, anti-IgD-FITC, anti-IgM-PE, anti-B220-FITC or –PerCP, anti-CD3-PE. Fc receptor-mediated unspecific binding was blocked by pre-incubation with unlabelled anti-CD16/anti-CD32 antibody (Pharmingen). Absolute

lymphocyte numbers in EDTA-anticoagulated peripheral blood from tail veins were counted using an automated hematology instrument calibrated for mouse samples. The B and T cell percentages of the total lymphocytes were determined by flow cytometry in parallel samples stained with anti-B220-FITC and anti-CD3-PE, and the B and T cell counts were calculated. T cells from blood, spleen and thymus were stained for flow cytometric analysis with the following monoclonal antibodies (Invitrogen, Carlsbad, CA): anti-CD4-FITC, and anti-CD8-PE. Flow cytometry was performed on a FACSCalibur flow cytometer (Becton Dickinson, San Diego, CA) and the data were analyzed using the CellQuest software (Becton Dickinson).

bFGF Binding. The binding of basic Fibroblast Growth Factor (bFGF) was determined using flow cytometry. Isolated T cells were incubated with biotinylated bFGF in Hams F12 medium (Invitrogen, Carlsbad, CA) with 0.5 % BSA (Sigma, St. Louis, MO) for 1 hour with shaking at 4ºC. Cells were washed twice in PBS and incubated in PBS containing streptavidin-APC for 20 minutes with shaking at 4ºC. Samples where bFGF was omitted were included as negative controls. bFGF binding to B cells from bone marrow, peripheral blood, and spleen was also determined, and the B cell sub-populations were gated using antibody staining as indicated above. To show that bFGF binding was related to heparan sulfate expression, controls were also performed after pre-treatment of T and B cells with heparin lyases I, II, and III (Seikagaku, East Falmouth, MA) for 4 hours at 37 ºC.

Proteoglycan Expression. The expression of syndecan-1 on B cell subpopulations in bone marrow, peripheral blood, and spleen was determined using flow cytometry. The cells were incubated with a rat anti-syndecan-1 antibody (Research Diagnostics, Flanders, NJ) at 1.7mg/10^6 cells for 20 min at 37 ºC. Binding was detected in a two-step procedure, using a biotinylated rabbit anti-rat antibody (Pharmingen) followed by streptavidin-APC. The B cell subpopulations were gated using antibody staining as indicated above. Samples where anti-syndecan-1 antibody was omitted were used as controls for unspecific binding.

B Cell Responses. Littermate pairs of *Ext1*$^{f/f}$ *CD19 Cre*$^{+}$ and *Ext1*$^{f/f}$ *CD19 Cre*$^{-}$ mice were immunized with dinitrophenol conjugated either to keyhole limpet hemocyanin (DNP-KLH, Biosearch Technologies, Novato, California) to test T-dependent B cell responses or to ficoll (DNP-ficoll, Biosearch Technologies) to test T-independent B cell responses. The mice were given metoxyflurane anesthesia (Medical Developments International, Springvale, Victoria, Australia) and all blood samples were obtained from tail veins. Immunizations with DNP-KLH: After obtaining a pre-immune blood sample, 10 ug DNP-KLH in 100 uL Freund's complete adjuvant (Sigma, St. Louis, Missouri, USA) was given subcutaneously in the first series of experiments (n= 7 littermate pairs). Samples were drawn after 7, 14, and 28 days, and a booster dose of 10 ug DNP-KLH in 100 uL Freund's incomplete adjuvant (Sigma) was given immediately after the 28-day sample. A final sample was drawn on day 35, whereafter the mice were killed. In a second series (n=5 littermate pairs),

immunizations were given intraperitoneally, samples were drawn on days 0, 14, 21 and 28, and the booster dose was given on day 21. Immunizations with DNP-ficoll: After obtaining a pre-immune blood sample, 10 ug DNP-ficoll in 100 uL sterile PBS was given subcutaneously in the first series of experiments (n=7 littermate pairs). Samples were drawn after 7 and 14 days, and the mice were killed. The second series was performed similarly (n=5 littermate pairs), except that the immunizations were given intraperitoneally. Serum was kept at – 20 ºC and analyzed in one batch.

Quantification of DNP-specific antibodies was done in enzyme immunoassays. The plates were coated with DNP-BSA (Biosearch Technologies) 200 ug/mL and blocked with 10 % FCS in PBS. Serum was diluted 1/200 for measurement of IgM (all samples), 1/1000 for measurement of IgG1 (DNP-KLH-immunized mice), and 1/800 for measurement of IgG3 (DNP-ficoll-immunized mice). Detection was performed using alkaline phosphatase-conjugated goat anti-mouse isotype-specific antibodies (IgM, IgG1, or IgG3, Southern Biotechnology Associates, Birmingham, Alabama, USA). The substrate was pNPP (Southern Biotechnology Associates), and the reactions were stopped after 20 min using 2 M NaOH. Optical density at 405 nm was read spectrophotometrically (Molecular Devices, Sunnyvale, CA), and the results are given as mean optical density of duplicate wells.

T cell proliferation after activation.24 well tissue culture plates (BD Falcon, Franklin Lakes, NJ) were coated with goat anti-hamster IgG (Sigma) at 37 ºC for 2 hours and washed with PBS. Hamster anti-mouse CD3 antibody (Pharmingen) was

added to the wells at increasing concentrations from 25 ng/ml to 800 ng/ml, and the plates were incubated at 37 ºC for 1 hour. Isolated T cells (10 x 10^6 cells/ml) were incubated in 2.5 mM Carboxy-fluorescein diacetate, succinimidyl ester (CFSE) (Invitrogen, Carlsbad, CA) in prewarmed PBS at 37 ºC for 10 minutes. CFSE is a cytoplasmic dye that becomes more diffuse with each cell division. The cells were washed in PBS and transferred to the anti-CD3 coated plates, permitting crossbinding of T cell receptors and induction of activation and proliferation. After two days of incubation at 37 ºC with 5 % CO_2, the cells were harvested and flow cytometry was performed.

Splenic Histology. Histological analyses were performed by the Cancer Center Histology Core at the University of California, San Diego. Frozen sections were cut and stained with a T cell specific antibody to CD3 (Abcam, Cambridge, MA), a macrophage specific antibody to F4/80 (Abcam), or a B cell specific antibody to B220 (R&D Systems, Minneapolis, MN).

IL-2 Secretion Supernatants from activated T cells were tested for IL-2 production using a commercial ELISA kit (eBioscience, San Diego, CA).

Statistics Due to small data sets and non-normal distribution of variables, non-parametric statistics were used. Data are given as medians with 95% non-parametric confidence intervals (six or more observations) or range (less than six observations) in

parenthesis. Differences between littermate pairs were compared using the Mann-Whitney U-test. The antibody responses after immunization were analyzed using two-way analysis of variance for repeated measures, employing logarithmic or rank transformation if necessary to get an appropriate model fit.

1.6 References

Ai, X., Do, A. T., Lozynska, O., Kusche-Gullberg, M., Lindahl, U., and Emerson, C. P., Jr. (2003). QSulf1 remodels the 6-O sulfation states of cell surface heparan sulfate proteoglycans to promote Wnt signaling. J Cell Biol *162*, 341-351.

Bobardt, M. D., Saphire, A. C., Hung, H. C., Yu, X., Van der Schueren, B., Zhang, Z., David, G., and Gallay, P. A. (2003). Syndecan captures, protects, and transmits HIV to T lymphocytes. Immunity *18*, 27-39.

Borghesi, L. A., Yamashita, Y., and Kincade, P. W. (1999). Heparan sulfate proteoglycans mediate interleukin-7-dependent B lymphopoiesis. Blood *93*, 140-148.

Bradl, H., Schuh, W., and Jack, H. M. (2004). CD44 is dispensable for B lymphopoiesis. Immunol Lett *95*, 71-75.

Chen, D., McKallip, R. J., Zeytun, A., Do, Y., Lombard, C., Robertson, J. L., Mak, T. W., Nagarkatti, P. S., and Nagarkatti, M. (2001). CD44-deficient mice exhibit enhanced hepatitis after concanavalin A injection: evidence for involvement of CD44 in activation-induced cell death. J Immunol *166*, 5889-5897.

Cladera, J., Martin, I., and O'Shea, P. (2001). The fusion domain of HIV gp41 interacts specifically with heparan sulfate on the T-lymphocyte cell surface. Embo J *20*, 19-26.

Demetriou, M., Granovsky, M., Quaggin, S., and Dennis, J. W. (2001). Negative regulation of T-cell activation and autoimmunity by Mgat5 N-glycosylation. Nature *409*, 733-739.

Diamond, M. S., Alon, R., Parkos, C. A., Quinn, M. T., and Springer, T. A. (1995). Heparin is an adhesive ligand for the leukocyte integrin Mac-1 (CD11b/CD1). J Cell Biol *130*, 1473-1482.

Ebert, L. M., Schaerli, P., and Moser, B. (2005). Chemokine-mediated control of T cell traffic in lymphoid and peripheral tissues. Mol Immunol *42*, 799-809.

Engelmann, S., Ebeling, O., and Schwartz-Albiez, R. (1995). Modulated glycosylation of proteoglycans during differentiation of human B lymphocytes. Biochim Biophys Acta *1267*, 6-14.

Esko, J. D., and Lindahl, U. (2001). Molecular diversity of heparan sulfate. J Clin Invest *108*, 169-173.

Forsberg, E., Pejler, G., Ringvall, M., Lunderius, C., Tomasini-Johansson, B., Kusche-Gullberg, M., Eriksson, I., Ledin, J., Hellman, L., and Kjellen, L. (1999). Abnormal mast cells in mice deficient in a heparin-synthesizing enzyme. Nature *400*, 773-776.

Gu, H., Marth, J. D., Orban, P. C., Mossmann, H., and Rajewsky, K. (1994). Deletion of a DNA polymerase beta gene segment in T cells using cell type-specific gene targeting. Science *265*, 103-106.

Hardy, R. R., and Hayakawa, K. (2001). B cell development pathways. Annu Rev Immunol *19*, 595-621.

Hardy, W. D. (1991). Combined ganciclovir and recombinant human granulocyte-macrophage colony-stimulating factor in the treatment of cytomegalovirus retinitis in AIDS patients. J Acquir Immune Defic Syndr *4 Suppl 1*, S22-28.

Hart, G. W. (1982). Biosynthesis of glycosaminoglycans by thymic lymphocytes. Effects of mitogenic activation. Biochemistry *21*, 6088-6096.

Horcher, M., Souabni, A., and Busslinger, M. (2001). Pax5/BSAP maintains the identity of B cells in late B lymphopoiesis. Immunity *14*, 779-790.

Inui, S., Maeda, K., Hua, D. R., Yamashita, T., Yamamoto, H., Miyamoto, E., Aizawa, S., and Sakaguchi, N. (2002). BCR signal through alpha 4 is involved in S6 kinase activation and required for B cell maturation including isotype switching and V region somatic hypermutation. Int Immunol *14*, 177-187.

Jackson, D. G. (1997). Human leucocyte heparan sulphate proteoglycans and their roles in inflammation. Biochem Soc Trans *25*, 220-224.

Kim, C. W., Goldberger, O. A., Gallo, R. L., and Bernfield, M. (1994). Members of the syndecan family of heparan sulfate proteoglycans are expressed in distinct cell-, tissue-, and development-specific patterns. Mol Biol Cell *5*, 797-805.

Kouro, T., Medina, K. L., Oritani, K., and Kincade, P. W. (2001). Characteristics of early murine B-lymphocyte precursors and their direct sensitivity to negative regulators. Blood *97*, 2708-2715.

Lin, X., Wei, G., Shi, Z., Dryer, L., Esko, J. D., Wells, D. E., and Matzuk, M. M. (2000). Disruption of gastrulation and heparan sulfate biosynthesis in EXT1-deficient mice. Dev Biol *224*, 299-311.

Lortat-Jacob, H., Grosdidier, A., and Imberty, A. (2002). Structural diversity of heparan sulfate binding domains in chemokines. Proc Natl Acad Sci U S A *99*, 1229-1234.

Rickert, R. C., Roes, J., and Rajewsky, K. (1997). B lymphocyte-specific, Cre-mediated mutagenesis in mice. Nucleic Acids Res *25*, 1317-1318.

Ringvall, M., Ledin, J., Holmborn, K., van Kuppevelt, T., Ellin, F., Eriksson, I., Olofsson, A. M., Kjellen, L., and Forsberg, E. (2000). Defective heparan sulfate biosynthesis and neonatal lethality in mice lacking N-deacetylase/N-sulfotransferase-1. J Biol Chem *275*, 25926-25930.

Rolink, A. G., Schaniel, C., Andersson, J., and Melchers, F. (2001). Selection events operating at various stages in B cell development. Curr Opin Immunol *13*, 202-207.

Sanderson, R. D., Lalor, P., and Bernfield, M. (1989). B lymphocytes express and lose syndecan at specific stages of differentiation. Cell Regul *1*, 27-35.

Stanley, M. J., Liebersbach, B. F., Liu, W., Anhalt, D. J., and Sanderson, R. D. (1995). Heparan sulfate-mediated cell aggregation. Syndecans-1 and -4 mediate intercellular adhesion following their transfection into human B lymphoid cells. J Biol Chem *270*, 5077-5083.

Stoop, R., Gal, I., Glant, T. T., McNeish, J. D., and Mikecz, K. (2002). Trafficking of CD44-deficient murine lymphocytes under normal and inflammatory conditions. Eur J Immunol *32*, 2532-2542.

Stoop, R., Kotani, H., McNeish, J. D., Otterness, I. G., and Mikecz, K. (2001). Increased resistance to collagen-induced arthritis in CD44-deficient DBA/1 mice. Arthritis Rheum *44*, 2922-2931.

van den Berg, T. K., van der Ende, M., Dopp, E. A., Kraal, G., and Dijkstra, C. D. (1993). Localization of beta 1 integrins and their extracellular ligands in human lymphoid tissues. Am J Pathol *143*, 1098-1110.

van der Voort, R., Keehnen, R. M., Beuling, E. A., Spaargaren, M., and Pals, S. T. (2000). Regulation of cytokine signaling by B cell antigen receptor and CD40-controlled expression of heparan sulfate proteoglycans. J Exp Med *192*, 1115-1124.

Wrenshall, L. E., and Platt, J. L. (1999). Regulation of T cell homeostasis by heparan sulfate-bound IL-2. J Immunol *163*, 3793-3800.

1.7 Acknowledgements

We would like to acknowledge the kind assistance of Dr. Lianchun Wang and Dr. Nissi Varki. This work was supported by an NRSA Minority Predoctoral Fellowship AI58916 (O.B.G.) and fellowships from the Fulbright Program and the Research Council of Norway (V.V).

Appendix 1 is a reprint of material intended to be submitted for publication by Garner, B. Omai; Esko, D. Jeffery; Videm, V. Vibeke. The dissertation author was the primary researcher and author of this paper.

Appendix 2: Guanidinylated Neomycin Delivers Large, Bioactive Cargo to Cells Through a Heparan Sulfate-Dependent Pathway

THE JOURNAL OF BIOLOGICAL CHEMISTRY VOL. 282, NO. 18, pp. 13585–13591, May 4, 2007

Guanidinylated Neomycin Delivers Large, Bioactive Cargo into Cells through a Heparan Sulfate-dependent Pathway*[S]

Received for publication, January 17, 2007, and in revised form, February 13, 2007 Published, JBC Papers in Press, February 20, 2007, DOI 10.1074/jbc.M700463200

Lev Elson-Schwab[‡], Omai B. Garner[§¶], Manuela Schuksz[§¶], Brett E. Crawford[§‖], Jeffrey D. Esko[§1], and Yitzhak Tor[‡2]

From the Departments of [‡]Chemistry and Biochemistry and [§]Cellular and Molecular Medicine, Glycobiology Research and Training Center, [¶]Biomedical Sciences Graduate Program, University of California, San Diego, La Jolla, California 92093 and [‖]Zacharon Pharmaceuticals, Inc., La Jolla, California 92037

Facilitating the uptake of molecules into living cells is of substantial interest for basic research and drug delivery applications. Arginine-rich peptides have been shown to facilitate uptake of high molecular mass cargos into cells, but the mechanism of uptake is complex and may involve multiple receptors. In this report, we show that a derivative of the aminoglycoside antibiotic neomycin, in which all of the ammonium groups have been converted into guanidinium groups, can carry large (>300 kDa) bioactive molecules across cell membranes. Delivery occurs at nanomolar transporter concentrations and under these conditions depends entirely on cell surface heparan sulfate proteoglycans. Conjugation of guanidinoneomycin to the plant toxin saporin, a ribosome-inactivating agent, results in proteoglycan-dependent cell toxicity. In contrast, an arginine-rich peptide shows both heparan sulfate-dependent and -independent cellular uptake. The high selectivity of guanidinoneomycin for heparan sulfate suggests the possibility of exploiting differences in proteoglycan compositions to target delivery to different cell types.

Advances in genomics and proteomics have identified high molecular mass biomolecules and their analogs as potential therapeutic agents. The ability of a cell to take up a high molecular mass drug and to release it into the cytoplasm in an active form represents, however, a major obstacle for the development of these agents. For biological macromolecules effective delivery entails minimal exposure to conditions that may denature or otherwise disrupt activity. Numerous approaches for the physical control of drug localization and release significantly improve the pharmacokinetic features of bioactive molecules, but they typically do not address the inherent challenge of transport of the therapeutic agent across cell membranes. Delivery procedures based on passive diffusion encounter problems due to charged groups, and carriers that exploit endogenous membrane transporters limit the size of potential drug candidates.

Certain polybasic proteins have been shown to enhance the cellular uptake of biomolecules (1). Over the past 15 years, tremendous progress has been made in advancing the basic science, applications, and preclinical evaluation of these and other cationic cell transduction domains (2, 3). In 1988, the human immunodeficiency virus 1 Tat protein was shown to cross lipid bilayers and enter the nucleus (4, 5). Subsequently, numerous other naturally occurring and chimeric peptides have been found to exhibit efficient translocation properties. A data base search, inspired by Tat, identified a number of membrane-permeable peptides that contain clustered arginine residues (6, 7). Further exploration of stereochemistry and composition identified D-Tat and Arg_9 as competent transporters (6, 7). Additionally, significant activity was observed for branched arginine-rich oligomers (8). These observations suggested that the presence of guanidinium moieties represents the critical feature responsible for efficient cell membrane permeability. In fact, guanidinium-containing peptoids (9) and β-peptides exhibit useful cell uptake properties (10). Short polyproline-based helices appended with guanidinium groups (11), highly branched guanidinium-rich dendritic oligomers (12), and heterocyclic guanidinium vectors also serve as cell transporters (13).

The mechanistic understanding of the cellular uptake and internalization of arginine-rich peptides and their analogs has yet to be fully elucidated. Endocytosis-based mechanisms have been both supported and questioned, but some of the early studies may have suffered from artifacts generated by cell fixation. Electrostatic interactions of the positively charged peptides with membrane phospholipids have been proposed as the first step in the transduction process (14–17). An alternative model that has recently been gaining support is the interaction of the positively charged peptides with negatively charged cell surface proteoglycan receptors (18–20).

Recently, we described a new family of synthetic RNA ligands, coined "guanidinoglycosides" (Fig. 1), in which the amino groups of naturally occurring aminoglycoside antibiotics were converted to guanidinium groups. These compounds exhibit high affinity and selectivity for RNA targets that are naturally recognized by Arg-rich domains (21). Guanidinoglycosides also display cellular uptake properties (22). Here, we explore the cellular requirement for uptake, as well as the delivery potential of guanidinoglycosides. We demonstrate that (i) the cellular binding and uptake of guanidinoneomycin at low concentration depends exclusively on heparan sulfate; (ii) in

* This work was supported by National Institutes of Health Grants CA11227 and GM33063 (to J. D. E.) and AI47673 and GM77471 (to Y. T.), Cancer Cell Biology Training Grant CA67754 (to M. S.), and National Research Service Award Individual Fellowship 5F31AI05891602 (to O. G.). The UCSD Neuroscience Microscopy Shared Facility was supported by National Institutes of Health Grant NS047101. The costs of publication of this article were defrayed in part by the payment of page charges. This article must therefore be hereby marked "*advertisement*" in accordance with 18 U.S.C. Section 1734 solely to indicate this fact.

[S] The on-line version of this article (available at http://www.jbc.org) contains supplemental Schemes S1 and S2 and supplemental data.

[1] To whom correspondence may be addressed. E-mail: jesko@ucsd.edu.
[2] To whom correspondence may be addressed. E-mail: ytor@ucsd.edu.

The Journal of Biological Chemistry

contrast, the uptake of arginine-rich peptides in the same concentration range follows both heparan sulfate-dependent and -independent pathways; (iii) guanidinoneomycin will transport high molecular mass and bioactive cargo into cells at low concentration in a completely proteoglycan-dependent manner; and (iv) effective guanidinoneomycin-mediated delivery can be achieved with little or no cellular toxicity.

EXPERIMENTAL PROCEDURES

Cell Culture—Chinese hamster ovary cells (CHO-K1)[3] (ATCC CCL-61) and Lec 2 (ATCC CRL-1736) were obtained from the American Type Culture Collection (Rockville, MD). Mutants pgsA745 and pgsG224 were described previously (23, 24). All cell lines were grown under an atmosphere of 5% CO_2 in air and 100% relative humidity in F12 growth medium supplemented with 7.5% (v/v) fetal bovine serum, 100 μg/ml of streptomycin sulfate, and 100 units/ml of penicillin G.

Synthesis of Guanidinoneomycin-Biotin, Neomycin-Biotin, and Arg_9-Biotin—Synthesis of guanidinoneomycin-biotin and neomycin-biotin is described in the supporting information. Arg_9-biotin and Arg_9-BODIPY were synthesized using standard Fmoc (*N*-(9-fluorenyl)methoxycarbonyl)/HBTU (*O*-(1*H*-benzotriazole-1-yl)-*N*,*N*,*N*′,*N*′-tetramethyluronium hexafluorophosphate) chemistry as described in the supporting information.

Inhibition Experiments—Wild-type CHO cells were grown to confluence on 6-well tissue culture plates, harvested with 10 mM EDTA (37 °C, 10 min), washed with phosphate-buffered saline (PBS), and incubated in suspension with biotinylated FGF-2 (10 ng/ml) (25) in F12 medium for 1 h at 4 °C in the presence of increasing concentrations of guanidinoneomycin (100 nM to 1.8 mM). The cells were then stained with streptavidin-phycoerythrin-Cy5 (BD Biosciences) for 20 min, washed three times with PBS, and analyzed by flow cytometry. Cells were also incubated in F12 medium containing 0.5 μM Arg_9-BODIPY and increasing concentrations of guanidinoneomycin (1–300 μM) for 1 h at 37 °C and analyzed by flow cytometry.

Preparation of Fluorescently Tagged Guanidinoneomycin-Biotin, Neomycin-Biotin, and Arg_9-Biotin and Cell Uptake Studies—Biotinylated compounds were stored in water at −20 °C. After thawing at room temperature, compounds were diluted into F12 medium to 1 μM. To this solution, streptavidin-PE-Cy5 (BD Biosciences) was added in a 1:1000 dilution to achieve a ratio of 1:3 of fluorophore to biotin. To ensure completion of the biotin-streptavidin reaction, the solution was gently mixed and allowed to incubate at room temperature, shielded from light for 30 min. Following this incubation, compounds were diluted to the desired concentration in growth medium. For experiments done at 4 °C solutions were incubated on ice for 30 min.

Wild-type and mutant CHO cells were grown to confluency on 6-well tissue culture plates. After washing with PBS, cells were incubated with the fluorescent-tagged guanidinoneomycin-, neomycin-, or Arg_9-biotin for 1 h at 37 °C under an atmosphere of 5% CO_2. Cells were washed with PBS, released with EDTA, and analyzed by flow cytometry.

[3] The abbreviations used are: CHO, Chinese hamster ovary; FGF, fibroblast growth factor; PE, phycoerythrin; PBS, phosphate-buffered saline.

Microscopy—Cells were cultured on Lab-Tek chambered coverglass slides (Electron Microscopy Sciences) in F12 medium. After washing with PBS, cells were incubated for 1 h in 1 ml of 60 nM guanidinoneomycin coupled to streptavidin-Alexa-488 (Molecular Probes) at 37 °C. Guanidinoneomycin-A488 was prepared by incubating 1 μM guanidinoneomycin-biotin with 6 μg of streptavidin-Alexa-488 in 1 ml of medium. Hoechst 33342 (2 μg/ml; Molecular Probes) was added to cells for the last 20 min of incubation. Cells were washed three times with F12 medium before live cell imaging. Microscopic images were acquired on an Olympus IX70 DeltaVision Spectris Image Deconvolution system, equipped with a temperature and atmospherically controlled stage. Images were deconvolved (10 cycles) using SoftWoRx Explorer Suite software.

Saporin Delivery—A conjugate of saporin and biotinylated guanidinoneomycin was prepared by mixing streptavidinylated saporin (Advanced Targeting Systems) with biotinylated compound in 1:4 ratio. Wild-type CHO and pgsA cells were incubated with guanidinoneomycin-biotin, guanidinoneomycin-biotin and saporin or the conjugate of guanidinoneomycin-biotin and streptavidinylated saporin in complete growth medium for 4 days at 37 °C. CellTiter-Blue (Promega) was added to the medium and cells were incubated for an additional 4 h to measure viability.

RESULTS

Uptake of Guanidinoneomycin Depends on Heparan Sulfate—Neomycin is a member of a family of aminoglycoside antibiotics that inhibit protein synthesis in bacteria (26). Conversion of the amino groups to guanidinium groups alters the properties of the glycoside, allowing it to interact with cell surface heparan sulfate. To study its interactions with cells, we synthesized biotinylated guanidinoneomycin, as well as biotinylated neomycin and biotinylated Arg_9 for comparison (Fig. 1). Biotinylation facilitates conjugation of the carriers to fluorophores and its versatility allows for the preparation and testing of a variety of analogs in different assays.

Fluorescent streptavidin-phycoerythrin-cychrome (streptavidin-PE-Cy5) conjugates of biotinylated guanidinoneomycin, neomycin, and Arg_9 were incubated with CHO cells and uptake was measured by flow cytometry. As described below, these measurements reflect both binding and internalization of the conjugates but are referred to as "uptake" for the sake of clarity. Uptake of the fluorescent guanidinoneomycin conjugate occurred at concentrations as low as 10 nM and proportionately increased up to a concentration of 1 μM, the highest concentration tested (Fig. 2, *upper panels*, *blue lines*). Cells also took up the neomycin conjugate but much less efficiently than the guanidinylated derivative (*middle panel*, *blue lines*). Uptake of the Arg_9 peptide occurred in a more complex manner, exhibiting two classes of receptors expressed by different cells in the population (*lower panel*, *blue lines*).

Incubation with heparin at concentrations as low as 100 ng/ml blocked uptake of the fluorescent guanidinoneomycin conjugate (Fig. 3), suggesting a high affinity of the compound for the negatively charged residues in heparin. These data also suggested the possibility that cell surface heparan sulfate proteoglycans might represent one class of receptors that mediate

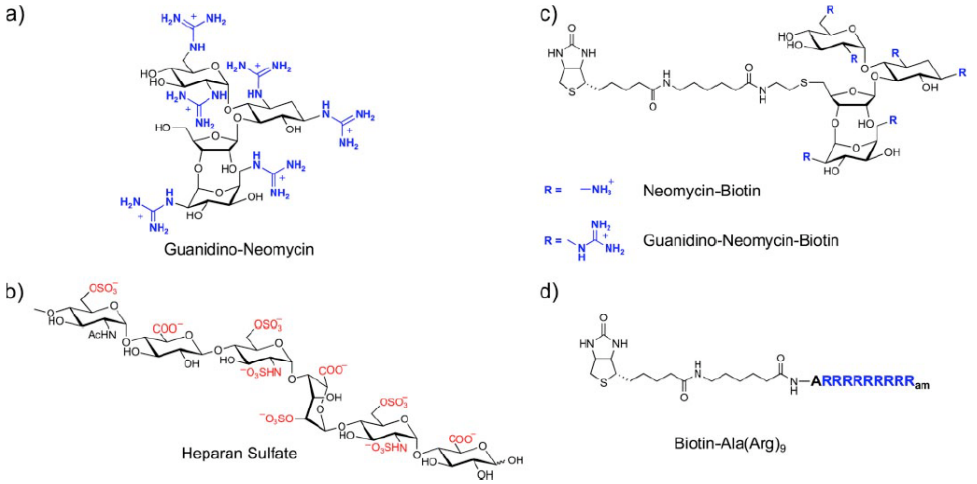

FIGURE 1. **Molecules utilized.** *a*, guanidinoneomycin. *b*, a hexasaccharide fragment of heparan sulfate. Interactions between the negatively charged sulfate groups on the heparan sulfate chain and positively charged guanidinium groups on the guanidinoglycoside are likely key for recognition. *c*, biotinylated guanidinoneomycin and biotinylated neomycin. *d*, biotinylated Arg_9. Details for the synthesis of the biotinylated derivates can be found in the supplemental materials.

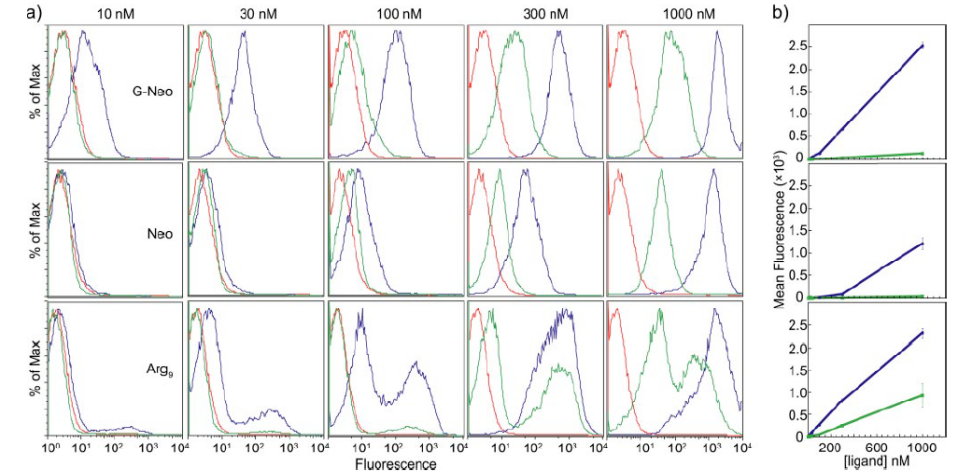

FIGURE 2. **Uptake of fluorescent carriers in CHO cells.** *a*, biotinylated guanidinoneomycin (*G-Neo*), biotinylated neomycin (*Neo*), and biotinylated Arg_9 (Arg_9) were conjugated to streptavidin-PE-Cy5 (~300 kDa). Wild-type (*blue*) and heparan/chondroitin sulfate-deficient pgsA cells (*green*) were incubated with the different conjugates at concentrations from 10 to 1000 nM for 1 h at 37 °C. After washing the cells, they were released with EDTA and analyzed by flow cytometry. Cells incubated with streptavidin-PE-Cy5 alone are shown in *red*. *b*, mean fluorescence values show that both guanidinoneomycin and neomycin display glycosaminoglycan-dependent uptake; however, guanidinoneomycin has a considerably higher uptake efficiency than neomycin. The uptake of Arg_9 does not appear to depend exclusively on heparan/chondroitin sulfate glycosaminoglycans.

binding and uptake. To test this idea, the fluorescent guanidinoneomycin conjugate was incubated with pgsA cells, a mutant that makes <2% of the wild-type level of chondroitin sulfate and heparan sulfate chains (Table 1) (23). Guanidinoneomycin uptake in pgsA cells was barely detectable up to concentrations of 100 nM and was over 20-fold lower than that observed with wild-type cells, even at 1 μM (Fig. 2, *upper panels, green lines*). At higher concentrations, a second, glycosaminoglycan-independent mode of uptake began to emerge. The same trend was observed for the fluorescently tagged neomycin, with internal-

The Journal of Biological Chemistry

ization being more efficient in wild-type cells than pgsA cells (Fig. 2, *middle panels*, *green lines*). The signal from pgsA cells was not affected by trypsin, indicating interactions with a non-proteinaceous receptor.

Whereas the uptake of guanidinoneomycin was strongly dependent on cell surface glycosaminoglycans, fluorescently labeled Arg_9 exhibited multiple modes of uptake in pgsA cells even at low concentrations (Fig. 2, *lower panels*, *green lines*). Multiple populations of cells exhibiting differential binding or uptake capacity were observed in pgsA cells and in wild-type cells. These data suggest that the internalization of Arg_9 follows both glycosaminoglycan-dependent and -independent pathways. Analysis of the mean fluorescence values showed that uptake of the compounds occurred in proportion to concentration, but did not saturate (Fig. 2*b*). Because of this, no further experiments to measure affinity were attempted.

To further study the uptake of guanidinoglycosides, other mutant CHO cells were examined (Table 1, Fig. 3). pgsG cells, mutants lacking all glycosaminoglycans due to a deficiency in glucuronyltransferase I (24), showed a reduction in binding and uptake similar to pgsA cells. Reintroduction of the gene for glucuronosyltransferase I (pgsG + GlcATI) restored binding and uptake, demonstrating their dependence on glycosaminoglycans. Cells selectively lacking heparan sulfate (pgsD) 27) also exhibited dramatically reduced binding and uptake of fluorescent guanidinoneomycin. Because pgsD cells express higher than normal levels of chondroitin sulfate on the cell surface, these findings demonstrate the specificity of binding and uptake for heparan sulfate. Examination of Lec2 cells, which lack sialic acid residues, excluded participation of sialylated glycoproteins and glycolipids (data not shown).

To test the dependence of guanidinoglycoside uptake on heparan sulfate in other cells, we incubated human HeLa ovarian carcinoma cells with fluorescent guanidinoneomycin. A robust signal was obtained, and treatment of the cells with heparin lyases reduced uptake (Fig. 3). The extent of reduction was not as great by enzymatic treatment as by genetic inactivation of heparan sulfate formation in CHO cells, presumably due to incomplete digestion of heparan sulfate chains. Similar results were also obtained for STO mouse fibroblast cells (data not shown), indicating that heparan sulfate on other cells can also mediate uptake of guanidinoneomycin.

To distinguish between cell surface binding and internalization, wild-type CHO cells were incubated with the fluorescent guanidinoneomycin conjugate at 4 °C, where only surface binding occurs. The extent of labeling at 4 °C was reduced by ~6-fold compared with incubations performed at 37 °C (Fig. 4, *inset*), suggesting that ~85% of the fluorescence signal at 37 °C was due to internalization. Binding at 4 °C was sensitive to tryp-

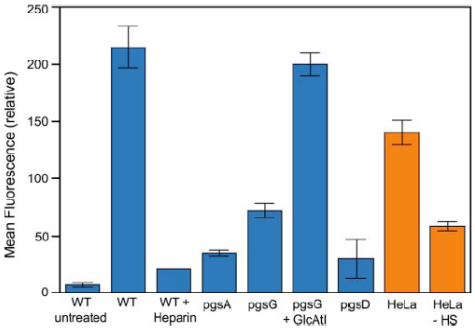

FIGURE 3. **Binding and uptake of guanidinoneomycin by CHO cells and mutants.** Guanidinoneomycin-biotin streptavidin-PE-Cy5 conjugates were incubated with wild-type and mutant CHO cells at 60 nM for 1 h at 37 °C under the indicated conditions. Binding and uptake was analyzed by flow cytometry, and the mean fluorescence values were determined. These data show that the cellular uptake of guanidinoneomycin depends on the presence of cell surface heparan sulfate.

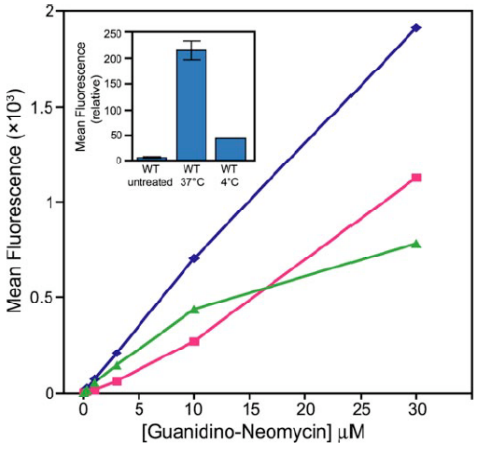

FIGURE 4. **CHO cell binding of guanidinoneomycin at 4 °C.** Guanidinoneomycin-biotin streptavidin-PE-Cy5 conjugates were incubated with wild-type (*blue*) and pgsA (*pink*) cells at concentrations from 10 nM to 30 μM at 4 °C. Binding was analyzed by flow cytometry, and the mean fluorescence values were determined. The difference between mean values (*green*) shows that proteoglycan-dependent binding sites for guanidinoneomycin start to become saturated at low to mid micromolar concentrations. The *inset* shows relative mean fluorescence values for untreated wild-type cells and wild-type cells treated with guanidinoneomycin at 37 and 4 °C.

TABLE 1
Glycan-deficient cell lines
CHO, Chinese hamster ovary cells.

Strain	Glycan alteration	Enzymatic defect
Wild-type CHO	Normal	None
CHO pgsA	Glycosaminoglycan-deficient	Xylosyltransferase (XTII) (23)
CHO pgsG	Glycosaminoglycan-deficient	Glucuronosyltransferase I (GlcAT1) (24)
CHO pgsD	Heparan sulfate-deficient	Copolymerase (EXT1) (27)
CHO Lec2	Sialic acid deficient	CMP-sialic acid transporter (28)
HeLa	Normal	None

sin and heparinase treatment, consistent with binding to membrane proteoglycans. Incubation of pgsA cells showed that at low concentrations binding was entirely dependent on expression of glycosaminoglycans. At higher concentrations, a second class of binding sites was detected that did not show saturability (Fig. 4). Binding to wild-type cells at higher concentrations represents the sum of both classes of binding sites. Subtraction of the fluorescent values obtained from the mutant (*pink line*) from those obtained from the wild-type (*blue line*) yielded a binding curve (*green line*) that presumably reflects the contribution of the proteoglycans (Fig. 4).

Guanidinoneomycin Inhibition of FGF-2 and Arg_9 Binding to Cell Surface Heparan Sulfate—The binding and uptake studies described above predicted that guanidinoneomycin would inhibit binding of ligands that are known to interact with heparan sulfate, such as basic fibroblast growth factor (FGF-2) (29, 30). Prior studies have shown that biotinylated FGF-2 will bind to wild-type CHO cells in a heparan sulfate-dependent manner (24). When mixed with increasing concentrations of guanidinoneomycin, binding was inhibited, with an IC_{50} value of ~20 μM (Fig. 5*a*). In contrast, neomycin, the parent aminoglycoside, did not inhibit binding of FGF-2, which is consistent with its reduced affinity for heparan sulfate (data not shown). Guanidinoneomycin also blocked fluorescent-Arg_9 binding and uptake (Fig. 5*b*). However, inhibition of Arg_9 was incomplete, saturating at the same level of fluorescence intensity as observed when fluorescent Arg_9 was incubated with pgsA cells (Fig. 5*b*, *inset*). These data show that Arg_9 and guanidinoneomycin bind to a common set of glycosaminoglycan-dependent sites and support the idea that Arg_9 also has one or more glycosaminoglycan-independent mechanisms of uptake.

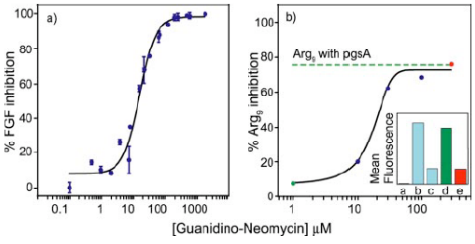

FIGURE 5. **Inhibition of FGF and Arg_9 binding by guanidinoneomycin.** *a*, wild-type CHO cells were incubated with biotinylated FGF-2 (10 ng/ml) for 1 h in the presence of increasing concentrations of guanidinoneomycin. Cells were then stained with streptavidin-phycoerythrin-cychrome and analyzed by flow cytometry. Guanidinoneomycin inhibited FGF-2 binding to cells with an IC_{50} of ~20 μM. *b*, wild-type and pgsA cells were incubated with 0.5 mM Arg_9-BODIPY and increasing concentrations of guanidinoneomycin. After 1 h the cells were analyzed by flow cytometry. Guanidinoneomycin is able to partially block Arg_9 binding to the surface of cells. The signal saturates once it reaches that of pgsA cells incubated with the fluorescent peptide. *Inset*, relative fluorescence of untreated wild-type cells (*a*), wild-type cells treated with fluorescent Arg_9 (*b*), pgsA cells treated with Arg_9 (*c*), and wild-type cells treated with Arg_9 and 1 μM (*d*) or 300 μM guanidinoneomycin (*e*).

Guanidinoneomycin Internalization and Cytoplasmic Delivery of Cargo—To study uptake of guanidinoneomycin in live cells, wild-type and glycosaminoglycan-deficient pgsA cells were incubated with a conjugate prepared from guanidinoneomycin-biotin and streptavidin-Alexa-488. Deconvolution fluorescence microscopy demonstrated uptake into punctate vesicles (Fig. 6*a*), whereas uptake was not observed in pgsA cells (Fig. 6*b*). Inclusion of heparin (50 μg/ml) in the incubation medium completely abolished uptake in wild-type cells (data not shown), but washing the cells with heparin (350 μg/ml) after incubation with the fluorescent guanidinoglycoside conjugate had little effect on vesicle fluorescence, consistent with the idea that the punctate structures were intracellular. With longer incubation, more diffuse cytoplasmic staining was observed as well (data not shown).

To probe the mechanism of uptake, wild-type cells were incubated with the fluorescent guanidinoneomycin conjugate in the presence of sucrose, which has been shown to inhibit clathrin-mediated endocytosis through dissociation of the clathrin lattice (31), and amiloride, which specifically blocks macropinocytosis through inhibition of Na^+/H^+ exchange (23, 32). Cells treated with sucrose showed a marked decrease in internalization of guanidinoneomycin, whereas amiloride had no effect (Fig. 6*c*). These data indicate that guanidinoneomycin is likely internalized into cells via clathrin-dependent endocytosis, consistent with other studies indicating that proteoglycans undergo constitutive internalization (33).

These findings suggested that much of the internalized fluorescent guanidinoneomycin was present in endocytic vesicles or lysosomes but with time some will appear in the cytoplasm. To examine whether guanidinoneomycin could deliver large cargo into the cytoplasm, streptavidinylated saporin was conjugated to guanidinoneomycin-biotin. Saporin, a Type I ribosome-inactivating toxin from *Saponaria officinalis* seeds, does not kill cells due to lack of cell surface receptors (34). However, conjugation of saporin to a ligand for which receptors exist leads to cell death (34). As shown in Fig. 7, the guanidinoneomycin-saporin complex killed wild-type CHO cells with an LD_{50} of ~2

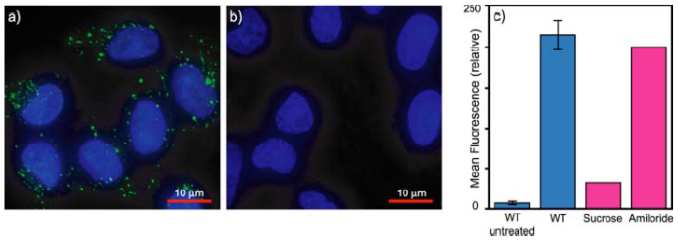

FIGURE 6. **Visualization of guanidinoneomycin uptake in CHO cells.** *a*, wild-type cells were incubated with a conjugate of biotinylated guanidinoneomycin and streptavidinylated Alexa-488 for 1 h at 37 °C. An overlay of the 4′,6 diamidino 2 phenylindole nuclear stain (*blue*) and fluorescent guanidinoneomycin conjugate (*green*) shows internalization in punctate vesicular structures. When the same experiment was performed with heparan/chondroitin sulfate-deficient pgsA cells (*b*), no cell-associated guanidinoglycoside fluorescence was observed. *c*, incubation of wild-type cells with 0.4 M sucrose inhibited uptake, whereas incubation with 5 mM amiloride had no effect.

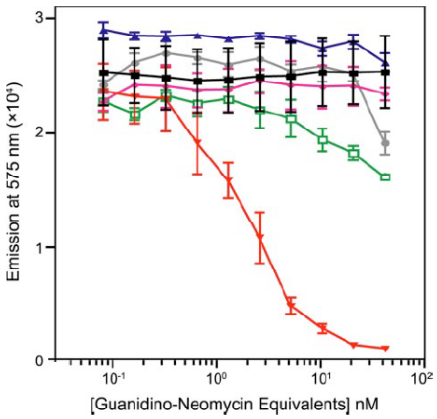

FIGURE 7. **Guanidinoneomycin can efficiently deliver large, bioactive cargo into the cell in a heparan/chondroitin sulfate-dependent manner.** Various combinations of guanidinoneomycin, saporin, and streptavidinylated saporin (~130 kDa) were added to cells. After 4 days, the number of viable cells was estimated using CellTiter assay ("Experimental Procedures"), where the emission at 575 nm corresponds to the relative number of viable cells. Guanidinoneomycin-biotin does not display cell lysis activity on wild-type (*black*) or pgsA (*pink*) cells up to the highest concentration examined (84 nM). Little to no cell death was observed in both wild-type (*blue*) and pgsA (*gray*) cells when incubated with a mixture of non-streptavidinylated saporin and guanidinoneomycin-biotin. Cell toxicity was observed when wild-type cells were incubated with guanidinoneomycin conjugated to saporin through biotin-streptavidin (*red*) with an LD_{50} of ~2 nM. pgsA cells were relatively resistant to the guanidinoglycoside-toxin conjugate (*green*).

nM. No cell toxicity was observed for unconjugated guanidinoneomycin-biotin or for free saporin at concentrations up to 100 nM. Mutant pgsA cells were resistant to toxin within this range of concentration but succumbed at higher concentrations, similarly to cells treated with neomycin-saporin or unconjugated saporin at high concentration. Taken together, these data show that guanidinoneomycin can deliver at very low concentrations large, bioactive cargo into the cytoplasm in a heparan sulfate-dependent manner.

DISCUSSION

Cationic transduction domains, such as the Arg-rich Tat peptide, have been demonstrated to effectively cross lipid bilayers and enter cells (7). Importantly, such relatively short peptides have also been shown to facilitate the uptake of diverse molecular cargos, from small molecules to oligonucleotides and proteins. These observations support the notion that such molecular transporting vehicles can eventually be used to facilitate cellular delivery of impermeable therapeutic agents. A natural peptidic backbone (or sequence) is unnecessary for delivery, because several guanidinium-containing derivatives have been shown to function in a similar manner to Arg-rich peptides. Here, we have evaluated the cell surface requirements for the uptake of guanidinoneomycin, a carbohydrate-based, non-oligomeric guanidinium-rich derivative of the naturally occurring aminoglycoside antibiotic. Like their oligo-arginine counterparts, guanidinoneomycin can deliver high molecular mass cargos, but with much greater selectivity for cell surface heparan sulfate. Thus, guanidinylated glycosides such as guanidinoneomycin may provide the opportunity to develop cell-selective delivery tools, exploiting the differences in proteoglycan expression among different cell types (35).

A universal feature of cell transduction domains, independent of backbone structure, is the presence of a number of guanidinium groups. Bearing a fixed positive charge, these groups can readily form charge-charge interactions with negatively charged groups present in macromolecules, such as phosphate groups in nucleic acids, sulfate and carboxyl groups in glycosaminoglycans, and polar head groups of acidic phospholipids enriched in the outer leaflet of the plasma membrane. The guanidinoglycosides bind more avidly than the corresponding aminoglycosides, presumably due to the higher basicity of the guanidinium groups and their ability to form charged, paired hydrogen bonds with sulfate groups. Apparently, net charge plays a key role in efficacy, as cell transduction domains typically contain between 5 and 11 clustered guanidino groups (3, 9, 22). The studies reported here also demonstrate that the three-dimensional distribution and density of guanidinium groups confer preferred interactions. Thus, exogenously supplied guanidinoneomycin preferentially interacts with heparan sulfate chains associated with cell surface proteoglycans, and not with other acidic glycans, such as chondroitin sulfate, which actually has a higher average charge density per unit length compared with heparan sulfate. Guanidinoneomycin can also bind to a second class of lower affinity receptors when added at higher concentrations. While the proteoglycan-dependent receptors became saturated at low micromolar concentrations of guanidinoneomycin,thebindingtothissecond,non-heparansulfate-dependent class of receptors did not plateau. This finding indicates that these receptors are abundant and may constitute a major part of the cell surface, such as the polar heads of the phospholipids (15). The ability to alter the number and spatial distribution of guanidinium groups on glycoside-based scaffolds may aid in the design of even more specific derivatives.

A major finding reported here is the use of guanidinoglycosides to facilitate the cytoplasmic delivery of bioactive cargo, such as streptavidinylated saporin (~130 kDa) and phycoerythrin (~300 kDa). The use of saporin as a probe of cytoplasmic delivery has several advantages, including greater sensitivity and the capacity to kill cells by inhibition of protein synthesis. The dependence of cytoplasmic delivery on heparan sulfate and its sensitivity to sucrose suggests that the guanidinoneomycin conjugates may bind to membrane proteoglycans and "piggy-back" into the cell during clathrin-dependent endocytosis. A portion of membrane proteoglycans undergoes constitutive internalization and degradation in lysosomes (33). Although it is tempting to speculate that the punctate structures labeled by fluorescent guanidinoneomycin represent a pool from which saporin complexes escape or are transported into the cytosol, further studies are needed to determine the actual compartment from which cytosolic cargo originates.

Guanidinoglycosides present several advantages over peptide/oligomer-based transport vehicles: 1) The mechanism of uptake and delivery of polyarginine appears to be more complicated, because both heparan sulfate-dependent and -independent pathways exist; 2) Non-peptidic and non-oligo-

The Journal of Biological Chemistry

meric structures may display enhanced *in vivo* stability; 3) Aminoglycoside-degrading enzymes, and by inference enzymes that degrade guanidinoglycosides, have not yet been described in animal cells, whereas multiple proteases exist that can degrade arginine-rich peptides; 4) Guanidinoglycosides may offer greater flexibility in conjugation chemistry as compared with peptide-based delivery agents; 5) The chemical synthesis of guanidinoglycosides allows for divergent synthesis of multiple conjugates; and 6) The use of cleavable linkers might further facilitate the delivery of small and large molecules and their release within the cytoplasm.

In summary, we have shown the capacity of guanidinoglycosides to deliver high molecular mass, bioactive cargos into cells. At low concentration, cellular uptake occurs exclusively by heparan sulfate-dependent receptors. This behavior may provide a window of opportunity to exploit differences in expression of cell surface proteoglycans for the development of more effective and selective cellular delivery vehicles.

Acknowledgment—We thank Arrate Mallabiabarrena for excellent assistance with deconvolution microscopy.

REFERENCES

1. Ryser, H. J.-P. (1968) *Science* **159,** 390–396
2. Dietz, G. P., and Bahr, M. (2004) *Mol. Cell. Neurosci.* **27,** 85–131
3. Wadia, J. S., and Dowdy, S. F. (2005) *Adv. Drug Del. Rev.* **57,** 579–596
4. Frankel, A. D., and Pabo, C. O. (1988) *Cell* **55,** 1189–1193
5. Green, M., and Loewenstein, P. M. (1988) *Cell* **55,** 1179–1188
6. Futaki, S. (2005) *Adv. Drug Deliv. Rev.* **57,** 547–558
7. Futaki, S. (2006) *Biopolymers Pept. Sci.* **84,** 241–249
8. Futaki, S., Nakase, I., Suzuki, T., Zhang, Y., and Sugiura, Y. (2002) *Biochemistry* **41,** 7925–7930
9. Wender, P. A., Mitchell, D. J., Pattabiraman, K., Pelkey, E. T., Steinman, L., and Rothbard, J. B. (2000) *Proc. Natl. Acad. Sci.* **97,** 13003–13008
10. Umezawa, N., Gelman, M. A., Haigis, M. C., Raines, R. T., and Gellman, S. H. (2002) *J. Am. Chem. Soc.* **124,** 368–369
11. Fillon, Y. A., Anderson, J. P., and Chmielewski, J. (2005) *J. Am. Chem. Soc.* **127,** 11798–11803
12. Chung, H. H., Harms, G., Seong, C. M., Choi, B. H., Min, C., Taulane, J. P., and Goodman, M. (2004) *Biopolymers* **76,** 83–96
13. Fernández-Carneado, J., Van Gool, M., Martos, V., Castel, S., Prados, P., de Mendoza, J., and Giralt, E. (2005) *J. Am. Chem. Soc.* **127,** 869–874
14. Rothbard, J. B., Jessop, T. C., and Wender, P. A. (2005) *Adv. Drug. Deliv. Rev.* **57,** 495–504
15. Rothbard, J. B., Jessop, T. C., Lewis, R. S., Murray, B. A., and Wender, P. A. (2004) *J. Am. Chem. Soc.* **126,** 9506–9507
16. Caesar, C. E. B., Esbjorner, E. K., Lincoln, P., and Nordén, B. (2006) *Biochemistry* **45,** 7682–7692
17. Hitz, T., Iten, R., Gardiner, J., Namoto, K., Walde, P., and Seebach, D. (2006) *Biochemistry* **45,** 5817–5829
18. Tyagi, M., Rusnati, M., Presta, M., and Giacca, M. (2001) *J. Biol. Chem.* **276,** 3254–3261
19. Fuchs, S. M., and Raines, R. T. (2004) *Biochemistry* **43,** 2438–2444
20. Richard, J. P., Melikov, K., Brooks, H., Prevot, P., Lebleu, B., and Chernomordik, L. V. (2005) *J. Biol. Chem.* **280,** 15300–15306
21. Luedtke, N. W., Baker, T. J., Goodman, M., and Tor, Y. (2000) *J. Am. Chem. Soc.* **122,** 12035–12036
22. Luedtke, N. W., Carmichael, P., and Tor, Y. (2003) *J. Am. Chem. Soc.* **125,** 12374–12375
23. Esko, J. D., Stewart, T. E., and Taylor, W. H. (1985) *Proc. Natl. Acad. Sci. U. S. A.* **82,** 3197–3201
24. Bai, X. M., Wei, G., Sinha, A., and Esko, J. D. (1999) *J. Biol. Chem.* **274,** 13017–13024
25. Wei, G., Bai, X., Sarkar, A. K., and Esko, J. D. (1999) *J. Biol. Chem.* **274,** 7857–7864
26. Chambers, H. F. (2006) in *Goodman & Gilman's The Pharmacological Basis of Therapeutics* (Brunton, L. L., Lazo, J. S., and Parker, K. L., eds) 11th Ed., pp. 1155–1171, McGraw-Hill, New York
27. Lidholt, K., Weinke, J. L., Kiser, C. S., Lugemwa, F. N., Bame, K. J., Cheifetz, S., Massaguo, J., Lindahl, U., and Esko, J. D. (1992) *Proc. Natl. Acad. Sci. U. S. A.* **89,** 2267–2271
28. Deutscher, S. L., Nuwayhid, N., Stanley, P., Briles, E. I., and Hirschberg, C. B. (1984) *Cell* **39,** 295–299
29. Yayon, A., Klagsbrun, M., Esko, J. D., Leder, P., and Ornitz, D. M. (1991) *Cell* **64,** 841–848
30. Rapraeger, A. C., Krufka, A., and Olwin, B. B. (1991) *Science* **252,** 1705–1708
31. Lamaze, C., and Schmid, S. L. (1995) *Curr. Opin. Cell Biol.* **7,** 573–580
32. Kaplan, I. M., Wadia, J. S., and Dowdy, S. F. (2005) *J. Controlled Release* **102,** 247–253
33. Williams, K. J., and Fuki, I. V. (1997) *Curr. Opin. Lipidol.* **8,** 253–262
34. Flavell, D. J. (1998) *Curr. Top Microbiol. Immunol.* **234,** 57–61
35. Esko, J. D., and Selleck, S. B. (2002) *Annu. Rev. Biochem.* **71,** 435–471

The Journal of Biological Chemistry

Appendix 2 is a reprint of material as it is published in the Journal of Biological Chemistry, Elson-Schwab, Lev; Garner, B. Omai; Schuksz, Manuela; Crawford, E. Brett; Esko, D. Jeffery; Tor, Yitzhak. The dissertation author was a secondary researcher and author of this paper.